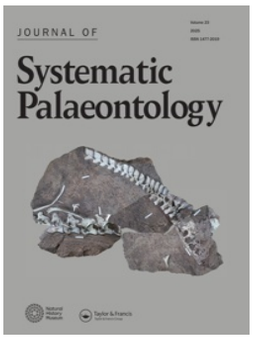

Journal of Systematic Palaeontology

ISSN: 1477-2019 (Print) 1478-0941 (Online) Journal homepage: www.tandfonline.com/journals/tjsp20

Critical reappraisal of a putative dicraeosaurid sauropod dinosaur from the Middle Jurassic of Gondwana and a revised view of diplodocoid evolutionary relationships and biogeography

Philip D. Mannion & Andrew J. Moore

To cite this article: Philip D. Mannion & Andrew J. Moore (2025) Critical reappraisal of a putative dicraeosaurid sauropod dinosaur from the Middle Jurassic of Gondwana and a revised view of diplodocoid evolutionary relationships and biogeography, Journal of Systematic Palaeontology, 23:1, 2550760, DOI: 10.1080/14772019.2025.2550760

To link to this article: https://doi.org/10.1080/14772019.2025.2550760

© 2025 The Author(s). Published by Informa UK Limited, trading as Taylor & Francis Group.

View supplementary material

Published online: 10 Oct 2025.

Submit your article to this journal

Article views: 2658

View related articles

View Crossmark data

Full Terms & Conditions of access and use can be found at
https://www.tandfonline.com/action/journalInformation?journalCode=tjsp20

Journal of Systematic Palaeontology, 2025
Vol. 23, No. 1, 2550760
http://dx.doi.org/10.1080/14772019.2025.2550760

Taylor & Francis
Taylor & Francis Group

OPEN ACCESS Check for updates

Critical reappraisal of a putative dicraeosaurid sauropod dinosaur from the Middle Jurassic of Gondwana and a revised view of diplodocoid evolutionary relationships and biogeography

Philip D. Mannion[a]* and Andrew J. Moore[b]

[a]*Department of Earth Sciences, University College London, Gower Street, London, WC1E 6BT, UK;* [b]*Department of Anatomical Sciences, Renaissance School of Medicine, Stony Brook University, Stony Brook, NY 11794, USA*

(Received 24 March 2025; accepted 21 July 2025)

Diplodocoidea is a diverse clade of sauropod dinosaurs that comprises three major lineages: Diplodocidae, Dicraeosauridae and Rebbachisauridae, with the former two united as Flagellicaudata. There has been a recent spate of newly described diplodocoid taxa, as well as additional information on existing species. Of particular significance is *Tharosaurus indicus*, from the Middle Jurassic of India, which was argued to represent a dicraeosaurid and to potentially evidence a Gondwanan origin for Flagellicaudata. Here, we critically reappraise the anatomy of *Tharosaurus* and use new morphological data to re-evaluate the phylogenetic relationships and biogeographical history of Diplodocoidea. We incorporated *Tharosaurus* and 12 diplodocoid operational taxonomic units (OTUs) into the largest existing character matrix for eusauropods, added new characters, and revised the characters and scores for previously included OTUs. The final matrix (563 characters scored for 139 OTUs) includes 38 uncontroversial diplodocoids. Topological results from phylogenetic analyses under maximum parsimony are sensitive to the application of equal versus extended implied weighting, but consistently agree that *Tharosaurus* is an indeterminate eusauropod that lacks diplodocoid synapomorphies. Favouring results produced under extended implied weighting with a concavity constant of 12, we present a revised view of diplodocoid relationships, provide new diagnoses and illustrate synapomorphies of major clades. The Upper Jurassic Morrison Formation sauropod *Haplocanthosaurus* is recovered as a non-diplodocimorph diplodocoid. In contrast with previous analyses, the Middle Jurassic Chinese diplodocoid *Lingwulong* is placed as a stem flagellicaudatan, outside of the diplodocid–dicraeosaurid split. We recover a diverse Dicraeosauridae that includes three Morrison Formation OTUs (*Smitanosaurus*, *Suuwassea*, BYU 17096) forming its earliest-branching members. Phylogenetically more-nested dicraeosaurids are all Late Jurassic–Early Cretaceous Gondwanan taxa, for which we formally define the clade Dicraeosaurinae. Diplodocidae includes the Morrison Formation taxon *Kaatedocus* as an early-diverging member, whilst *Tornieria* + *Leinkupal* forms a phylogenetically nested diplodocine clade. The Morrison Formation sauropod *Amphicoelias* is recovered as an early-branching diplodocoid of uncertain affinities, with equally parsimonious placement as a flagellicaudatan, rebbachisaurid, or non-diplodocimorph diplodocoid. Early-diverging rebbachisaurids include Gondwana taxa, as well as the earliest Cretaceous UK taxon *Xenoposeidon*. Within Khebbashia, Limaysaurinae is restricted to South America, whereas Rebbachisaurinae is present in Europe, North Africa, and South America. The stratigraphically youngest known flagellicaudatans are from the Barremian, whereas rebbachisaurids survived until the Turonian or Coniacian. The extinction of diplodocoids appears to have been spatiotemporally staggered. Our results reinforce the view that Flagellicaudata (and probably also Rebbachisauridae) likely originated in Laurasia, but the presence of diplodocoids across Eurasia in the Middle Jurassic suggests a potentially widespread distribution early in their evolutionary history that is likely obscured by sampling failure.

Keywords: Biogeography; Dinosauria; Diplodocoidea; Morrison Formation; phylogenetics; Sauropoda

Introduction

Diplodocoids include some of the most well-known sauropod dinosaurs, with taxa such as the diplodocids *Brontosaurus* and *Diplodocus* from the Upper Jurassic Morrison Formation of the USA shaping our earliest understanding of these megaherbivores (Mannion & Whitlock, in press; McIntosh, 1990; Tschopp et al., 2015; Upchurch, Barrett, et al., 2004). As the sister taxon to Macronaria, Diplodocoidea represents one of the two lineages of the diverse clade Neosauropoda (Wilson & Sereno, 1998). Diplodocoidea consists of three major lineages: Diplodocidae, Dicraeosauridae and Rebbachisauridae. Early phylogenetic analyses demonstrated that Diplodocidae is the sister taxon of Dicraeosauridae (Calvo & Salgado, 1995; Russell &

*Corresponding author. Email: philipdmannion@gmail.com

© 2025 The Author(s). Published by Informa UK Limited, trading as Taylor & Francis Group.
This is an Open Access article distributed under the terms of the Creative Commons Attribution-NonCommercial-NoDerivatives License (http://creativecommons.org/licenses/by-nc-nd/4.0/), which permits non-commercial re-use, distribution, and reproduction in any medium, provided the original work is properly cited, and is not altered, transformed, or built upon in any way. The terms on which this article has been published allow the posting of the Accepted Manuscript in a repository by the author(s) or with their consent.

Published online 10 Oct 2025

Zheng, 1993; Upchurch, 1995, 1998; Wilson & Sereno, 1998), subsequently grouped together as the clade Flagellicaudata (Harris & Dodson, 2004), which is in turn the sister taxon of Rebbachisauridae (Wilson, 2002). A small number of taxa from the Morrison Formation (*Haplocanthosaurus* spp. and *Amphicoelias altus*) are typically recovered as diplodocoids that lie outside of these three clades (Mannion et al., 2021), prompting the use of Diplodocimorpha to unite the less inclusive clade of Flagellicaudata + Rebbachisauridae (Taylor & Naish, 2005). These relationships continue to be well supported in more recent phylogenetic analyses that sample a large number of diplodocoids (e.g. Bellardini et al., 2025; Canudo et al., 2018; Gallina et al., 2019; Lerzo, Gallina, et al., 2025; Mannion, Upchurch, Schwarz, et al., 2019; Tschopp & Mateus, 2017; Whitlock & Wilson Mantilla, 2020).

Diplodocids are best known for having had long necks and tails, even by sauropod standards. As noted above, diplodocids include some of the earliest-named sauropods and several members of this clade have a long history of study (McIntosh, 1990; Upchurch, Barrett, et al., 2004). Much of known diplodocid diversity comes from the Morrison Formation, with at least 12 species currently considered to be valid (*Apatosaurus* spp., *Ardetosaurus viator*, *Barosaurus lentus*, *Brontosaurus* spp., *Diplodocus* spp., *Galeamopus* spp., *Supersaurus vivianae*), although some of these have only been recognized in recent decades (Mannion et al., 2021; Tschopp et al., 2015; van der Linden et al., 2024). The presence of this clade outside of North America was also recognized relatively early in the history of sauropod study, with the species now known as *Tornieria africana* identified in the Upper Jurassic Tendaguru Formation of Tanzania early in the twentieth century (Fraas, 1908; Remes, 2006). This distribution was extended into Europe with the description of *Dinheirosaurus lourinhanensis* from the Upper Jurassic Lourinhã Formation of Portugal (Bonaparte & Mateus, 1999; Mannion et al., 2012), and into South America through the discovery of *Leinkupal laticauda* in the lowermost Cretaceous Bajada Colorada Formation of Argentina (Gallina et al., 2014). By contrast with the long history of study and known diversity of diplodocids, members of the other two diplodocoid clades remained poorly known until recent decades.

Rebbachisaurids are perhaps best known for their highly specialized, lightly constructed skulls, including an anteriorly restricted dental battery, as well as their racquet-shaped scapulae (Calvo & Salgado, 1995; Sereno et al., 2007). Originally known from a single species, *Rebbachisaurus garasbae*, from the lower Upper Cretaceous Kem Kem Group of Morocco (Lavocat, 1954; Wilson & Allain, 2015), the diversity of Rebbachisauridae was expanded through the description of *Limaysaurus tessonei* (originally described as a species of *Rebbachisaurus*) and *Rayososaurus agrioensis* from the contemporaneous Candeleros Formation of Argentina (Bonaparte, 1996; Calvo & Salgado, 1995; Carballido et al., 2010; Salgado et al., 2004). An additional rebbachisaurid species, *Nigersaurus taqueti*, was described from the upper Lower Cretaceous Elrhaz Formation of Niger (Sereno et al., 1999), with north African diversity later augmented by the discovery of *Tataouinea hannibalis*, from the contemporaneous Aïn el Guettar Formation of Tunisia (Fanti et al., 2013). Numerous additional rebbachisaurid taxa have since been recognized from Argentina (Apesteguía, 2007; Bellardini et al., 2023, 2025; Canudo et al., 2018; Carballido et al., 2012; Gallina & Apesteguía, 2005; Ibiricu et al., 2013; Lerzo, Gallina, et al., 2025; Lerzo, Torcida Fernández-Baldor, et al., 2025; Salgado et al., 2006, 2022; Simón & Salgado, 2025), emanating from the upper Lower Cretaceous La Amarga, Lohan Cura and Rayoso formations (*Agustinia ligabuei*, *Comahuesaurus windhauseni*, *Lavocatisaurus agrioensis*, *Zapalasaurus bonapartei*), as well as the lower Upper Cretaceous Bajo Barreal, Candeleros, and Huincul formations (*Astigmasaura genuflexa*, *Campananeyen fragilissimus*, *Cathartesaura anaerobica*, *Cienciargentina sanchezi*, *Katepensaurus goicoecheai*, *Nopcsaspondylus alarconensis*, *Sidersaura marae*). Rebbachisaurids have also been described from Brazil, with *Amazonsaurus maranhensis* from the upper Lower Cretaceous Itapecuru Formation (Carvalho et al., 2003) and *Itapeuasaurus cajapioensis* from the lower Upper Cretaceous Alcântara Formation (Lindoso et al., 2019).

Although part of Europe today, the Lower Cretaceous deposits of Croatia that yielded the rebbachisaurid *Histriasaurus boscarollii* were formed when this was part of the Afro-Arabian continent (Dalla Vecchia, 1998, 2005). Genuine European rebbachisaurids have subsequently been recognized, with *Demandasaurus darwini* from the upper Lower Cretaceous Castrillo de la Reina Formation of Spain (Pereda Suberbiola et al., 2003; Torcida Fernández-Baldor et al., 2011) demonstrating that Rebbachisauridae was not endemic to Gondwana (see also Mannion, 2009). More recently, *Xenoposeidon proneneukos*, from the lowermost Cretaceous Ashdown Formation of the UK (Taylor & Naish, 2007), has been interpreted as a rebbachisaurid (Taylor, 2018), although this has yet to be tested via phylogenetic analysis. Finally, Carpenter (2018) interpreted a drawing of a long-lost specimen from the Morrison Formation as a rebbachisaurid, erecting *Maraapunisaurus fragillimus*. If correct, this would be the stratigraphically oldest known rebbachisaurid, and

the only occurrence of this clade currently known from North America.

Dicraeosaurids are best known for the hyper-elongate, bifid neural spines that characterize much of their presacral vertebral column (Gallina et al., 2022; Upchurch, Barrett, et al., 2004). The first described member of the group, *Dicraeosaurus*, was erected for two species (*D. hansemanni* and *D. sattleri*) from the Tendaguru Formation in the early twentieth century (Janensch, 1914). A second genus, *Amargasaurus cazaui*, from the Lower Cretaceous La Amarga Formation of Argentina, was only described in the last decade of the twentieth century (Salgado & Bonaparte, 1991). Dicraeosaurid diversity was expanded through the description of *Brachytrachelopan mesai* from the Upper Jurassic Cañadón Calcáreo Formation of Argentina (Rauhut et al., 2005), but remained a seemingly endemic Gondwanan clade until the recognition that *Suuwassea emilieae*, from the Upper Jurassic Morrison Formation of the USA (Harris & Dodson, 2004), was an additional member of Dicraeosauridae (Salgado et al., 2006; Whitlock, 2011a). Not only did this demonstrate that dicraeosaurids had a geographically broader distribution, but *Suuwassea* was recovered as the earliest-diverging member of the group, casting doubt on the clade's previously presumed Gondwanan origin (Whitlock, 2011a). Additional dicraeosaurid taxa have since been recognized from the Morrison (*Smitanosaurus agilis*, and possibly *Dyslocosaurus polyonychius* and *Kaatedocus siberi*) and La Amarga formations (*Amargatitanis macni*) (Gallina, 2016; Tschopp et al., 2015; Whitlock & Wilson Mantilla, 2020), along with *Bajadasaurus pronuspinax* and *Pilmatueia faundezi* from the Lower Cretaceous Bajada Colorada and Mulichinco formations, respectively, of Argentina (Coria et al., 2019; Gallina et al., 2019; Windholz et al., 2022).

The discovery of *Lingwulong shenqi* from the Middle Jurassic Yanan or Zhiluo Formation of China, recovered as a dicraeosaurid, extended the spatiotemporal distribution of the group further (Xu et al., 2018; see You et al., 2019 regarding stratigraphical provenance). It also demonstrated that the three main lineages of Diplodocoidea must have diverged no later than this time, implying unsampled ghost lineages for Diplodocidae and Rebbachisauridae, for which the stratigraphically earliest unequivocal occurrences are restricted to the Late Jurassic and Early Cretaceous, respectively (see above). It also supported the view that diplodocoids had a widespread distribution early in their evolutionary history (Xu et al., 2018) and provided additional evidence that major divergences in the clade might not necessarily have occurred in Gondwana (Mannion, Upchurch, Schwarz, et al., 2019). Recently, Bajpai et al. (2023) described fragmentary sauropod remains from the Middle Jurassic of India, then part of Gondwana, which they identified as a new dicraeosaurid, *Tharosaurus indicus*. This would make it one of the stratigraphically oldest known members of Dicraeosauridae, and, by extension, Diplodocoidea, and potentially challenge existing biogeographical hypotheses pertaining to the radiation of the major neosauropod lineages.

The recent spate of newly described dicraeosaurid and rebbachisaurid taxa, coupled with new information on existing species, means that the phylogenetic interrelationships of the two clades are in a state of flux (e.g. see topologies in Bellardini et al., 2023, 2025; Gallina et al., 2019; Lerzo, Gallina, et al., 2025; Lerzo, Torcida Fernández-Baldor, et al., 2025; Mannion, Upchurch, Schwarz, et al., 2019; Whitlock & Wilson Mantilla, 2020; Windholz et al., 2022). Here, we reassess the proposed dicraeosaurid affinities of *Tharosaurus indicus* and present an expanded version of the largest phylogenetic data matrix for eusauropods published to date, in which we focus on elucidating the evolutionary relationships of diplodocoid sauropod dinosaurs. Finally, we use this to provide a revised view of our current understanding of the evolutionary and biogeographical history of diplodocoids.

Institutional abbreviations

AMNH, American Museum of Natural History, New York, NY, USA; **ANS**, Academy of Natural Sciences, Philadelphia, PA, USA; **BYU**, Brigham Young University, Museum of Paleontology, Provo, UT, USA; **CM**, Carnegie Museum of Natural History, Pittsburgh, PA, USA; **CMNH**, Cleveland Museum of Natural History, Cleveland, OH, USA; **CPT**, Museo Fundación Conjunto Paleontológico de Teruel, Teruel, Spain; **DFMMh**, Dinosaurier-Freilichtmuseum Münchehagen, Münchehagen, Germany; **IVPP**, Institute of Vertebrate Paleontology and Paleoanthropology, Beijing, China; **LGP**, Lingwu Geopark, Lingwu, Ningxia Hui Autonomous Region, China; **LM**, Lingwu Museum, Lingwu, Ningxia Hui Autonomous Region, China; **MACN**, Museo Argentino de Ciencias Naturales Bernardino Rivadavia, Buenos Aires, Argentina; **MDPA**, Museo del Desierto Patagónico de Añelo, Neuquén, Argentina; **MDS**, Museo de Dinosaurios de Salas de los Infantes, Burgos, Spain; **MDT-PV**, Museo Desiderio Torres–Paleovertebrados, Sarmiento, Argentina; **MfN**, Museum für Naturkunde, Berlin, Germany; **MIWG**, Museum of Isle of Wight Geology (now Dinosaur Isle Visitor Centre), Isle of Wight, UK; **ML**, Museu da Lourinhã, Lourinhã, Portugal; **MMCH**, Museo Municipal 'Ernesto Bachmann', Villa El

Chocón, Neuquén, Argentina; **MN**, Museu Nacional, Rio de Janeiro, Brazil; **MNHN**, Muséum National d'Histoire Naturelle, Paris, France; **MNN**, Musée National du Niger, Niamey, Republic of Niger; **MOZ**, Museo Provincial de Ciencias Naturales 'Prof. Dr Juan A. Olsacher', Zapala, Neuquén, Argentina; **MPCA**, Museo Provincial Carlos Ameghino, Cipolletti, Río Negro, Argentina; **MPEF**, Museo Paleontológico Egidio Feruglio, Trelew, Argentina; **MUCPv**, Museo de Geología y Paleontología de la Universidad Nacional del Comahue, Neuquén, Argentina; **NHMUK**, Natural History Museum, London, UK; **SMNS**, Staatliches Museum für Naturkunde Stuttgart, Stuttgart, Germany; **TATE**, Tate Geological Museum, Casper College, Casper, WY, USA; **UFRJ-DG**, Universidade Federal do Rio de Janeiro, Departamento de Geologia, Rio de Janeiro, Brazil; **UNPSJB**, Universidad Nacional de la Patagonia San Juan Bosco, Comodoro Rivadavia, Argentina; **USNM**, National Museum of Natural History, Washington, DC, USA; **UWGM**, University of Wyoming Geological Museum, Laramie, WY, USA; **WDC**, Wyoming Dinosaur Center, Thermopolis, WY, USA; **YPM**, Yale Peabody Museum, New Haven, CT, USA; **ZDM**, Zigong Dinosaur Museum, Dashanpu, China.

Anatomical reinterpretation of *Tharosaurus*

Bajpai et al. (2023) only made anatomical comparisons with flagellicaudatans. In many instances, they noted that a feature is similar to a subset of flagellicaudatan taxa; however, in nearly all cases these features are similar to a much more inclusive sauropod group. Below we focus on anatomical features interpreted by Bajpai et al. (2023) as synapomorphic within Diplodocoidea, in addition to putative autapomorphies of *Tharosaurus* (Figs 1–3). Our reassessment of *Tharosaurus* is based entirely on the photographs and information presented in Bajpai et al. (2023) and not on first-hand observation of the material (RWR-241-A–K).

Cervical vertebral features

Bajpai et al. (2023) described the presence of paired fossae on the ventral surface of the posterior half of the cervical centrum, RWR-241-B (Fig. 1A), which they noted as a dicraeosaurid feature. However, ventral paramedian fossae are not exclusive to dicraeosaurids, and also occur in the cervical centra of some non-neosauropods, including *Tazoudasaurus* (Allain & Aquesbi, 2008), *Datousaurus* (Peng et al., 2005), and *Omeisaurus* (He et al., 1998; Tan et al., 2019), as well as the early-diverging diplodocoid *Haplocanthosaurus priscus* (Tschopp et al., 2015; Whitlock, 2011a), the rebbachisaurid *Katepensaurus* (Ibiricu et al., 2013), and the diplodocines *Supersaurus* (Lovelace et al., 2008) and *Galeamopus* (Tschopp & Mateus, 2017). In these taxa, as well as in dicraeosaurids, these fossae are distinct excavations with a clear break of slope from the remainder of the ventral surface; furthermore, in dicraeosaurids, they are usually restricted to the anterior region of the non-condylar centrum of anterior cervical centra (Fig. 1F) (Whitlock, 2011a). By contrast, the feature described by Bajpai et al. (2023) in RWR-241-B is not a distinct excavation, but is instead the flat to gently concave morphology (Fig. 1A) that characterizes the ventral surface of most sauropod cervical centra (e.g. Mannion et al., 2013; Upchurch, Barrett, et al., 2004). Bajpai et al. (2023) also described the presence of ventrolateral ridges along the cervical centrum of *Tharosaurus* (Fig. 1A), which contribute to the appearance of a shallowly concave ventral surface; however, these features are widespread amongst eusauropods (Fig. 1H) (e.g. Upchurch et al., 2021; Wilson & Upchurch, 2009) and the ridges in RWR-241-B are not the prominent structures delimiting a ventral longitudinal sulcus that characterizes some flagellicaudatans (Fig. 1G), such as *Apatosaurus*, *Dicraeosaurus* and *Diplodocus* (Upchurch, 1998).

There is a midline keel along the entirety of the preserved ventral surface of the cervical centrum (RWR-241-B) of *Tharosaurus* (Fig. 1A). Bajpai et al. (2023) noted that a ventral keel also characterizes many flagellicaudatans, including most dicraeosaurids (Fig. 1F) (see Upchurch, 1998; Whitlock, 2011a). However, the presence of a midline ventral keel is the plesiomorphic sauropod condition that is retained in the cervical centra of many non-neosauropod taxa, including *Bagualia*, *Barapasaurus*, *Lapparentosaurus*, *Omeisaurus*, *Patagosaurus* and *Tazoudasaurus* (Fig. 1H) (Allain & Aquesbi, 2008; Bandyopadhyay et al., 2010; Gomez et al., 2021; Holwerda et al., 2021; Upchurch, 1998). It also characterizes rebbachisaurids and is variably present in *Haplocanthosaurus priscus* (Mannion, Upchurch, Schwarz, et al., 2019; Upchurch, 1998; Whitlock, 2011a). In most of these taxa, the keel does not extend continuously as far posteriorly as the condition in *Tharosaurus* (Gomez et al., 2021), although *Tazoudasaurus* (Allain & Aquesbi, 2008) is also characterized by a posteriorly extensive ventral keel. As such, by itself, a midline ventral keel cannot be unequivocally used to support dicraeosaurid affinities for *Tharosaurus*. Bajpai et al. (2023) suggested that this keel autapomorphically bifurcates at its posterior end in *Tharosaurus*; however, the relevant area of RWR-241-B is poorly preserved (Fig. 1A) and such an interpretation cannot be substantiated without additional remains.

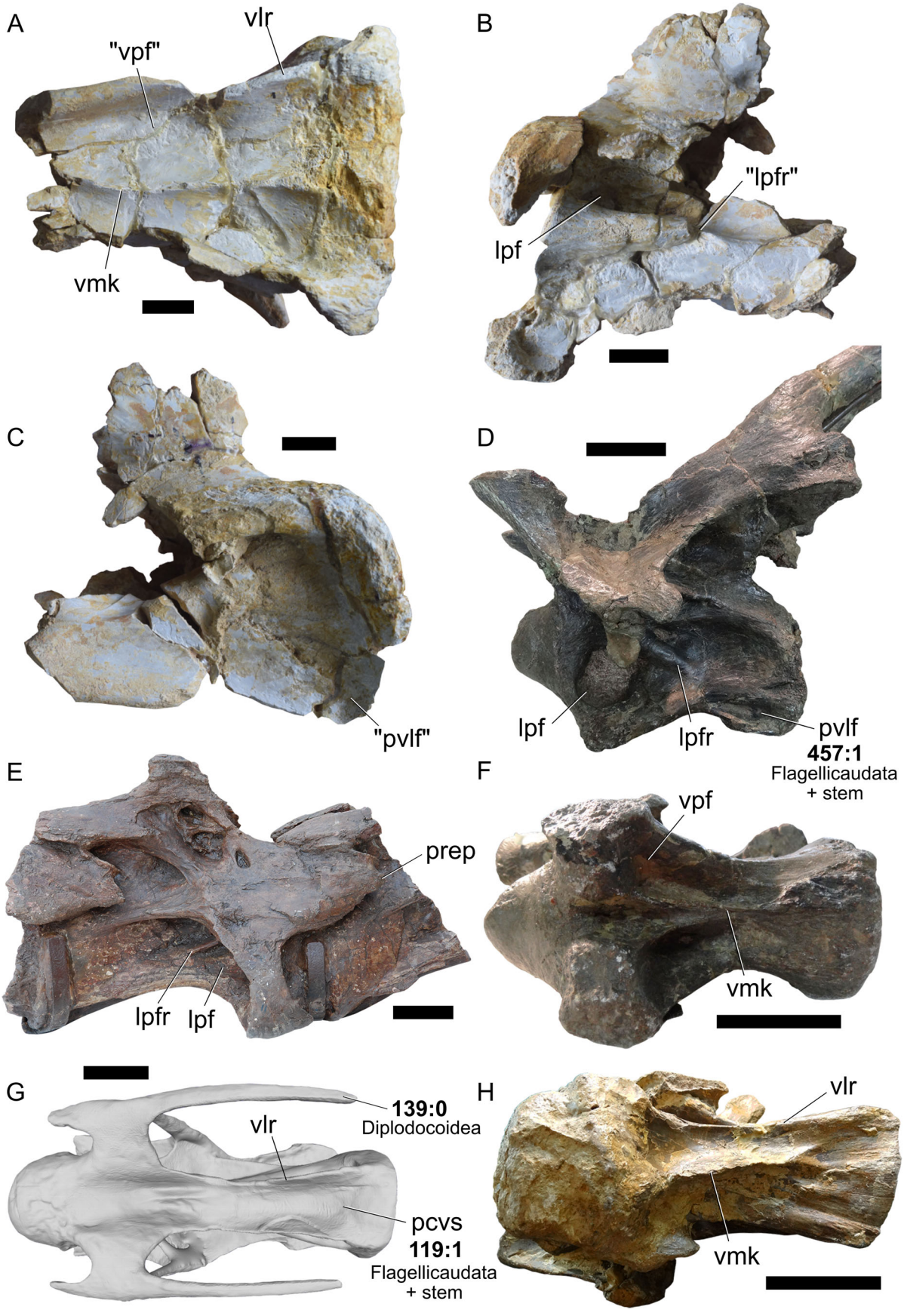
A
vlr
"vpf"
vmk
B
"lpfr"
lpf
C
"pvlf"
D
lpf
lpfr
pvlf
457:1
Flagellicaudata
+ stem
E
prep
lpfr
lpf
F
vpf
vmk
G
139:0
Diplodocoidea
vlr
pcvs
119:1
Flagellicaudata
+ stem
H
vlr
vmk

The presence of a divided lateral fossa on the cervical centrum (RWR-241-B) of *Tharosaurus* (Fig. 1B) was considered a flagellicaudatan synapomorphy by Bajpai et al. (2023); however, this morphology is more widespread amongst eusauropods, including taxa such as *Jobaria*, *Klamelisaurus* (Fig. 1E), and *Omeisaurus*, as well as other diplodocoids (Mannion, Upchurch, Schwarz, et al., 2019; McIntosh, 1990; Moore et al., 2020; Upchurch, 1998). Furthermore, there is no evidence of a dividing ridge in *Tharosaurus*, only a partially sheared and displaced portion of the centrum (Fig. 1B).

Bajpai et al. (2023) described a posteroventral fossa on the lateral surface of the centrum in RWR-241-B (Fig. 1C), which they noted also characterizes some flagellicaudatans (Fig. 1D). However, this feature is not restricted to flagellicaudatans, with a posteroventral fossa also present in *Omeisaurus* (Tan et al., 2019). Furthermore, it is distinct fossa in flagellicaudatans (Fig. 1D) and *Omeisaurus*, with a clear break of slope from the remainder of the lateral surface (Tschopp & Mateus, 2013; Whitlock, 2011a, 2011b). By contrast, in *Tharosaurus*, the relevant region of RWR-241-B lacks a distinct fossa (Fig. 1B, C). Some cervical centra of *Bagualia* are also characterized by a shallow posteroventral depression in this region (Gomez et al., 2021). Furthermore, the cervical vertebra (RWR-241-B) of *Tharosaurus* has clearly been broken and reassembled in this region (Fig. 1C), casting doubt as to whether any concavity is a genuine feature.

Bajpai et al. (2023) regarded the presence of triangular facets on the ventrolateral margins of the posterior cotyle (Fig. 2A) of RWR-241-B as an autapomorphy of *Tharosaurus*. However, we interpret these merely as the aforementioned ventrolateral ridges that appear accentuated in posterior view as a result of the incomplete margins of the cotyle (Fig. 2A).

The centroprezygapophyseal lamina (CPRL) was described as bifid in the cervical vertebra (RWR-241-C) of *Tharosaurus* (Bajpai et al., 2023), with the medial branch meeting the interprezygapophyseal lamina (TPRL) (Fig. 2B). This was regarded as a dicraeosaurid synapomorphy by Whitlock and Wilson Mantilla (2020). However, the latter authors used a restricted dataset, including only five non-diplodocoid taxa, and thus it can only be optimized therein as a feature distinguishing dicraeosaurids from other diplodocoids. As demonstrated in its original formulation as a character state by Carballido et al. (2012), this morphology is more widespread amongst eusauropods, including taxa such as *Bellusaurus* (Fig 2C), *Cetiosaurus*, *Omeisaurus*, and several macronarians (Tschopp et al., 2015). We also note that the 'medial CPRLs' in the case of dicraeosaurids and taxa such as *Bellusaurus* (Fig. 2C) are better considered as the lateral margins of the anterior neural canal opening that become pronounced as a result of the accentuated depth of the centroprezygapophyseal fossa (CPRF), rather than representing distinct laminae. This interpretation is supported by the presence of these struts of bone on either side of the anterior neural canal opening even in some diplodocids that are also characterized by a 'true' bifurcation of the CPRL (e.g. *Apatosaurus louisae*; Gilmore, 1936, pl. 21), i.e. one in which both the medial and lateral branches meet the prezygapophysis (Whitlock, 2011b).

The prezygapophyseal articular surfaces in RWR-241-C were described as transversely convex, although this is difficult to confirm from the figures in Bajpai et al. (2023) (Fig. 2B). A similar morphology, as described, is present in the cervical vertebrae of some diplodocines and *Kaatedocus* (Tschopp & Mateus, 2013; Upchurch, 1995), as noted by Bajpai et al. (2023); nevertheless, it also characterizes some mamenchisaurids (Fig. 2E) (Moore et al., 2020; Upchurch et al., 2021; Zhang et al., 2020), indicating a more widespread distribution for transversely convex prezygapophyseal articular surfaces (see also Whitlock, 2011b). The presence of pre-epipophyses in RWR-241-C was also regarded as a feature that *Tharosaurus* shares with flagellicaudatans (Bajpai et al., 2023), but these processes have a much more widespread distribution among eusauropods, including taxa such as *Bagualia*, *Jobaria*, *Haplocanthosaurus priscus*, *Klamelisaurus* and *Turiasaurus* (Fig. 1E) (Gomez et al., 2021; Mannion et al., 2013; Mannion, Upchurch, Schwarz, et al., 2019; Moore et al., 2020; Whitlock, 2011b; Wilson & Upchurch, 2009). Furthermore, they are absent in nearly all dicraeosaurids for which this feature can be assessed

Figure 1. Photographs showing comparisons of cervical vertebral anatomical features described in *Tharosaurus* with other eusauropods. Cervical vertebra of *Tharosaurus*: **A,** ventral (anterior towards the left); **B,** right lateral; and **C,** left lateral views. **D,** Cervical vertebra 4 of *Amargasaurus* (MACN PV N15) in left lateral view (neural spine partly cropped). **E,** Cervical vertebrae 11 and 12 of *Klamelisaurus* (IVPP V9492) in right lateral view. **F,** Cervical vertebra 3 of *Amargasaurus* (MACN PV N15) in ventral view. **G,** Cervical vertebra 10 of *Diplodocus carnegii* (CM 84) in ventral view. **H,** Middle–posterior cervical vertebra of *Patagosaurus* (MACN-CH 936) in ventral view. Selected diplodocoid synapomorphies are highlighted, consisting of the presence of a posteroventral lateral fossa on the centrum (457:1), a posteriorly concave ventral surface (119:1) and short cervical ribs (139:0). **Abbreviations: lpf**, lateral pneumatic foramen; **lpfr**, lateral pneumatic foramen ridge; **pcvs**, posteriorly concave ventral surface; **prep**, pre-epipophysis; **pvlf**, posteroventral lateral fossa; **vlr**, ventrolateral ridge; **vmk**, ventral midline keel; **vpf**, ventral paramedian fossa. Putative diplodocoid features of *Tharosaurus*, reinterpreted in the main text, are placed in quotation marks. Scale bar equals 50 mm in A–D and F, and 100 mm in E, G and H. Image credits: A–C, Debajit Datta and Bajpai Sunil; G, Matt Lamanna/Carnegie Museum of Natural History.

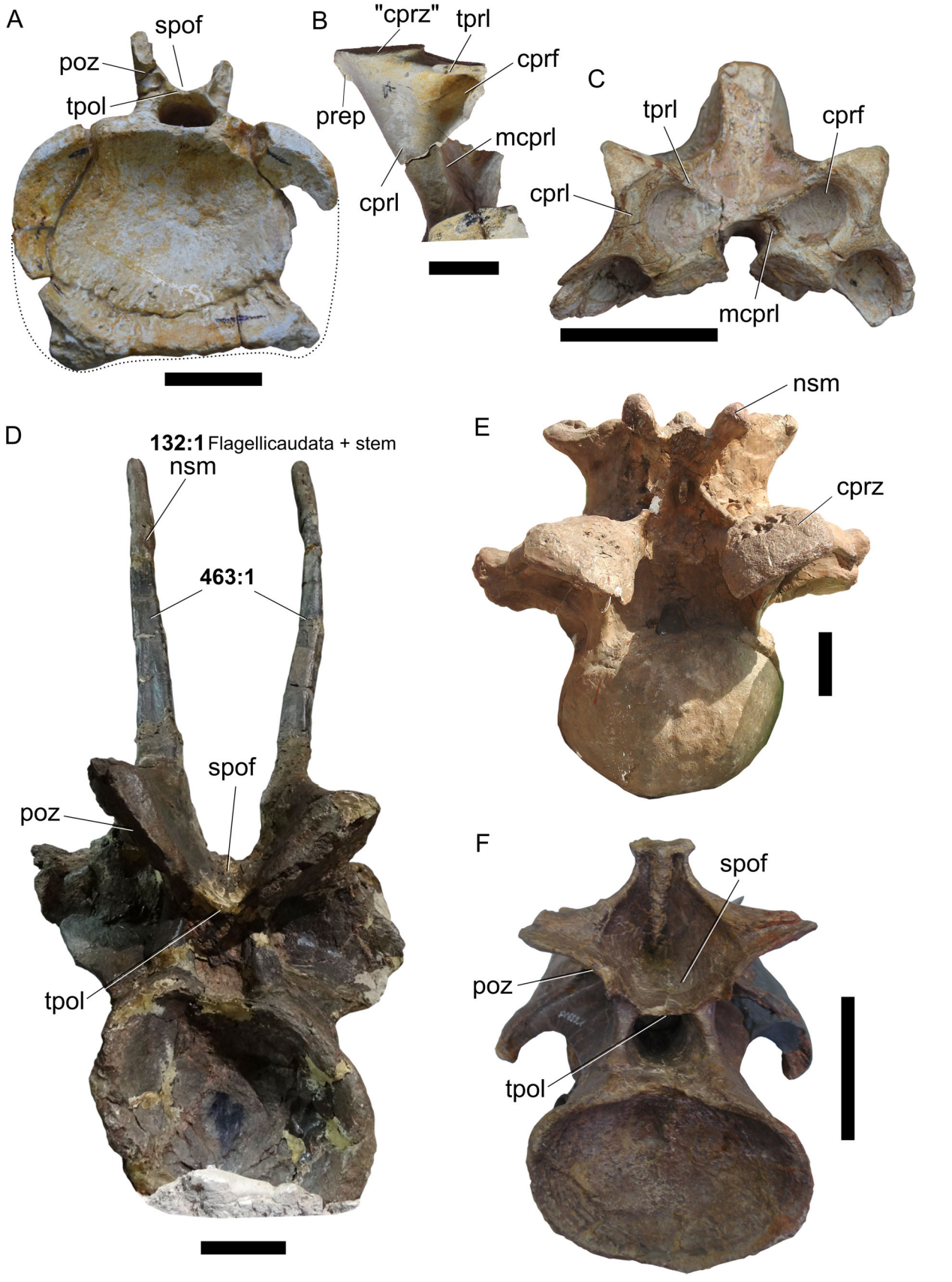
A
spof
poz
tpol
B
"cprz"
tprl
cprf
prep
mcprl
cprl
C
tprl
cprf
cprl
mcprl
D
132:1 Flagellicaudata + stem
nsm
463:1
spof
poz
tpol
E
nsm
cprz
F
spof
poz
tpol

(Fig. 1D) (Mannion, Upchurch, Schwarz, et al., 2019), with the exception of *Suuwassea* (ANS 21122: AJM pers. obs.) and the putative member *Kaatedocus* (Tschopp & Mateus, 2013; though see below regarding its affinities).

Despite only preserving the lowermost portion of the neural arch (Fig. 2A), Bajpai et al. (2023) interpreted the cervical neural spine of RWR-241-B as bifid, with this bifurcation extending down to the roof of the neural canal, which they regarded as the interpostzygapophyseal lamina (TPOL). They also stated that this same extreme bifid morphology characterizes the dicraeosaurids *Amargasaurus* and *Pilmatueia*, although in those two taxa there is clearly a dorsoventral separation between the roof of the neural canal and the TPOL (e.g. Coria et al., 2019, fig. 5; Fig. 2D). Part of their reasoning for interpreting the cervical neural spine of *Tharosaurus* as bifid is that the surface dorsal to the neural canal/TPOL is finished bone, which Bajpai et al. (2023) therefore regarded as the region in between paired metapophyses. However, an alternative explanation is that this region is the spinopostzygapophyseal (=postspinal) fossa (Fig. 2A), which is often an extensive, anteroposteriorly deep opening in cervical vertebrae, forming a shelf-like platform (Fig. 2F). Under this scenario, the otherwise highly unusual 'metapophyses' in RWR-241-B are herein reinterpreted as the bases of the postzygapophyses or the bone immediately ventral to these processes (Fig. 2A, D, F). Finally, we note that bifid cervical neural spines are present in several eusauropod lineages, with members of Mamenchisauridae (Fig. 1E), Turiasauria and Macronaria, in addition to Flagellicaudata (Fig. 1D), characterized by this morphology (e.g. McIntosh, 1990; Royo-Torres et al., 2006; Upchurch, 1995; Wilson & Sereno, 1998).

Dorsal vertebral features

Bajpai et al. (2023) stated that the orientation of the lateral margins of the incomplete dorsal neural spine (RWR-241-G) of *Tharosaurus* (Fig. 3A) indicate that it would have expanded dorsally, comparable to the morphology exhibited by dicraeosaurids (Fig. 3E) (Calvo & Salgado, 1995; Upchurch, 1998). However, the lateral margins are subparallel, with a subtle degree of convergence, and thus there is no evidence to suggest that they might have flared dorsally.

The presence of a smooth and narrow prespinal lamina (Fig. 3A) on the element interpreted as an anterior dorsal neural spine (RWR-241-G) was described as an autapomorphy of *Tharosaurus* by Bajpai et al. (2023). This lamina is primarily known only in the presacral vertebrae of neosauropods (Fig. 3E) (D'Emic, 2012; Mannion et al., 2013; Salgado et al., 1997), although it is also present in the anterior dorsal vertebrae of *Tendaguria* (Mannion, Upchurch, Schwarz, et al., 2019). Unlike the dorsally restricted lamina in *Tharosaurus* (Fig. 3A), this lamina extends along the ventral portion of the neural spine in all diplodocoids in which it is present (Fig. 3E) (Mannion, Upchurch, Schwarz, et al., 2019). Furthermore, we are uncertain that the identification of RWR-241-G (Fig. 3A) as a dorsal neural spine is correct, and it could conceivably represent a partial diapophysis instead.

Caudal vertebral features

The anterior caudal centrum of *Tharosaurus* (RWR-241-J; Fig. 3B) was described as heart-shaped by Bajpai et al. (2023), similar to the morphology in some flagellicaudatans, such as *Apatosaurus* and *Suuwassea* (Fig. 3F) (e.g. Harris, 2006a). However, the centrum of RWR-241-J has clearly undergone some compression and breakage, with much of the lateral surface not preserved; furthermore, even as preserved, it lacks any discernible heart-shape (Fig. 3B). Bajpai et al. (2023, fig. 5c) also stated that a ventral keel is present, but no such feature is apparent in their figure.

A lateral foramen is present on one side of the anterior caudal centrum (RWR-241-J) of *Tharosaurus* (Fig. 3C). Bajpai et al. (2023) listed this as an autapomorphy and compared it with the lateral pneumatic foramen that primarily characterizes the anterior caudal centra of diplodocids (Fig. 3G) (McIntosh, 1990; Upchurch, 1995), as well as some rebbachisaurids (Carballido et al., 2012; Mannion et al., 2011; Mannion & Barrett, 2013).

Figure 2. Photographs showing comparisons of cervical vertebral anatomical features described in *Tharosaurus* with other eusauropods. **A,** Cervical centrum and base of neural arch of *Tharosaurus* in posterior view (dotted line represents an estimated outline). **B,** Cervical prezygapophysis of *Tharosaurus* in anteromedial view. **C,** Posterior cervical neural arch of *Bellusaurus* (IVPP V17768) in anterior view. **D,** Cervical vertebra 12 of *Amargasaurus* (MACN PV N15) in posterior view. **E,** Posterior cervical vertebra of *Hudiesaurus* (IVPP V11120) in anterior/anterodorsal view. **F,** Cervical vertebra of *Europasaurus* (DFMMh/FV 652) in posterior/posterodorsal view. The flagellicaudatan + stem taxa synapomorphy of bifurcated neural spines in postaxial cervical and anterior dorsal vertebrae (132:1) is highlighted. **Abbreviations: cprf**, centroprezygapophyseal fossa; **cprl**, centroprezygapophyseal lamina; **cprz**, convex prezygapophysis; **mcprl**, medial centroprezygapophyseal lamina; **nsm**, neural spine metapophysis; **prep**, pre-epipophysis; **poz**, postzygapophysis; **spof**, spinopostzygapophyseal fossa; **tpol**, interpostzygapophyseal lamina; **tprl**, interprezygapophyseal lamina. Putative diplodocoid features of *Tharosaurus*, reinterpreted in the main text, are placed in quotation marks. Scale bar equals 100 mm in A and E, and 50 mm in B–D and F. Image credits: A and B, Debajit Datta and Bajpai Suni.

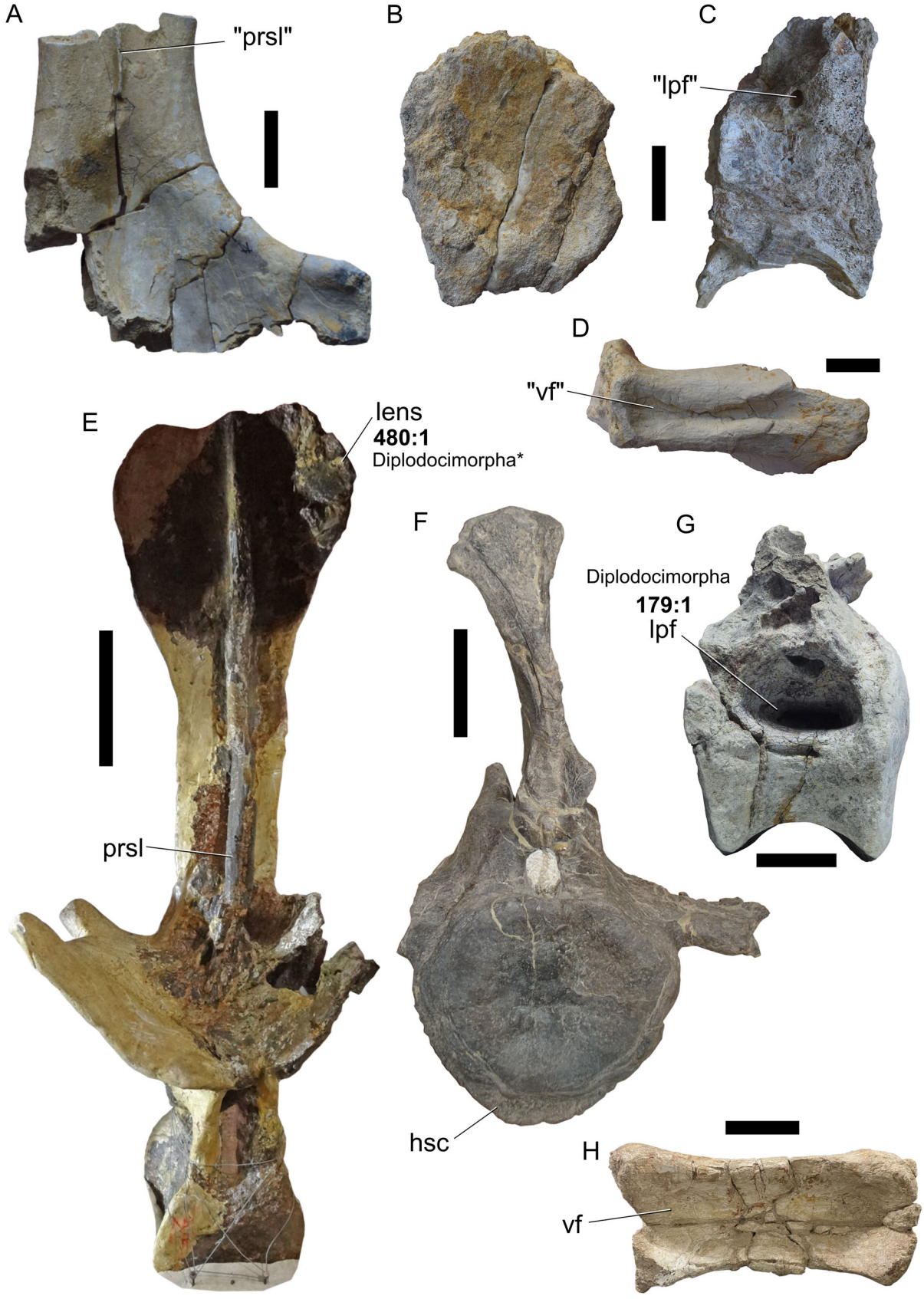
A
"prsl"
B
C
"lpf"
D
"vf"
E
lens
480:1
Diplodocimorpha*
prsl
F
hsc
G
Diplodocimorpha
179:1
lpf
H
vf

However, the foramina in diplodocids are connected to camerae within the centrum (Schwarz et al., 2007; Wedel, 2003; Wedel & Taylor, 2013), whereas there is no clear evidence that this is the case in RWR-241-J. There are also similar foramina on the ventral surface of the centrum. Given these observations, and that it is only present on one side, we suggest that it might not be comparable to the lateral pneumatic foramen that primarily characterizes diplodocids. Based on its size and the absence of internal ramification, we propose that it might instead represent an asymmetrically developed nutrient foramen.

A middle caudal centrum (RWR-241-K) was described as quadrangular, which was regarded as a diplodocoid synapomorphy by Bajpai et al. (2023); however, the margins of this centrum are incomplete and it has clearly undergone severe transverse crushing, making it impossible to discern its true shape. RWR-241-K was also described as being characterized by a ventral fossa (Fig. 3D), such as that present in diplodocines (Fig. 3H) (McIntosh, 1990; Upchurch, 1995), but the concavity is most likely a product of the aforementioned crushing, as exemplified by its inconsistent width and depth, as well as several areas of broken and sheared bone (Fig. 3D).

Phylogenetic dataset and analyses

Reassessment of the placement of *Tharosaurus*

Bajpai et al. (2023) incorporated *Tharosaurus* into an expanded version of the phylogenetic data matrix published by Gallina et al. (2019), comprising 76 operational taxonomic units (OTUs), including 21 unequivocal diplodocoids, scored for 393 characters. Following our reinterpretation of numerous anatomical features, we rescored *Tharosaurus* for this matrix. We focused on instances in which a character was clearly incorrectly scored and those for which the presence of the feature was equivocal or could not be assessed (e.g. because of incompleteness). In total, we made 23 score changes (documented in Supplemental material), with 21 of these representing scores revised to a '?'. Using the same protocol applied by Bajpai et al. (2023), including ordering 25 characters (see Gallina et al., 2019), we then re-ran the phylogenetic analysis in TNT v.1.6 (Goloboff & Morales, 2023). The revised nexus and TNT files are presented in Supplemental material.

Main phylogenetic data matrix

To produce a revised view of diplodocoid evolutionary relationships, we utilized the phylogenetic data matrix of Poropat et al. (2023), which is the most recent iteration of the matrix presented by Mannion, Upchurch, Schwarz, et al. (2019). It is currently the largest data matrix in terms of character and taxon sampling for eusauropods (556 characters scored for 126 OTUs), including 27 unequivocal diplodocoid OTUs. Based on personal observations of specimens, we substantially revised scores for seven OTUs already included in this data matrix (see Supplemental material). This included three OTUs that have been previously recovered as a diplodocoid in at least some analyses: *Cetiosauriscus stewarti* (NHMUK R3078; PDM & AJM), *Suuwassea emiliae* (ANS 21122; AJM), and the 'El Chocon rebbachisaurid' (MMCH-Pv-49; PDM). The other four revised OTUs had been previously scored in parallel, independently, by Mannion, Upchurch, Schwarz, et al. (2019) and Moore et al. (2020): we reconciled scoring differences herein for *Bellusaurus sui*, *Jobaria tiguidensis*, *Losillasaurus giganteus*, and *Turiasaurus riodevensis*, all of which have been typically recovered as non-neosauropod eusauropods. We also made a number of score revisions to additional existing OTUs (see Supplemental material).

We incorporated *Tharosaurus* based on our reinterpretation of its anatomy, alongside 12 newly added diplodocoid OTUs, comprising: (1) *Amargatitanis macni*, scored based on Gallina (2016) and personal observations of MACN PV N53 (PDM); (2) *Astigmasaura genuflexa*, scored based on information presented in Bellardini et al. (2024), primarily on the hind limb (note that additional anatomical data on this species, presented in Bellardini et al. [2025], was published after the current work was finalized); (3)

Figure 3. Photographs showing comparisons of dorsal and caudal vertebral anatomical features described in *Tharosaurus* with diplodocoids. **A,** Putative dorsal neural spine of *Tharosaurus* in anterior view. Anterior caudal vertebra of *Tharosaurus* in **B,** anterior and **C,** right lateral views. **D,** Middle caudal centrum of *Tharosaurus* in ventral view. **E,** Dorsal vertebra 9 of *Amargasaurus* (MACN PV N15) in anterior/anterodorsal view. **F,** Anterior caudal vertebra of *Brontosaurus yahnahpin* (TATE-001) in posterior view. **G,** Anterior caudal centrum of *Tornieria* (MfN MB.R. 2957) in left lateral view. **H,** Middle caudal centrum of *Tornieria* (MfN MB.R. 2913) in ventral view. Two synapomorphies of Diplodocimorpha are highlighted, consisting of petal-shaped middle–posterior dorsal neural spines (480:1) and the presence of a sharp-lipped lateral pneumatic foramen in anterior caudal centra (179:1). Unique and exclusive synapomorphies are denoted with an asterisk. **Abbreviations: hsc**, heart-shaped centrum; **lens**, laterally expanded neural spine; **lpf**, lateral pneumatic foramen; **prsl**, prespinal lamina; **vf**, ventral fossa. Putative diplodocoid features of *Tharosaurus*, reinterpreted in the main text, are placed in quotation marks. Scale bar equals 50 mm in A–D, G and H, and 100 mm in E and F. Image credits: A–D, Debajit Datta and Bajpai Sunil.

Table 1. Diplodocoid taxa and specimens included as operational taxonomic units (OTUs) in the phylogenetic analysis, including information on geological age, stratigraphical and geographical provenance, and the basis for scoring of characters. Taxa highlighted with an asterisk are newly incorporated to this data matrix in this study, whereas all other OTUs were already included in Mannion, Upchurch, Schwarz, et al. (2019).

Taxon/OTU	Geological age, stratigraphical + geographical provenance	Basis for scoring in phylogenetic analysis
Haplocanthosaurus delfsi	Kimmeridgian (Late Jurassic), Morrison Formation, USA	McIntosh and Williams (1988); CMNH 10380 (PDM pers. obs.)
Haplocanthosaurus priscus	Kimmeridgian–Tithonian (Late Jurassic), Morrison Formation, USA	Hatcher (1903); CM 572 and CM 879 (PDM pers. obs.)
Amphicoelias altus	Early Tithonian (Late Jurassic), Morrison Formation, USA	Osborn and Mook (1921); Mannion et al. (2021); AMNH FARB 5764 (PDM pers. obs.)
Cetiosauriscus stewarti	Callovian (Middle Jurassic), Oxford Clay Formation, UK	NHMUK R3078 (PDM & AJM pers. obs.)
Lingwulong shenqi	Aalenian or Bathonian–Callovian (Middle Jurassic), Yanan or Zhiluo Formation, China	Xu et al. (2018); LM V001a, LGP V001–006 and IVPP V23704 (PDM pers. obs.)
*Smitanosaurus agilis**	Kimmeridgian (Late Jurassic), Morrison Formation, USA	Whitlock and Wilson Mantilla (2020); USNM 5384 (AJM pers. obs.)
Suuwassea emilieae	Late Kimmeridgian (Late Jurassic), Morrison Formation, USA	Harris and Dodson (2004); Harris (2006a, 2006b, 2006c, 2007), Whitlock and Harris (2010); ANS 21122 (AJM pers. obs.)
*BYU 17096**	Kimmeridgian–Tithonian (Late Jurassic), Morrison Formation, USA	Balanoff et al. (2010); BYU 17096 (AJM pers. obs.)
Amargasaurus cazaui	Barremian (Early Cretaceous), La Amarga Formation, Argentina	Salgado and Bonaparte (1991); Salgado and Calvo (1992); Paulina Carabajal et al. (2014); MACN PV N15 (PDM pers. obs.)
*Bajadasaurus pronuspinax**	Late Berriasian–Valanginian (Early Cretaceous), Bajada Colorada Formation, Argentina	Gallina et al. (2019); Garderes et al. (2024)
Brachytrachelopan mesai	Kimmeridgian – early Tithonian (Late Jurassic), Cañadón Calcáreo Formation, Argentina	Rauhut et al. (2005); MPEF PV 1716 (PDM pers. obs.)
Dicraeosaurus spp.	Late Kimmeridgian–Tithonian (Late Jurassic), Tendaguru Formation, Tanzania	Janensch (1929b, 1935–1936, 1961); Schwarz-Wings and Böhm (2014); MfN MB.R. specimens (PDM & AJM pers. obs.)
*Pilmatueia faundezi**	Valanginian (Early Cretaceous), Mulichinco Formation, Argentina	Coria et al. (2019); Windholz et al. (2020, 2022)
*Kaatedocus siberi**	Kimmeridgian (Late Jurassic), Morrison Formation, USA	Tschopp and Mateus (2013); AMNH FARB 7530 (AJM pers. obs.)
Apatosaurus spp.	Kimmeridgian–Tithonian (Late Jurassic), Morrison Formation, USA	Gilmore (1936); Ostrom and McIntosh (1966); Berman and McIntosh (1978); Upchurch, Tomida, et al. (2004); Whitlock (2011a); Tschopp et al. (2015); CM & YPM specimens and UWGM 15556 (PDM & AJM pers. obs.)
Dinheirosaurus lourinhanensis	Late Kimmeridgian–early Tithonian (Late Jurassic), Lourinhã Formation, Portugal	Bonaparte and Mateus (1999); Mannion et al. (2012); ML 414 (PDM pers. obs.)
Supersaurus vivianae	Kimmeridgian–Tithonian (Late Jurassic), Morrison Formation, USA	Jensen (1985); Curtice and Stadtman (2001); Lovelace et al. (2008); WDC DMJ-021 (PDM pers. obs.)
Diplodocus spp.	Kimmeridgian–Tithonian (Late Jurassic), Morrison Formation, USA	Hatcher (1901); Holland (1906, 1910, 1924); Mook (1917); McIntosh and Berman (1975); Whitlock (2011a); Tschopp et al. (2015); CM specimens (PDM & AJM pers. obs.)
Leinkupal laticauda	Late Berriasian–Valanginian (Early Cretaceous), Bajada Colorada Formation, Argentina	Gallina et al. (2014)
Tornieria africana	Tithonian (Late Jurassic), Tendaguru Formation, Tanzania	Janensch (1935–1936); Remes (2006, 2007, 2009); MfN MB.R. and SMNS specimens (PDM & AJM pers. obs.)
*Amargatitanis macni**	Barremian (Early Cretaceous), La Amarga Formation, Argentina	Gallina (2016); MACN PV N53 (PDM pers. obs.)
Amazonsaurus maranhensis	Aptian–Albian (Early Cretaceous), Itapecuru Formation, Brazil	Carvalho et al. (2003); MN 4555–4564 and UFRJ-DG 58 (PDM pers. obs.)

(*Continued*)

Table 1. (*Continued*).

Taxon/OTU	Geological age, stratigraphical + geographical provenance	Basis for scoring in phylogenetic analysis
*Astigmasaura genuflexa**	Late Cenomanian–Turonian (Late Cretaceous), Huincul Formation, Argentina	Bellardini et al. (2024)
Comahuesaurus windhauseni	Late Aptian–early Albian (Early Cretaceous), Lohan Cura Formation, Argentina	Salgado et al. (2004); Carballido et al. (2012); MOZ-PV specimens (PDM pers. obs.)
*Campananeyen fragilissimus**	Cenomanian (Late Cretaceous), Candeleros Formation, Argentina	Paulina Carabajal et al. (2016); Lerzo, Gallina, et al. (2025)
*Lavocatisaurus agrioensis**	Aptian–early Albian (Early Cretaceous), Rayoso Formation, Argentina	Salgado et al. (2012); Canudo et al. (2018)
*Sidersaura marae**	Late Cenomanian–Turonian (Late Cretaceous), Huincul Formation, Argentina	Lerzo, Torcida Fernández-Baldor, et al., (2025)
Histriasaurus boscarollii	Late Hauterivian–early Barremian (Early Cretaceous), Unnamed unit, Croatia	Dalla Vecchia (1998, 1999, 2005)
*Xenoposeidon proneneukos**	Late Berriasian–early Valanginian (Early Cretaceous), Ashdown Formation, UK	Taylor (2018); NHMUK R2095 (PDM pers. obs.)
Rayososaurus agrioensis	Cenomanian (Late Cretaceous), Candeleros Formation, Argentina	Carballido et al. (2010); MACN PV N41 (PDM pers. obs.)
Katepensaurus goicoecheai	Late Cenomanian–Turonian (Late Cretaceous), Bajo Barreal Formation, Argentina	Ibiricu et al. (2013, 2015); UNPSJB-PV 1007 (PDM pers. obs.)
Zapalasaurus bonapartei	Late Barremian–early Aptian (Early Cretaceous), La Amarga Formation, Argentina	Salgado et al. (2006); MOZ-PV specimens (PDM pers. obs.)
Cathartesaura anaerobica	Late Cenomanian–Turonian (Late Cretaceous), Huincul Formation, Argentina	Gallina and Apesteguía (2005); MPCA 232 (PDM pers. obs.)
Limaysaurus tessonei	Cenomanian (Late Cretaceous), Candeleros Formation, Argentina	Calvo and Salgado (1995); Paulina Carabajal and Calvo (2021); MUCPv specimens (PDM pers. obs.)
Nopcsaspondylus alarconensis	Cenomanian (Late Cretaceous), Candeleros Formation, Argentina	Nopcsa (1902)
MMCH-Pv-49 ('El Chocon rebbachisaurid')	Late Cenomanian–Turonian (Late Cretaceous), Huincul Formation, Argentina	Apesteguía et al. (2010); Haluza et al. (2012); MMCH-Pv-49 (PDM pers. obs.)
*Itapeuasaurus cajapioensis**	Cenomanian (Late Cretaceous), Alcântara Formation, Brazil	Lindoso et al. (2019)
Nigersaurus taqueti	Aptian–Albian (Early Cretaceous), Elrhaz Formation, Niger	Sereno et al. (1999, 2007); Sereno and Wilson (2005); MNN specimens (PDM & AJM pers. obs.)
Rebbachisaurus garasbae	Cenomanian (Late Cretaceous), Gara Sbaa Formation, Morocco	Wilson and Allain (2015); MNHN MRS 1958 (PDM pers. obs.)
Tataouinea hannibalis	Early Albian (Early Cretaceous), Aïn el Guettar Formation, Tunisia	Fanti et al. (2013, 2015)
Demandasaurus darwini	Late Barremian–early Aptian (Early Cretaceous), Castrillo la Reina Formation, Spain	Pereda Suberbiola et al. (2003); Torcida Fernández-Baldor et al. (2011); Torcida Fernández-Baldor (2012); MDS-RVII (PDM pers. obs.)
MIWG 5384 ('IOW rebbachisaurid')	Barremian (Early Cretaceous), Wessex Formation, UK	Mannion et al. (2011); MIWG 5384 (PDM pers. obs.)

Bajadasaurus pronuspinax, scored based on Gallina et al. (2019) and Garderes et al. (2024); (4) *Campananeyen fragilissimus*, scored based on Paulina Carabajal et al. (2016) and Lerzo, Torcida Fernández-Baldor, et al., (2025); (5) *Itapeuasaurus cajapioensis*, scored based on Lindoso et al. (2019); (6) *Kaatedocus siberi*, scored based on Tschopp and Mateus (2013) and personal observations of AMNH FARB 7530 (AJM); (7) *Lavocatisaurus agrioensis*, scored based on Salgado et al. (2012) and Canudo et al. (2018); (8) *Pilmatueia faundezi*, scored based on Coria et al. (2019) and Windholz et al. (2020, 2022); (9) *Sidersaura marae*,

scored based on Lerzo, Gallina, et al. (2025); (10) *Smitanosaurus agilis*, scored based on Whitlock and Wilson Mantilla (2020) and personal observations of USNM 5384 (AJM); (11) *Xenoposeidon proneneukos*, scored based on Taylor (2018) and personal observations of NHMUK R2095 (PDM); and (12) BYU 17096, a braincase previously referred to *Apatosaurus*, scored based on Balanoff et al. (2010) and personal observations (AJM). Seven characters were also newly included, based on the recent literature (Canudo et al., 2018; Whitlock & Wilson Mantilla, 2020) and our observations, and six existing characters (C150, 207, 271, 327, 336 and 440) were modified (see Supplemental material). Other recently proposed characters (e.g. Lerzo, 2024; Whitlock & Wilson Mantilla, 2020; Windholz et al., 2022) were either already represented in earlier iterations of this data matrix or did not withstand scrutiny. Our revised and expanded data matrix comprises 139 OTUs, including 38 uncontroversial diplodocoids (see Table 1), scored for 563 characters, and is provided as nexus and TNT files, along with the full character list (Supplemental material).

Following the protocol applied in analyses of previous iterations of this data matrix (e.g. Poropat et al., 2023), phylogenetic analyses using maximum parsimony were run in TNT v.1.6 (Goloboff & Morales, 2023). Twenty characters were treated as ordered (11, 14, 15, 27, 40, 51, 104, 122, 147, 148, 195, 205, 259, 286, 297, 426, 435, 472, 510, and 557) and eight non-diplodocoid taxa identified as unstable in previous analyses were excluded *a priori* (i.e. *Astrophocaudia slaughteri*, *Australodocus bohetii*, *Brontomerus mcintoshi*, *Fukuititan nipponensis*, *Fusuisaurus zhaoi*, *Liubangosaurus hei*, *Malarguesaurus florenciae* and *Mongolosaurus haplodon*). Following preliminary analyses, we also excluded *Bellusaurus sui*. This taxon was recently argued to represent an immature mamenchisaurid (Moore et al., 2023), but the present version of the matrix lacks the character and taxon sampling necessary to adequately test this hypothesis. *Bellusaurus* was therefore omitted from the analyses, pending incorporation of a broader sample of Middle–Late Jurassic East Asian sauropods. Two further unstable non-diplodocoid taxa were excluded *a priori* from analyses applying equal character weighting (the 'Cloverly titanosauriform' and *Ruyangosaurus giganteus*). We initially ran a 'New Technology Search', using the 'Stabilize Consensus' option, applying sectorial searches, drift, and tree fusing. The resultant trees were then used as the starting topologies for a 'Traditional Search', using tree bisection–reconnection, collecting up to 500,000 most parsimonious trees (MPTs). Three versions of the analysis were run: one with equal character weighting (EQW), and the other two with extended implied weighting (EIW) (Goloboff, 2014). In one of these EIW analyses, we applied a concavity constant (=*k*-value) of 9, in keeping with recent iterations of this matrix (e.g. Poropat et al., 2021, 2023), whereas we applied a *k*-value of 12 for the other EIW analysis, which is the value used in simulations by Goloboff et al. (2018) to demonstrate the superiority of EIW over EQW. Both *k*-values are appropriate for the number of OTUs in our data matrix (Ezcurra, 2024). Unstable OTUs were identified using the *pcrprune* command, and equally parsimonious positions for these labile taxa were visualized using the *nelsen* consensus command.

Phylogenetic results

Reassessed placement of *Tharosaurus indicus*

Our re-analysis of the data matrix published by Bajpai et al. (2023) yields 8 MPTs of length 1186 steps. This is 12 steps fewer than when the analysis is run without any character score changes (1198 steps), although this partly reflects the number of scores changed to missing data. *Tharosaurus* is recovered outside of Neosauropoda, as the sister taxon of the clade comprising Mamenchisauridae + (Turiasauria + (*Jobaria* + Neosauropoda)). Most eusauropod clades have Bremer supports of at least 2, including the neosauropod and diplodocoid nodes. Enforcing our revised *Tharosaurus* OTU to be a diplodocoid results in only two extra steps, wherein it is recovered within Dicraeosauridae.

Diplodocoid relationships

The results of our main phylogenetic analyses, expanding on the data matrix of Poropat et al. (2023), are highly sensitive to the application of EQW versus EIW, and, to a lesser extent, to the value of the concavity constant used in implied weighting (Figs 4–7; Table 2). However, all analyses agree in recovering *Tharosaurus* as a eusauropod of uncertain affinities. In both EIW analyses, *Tharosaurus* is consistently found outside the Turiasauria + Neosauropoda clade, whereas the EQW analysis also permits positions as an early-branching rebbachisaurid, stem flagellicaudatan, or earliest-branching macronarian. In addition, all three analyses agree in recovering a traditional arrangement of diplodocoid taxa, with a speciose Rebbachisauridae that is sister taxon to a lineage of flagellicaudatans (and close relatives) that includes a diverse Diplodocidae and Dicraeosauridae. Other commonalities across analyses include the consistent recovery of *Haplocanthosaurus* spp. outside of Diplodocimorpha and the presence of a nested clade of Gondwanan dicraeosaurid taxa comprising

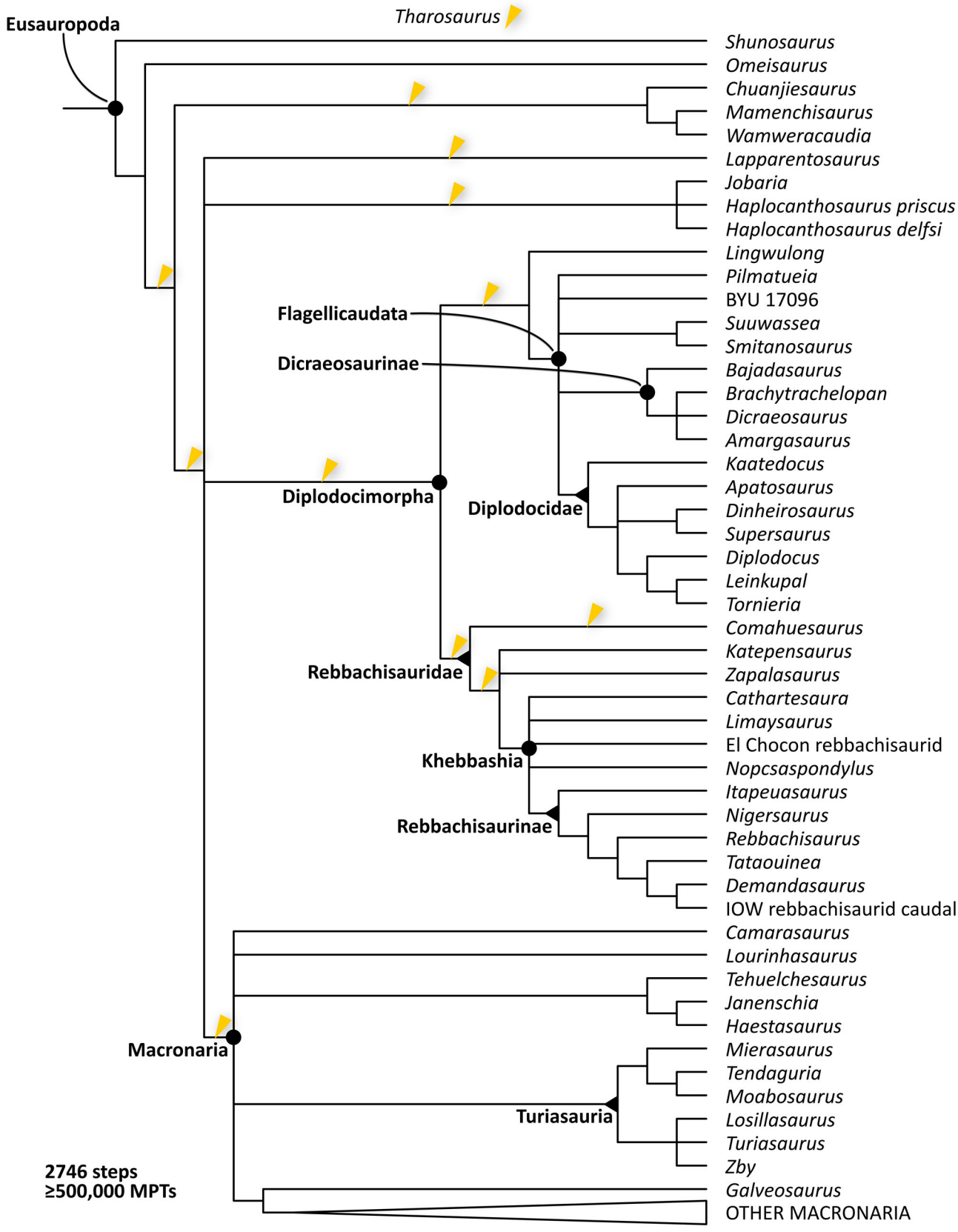

Figure 4. Reduced strict consensus of the equal weights parsimony analysis (EQW) following *a posteriori* pruning of numerous labile OTUs, including: *Tharosaurus*, *Aragosaurus*, *Atlasaurus*, *Cetiosauriscus*, *Amazonsaurus*, *Histriasaurus*, *Rayososaurus*, *Amphicoelias*, *Xenoposeidon*, *Amargatitanis*, *Lavocatisaurus*, *Sidersaura*, *Astigmasaura* and *Campananeyen.* Alternative placements for labile diplodocoids are outlined in Table 2. Note that poor resolution prevents labelling several clades (e.g. Diplodocoidea, Limaysaurinae).

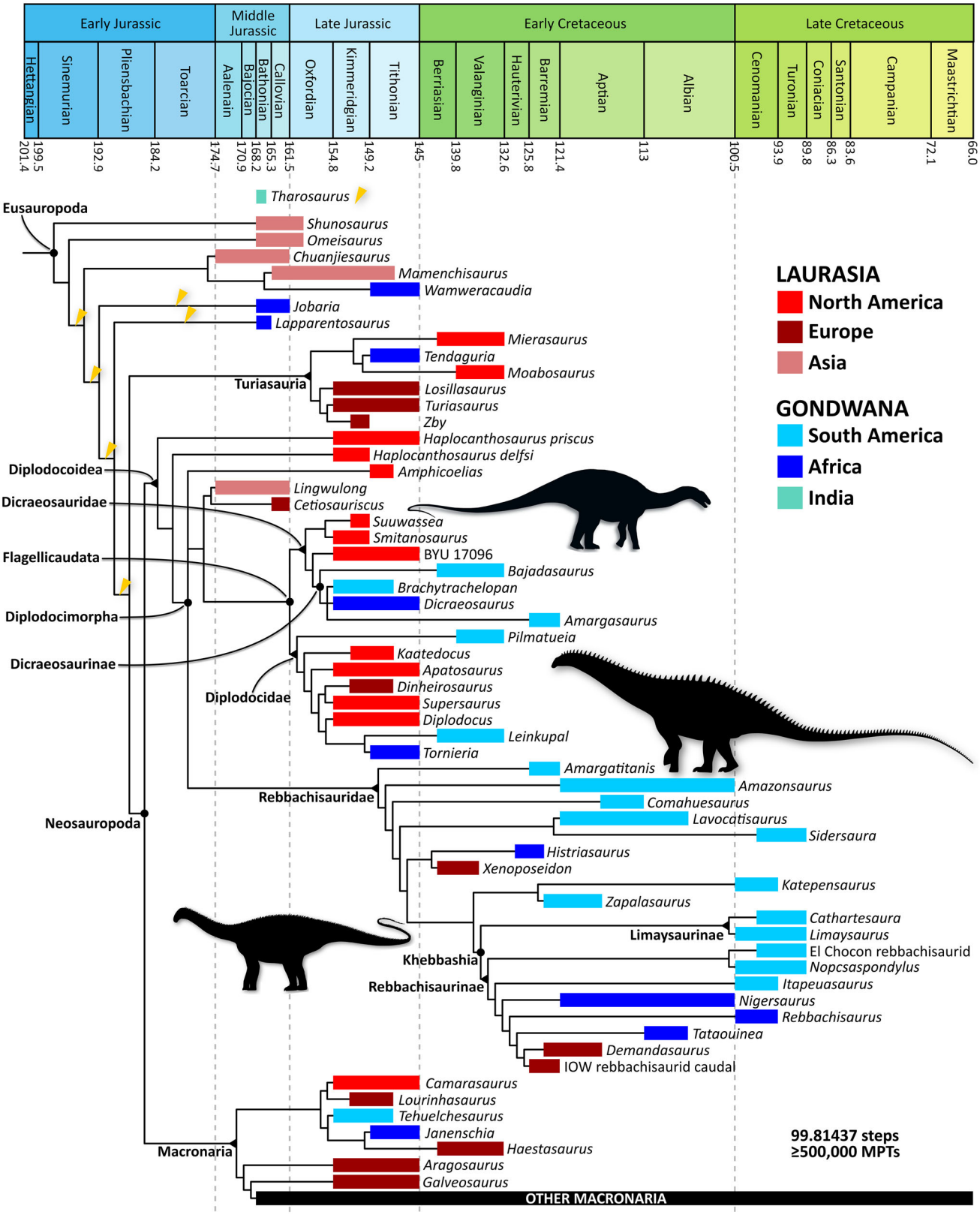

Figure 5. Time-calibrated reduced strict consensus of the extended implied weights analysis with $k = 12$ (EIW12), following *a posteriori* pruning of four labile OTUs: *Tharosaurus* (placements for which are indicated with yellow arrows), *Campananeyen*, *Astigmasaura* and *Rayososaurus* (the latter three are recovered as non-khebbashian rebbachisaurids – see Figure 7 for specific placements).

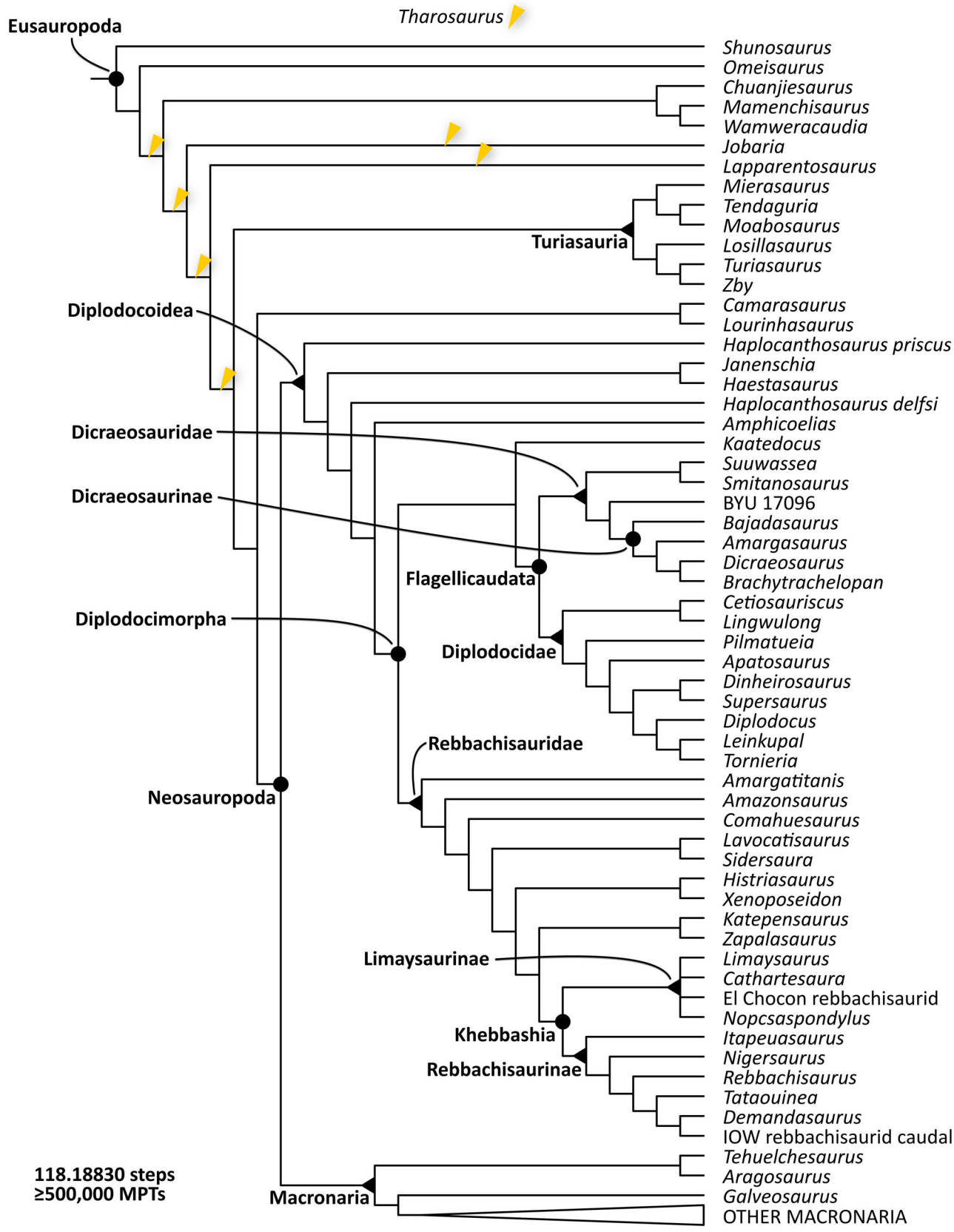

Figure 6. Reduced strict consensus of the extended implied weights analysis with $k = 9$ (EIW9), following *a posteriori* pruning of four labile OTUs: *Tharosaurus* (placements for which are indicated with yellow arrows), *Campananeyen*, *Astigmasaura* and *Rayososaurus* (the latter three are recovered as non-khebbashian rebbachisaurids – see Figure 7 for specific placements).

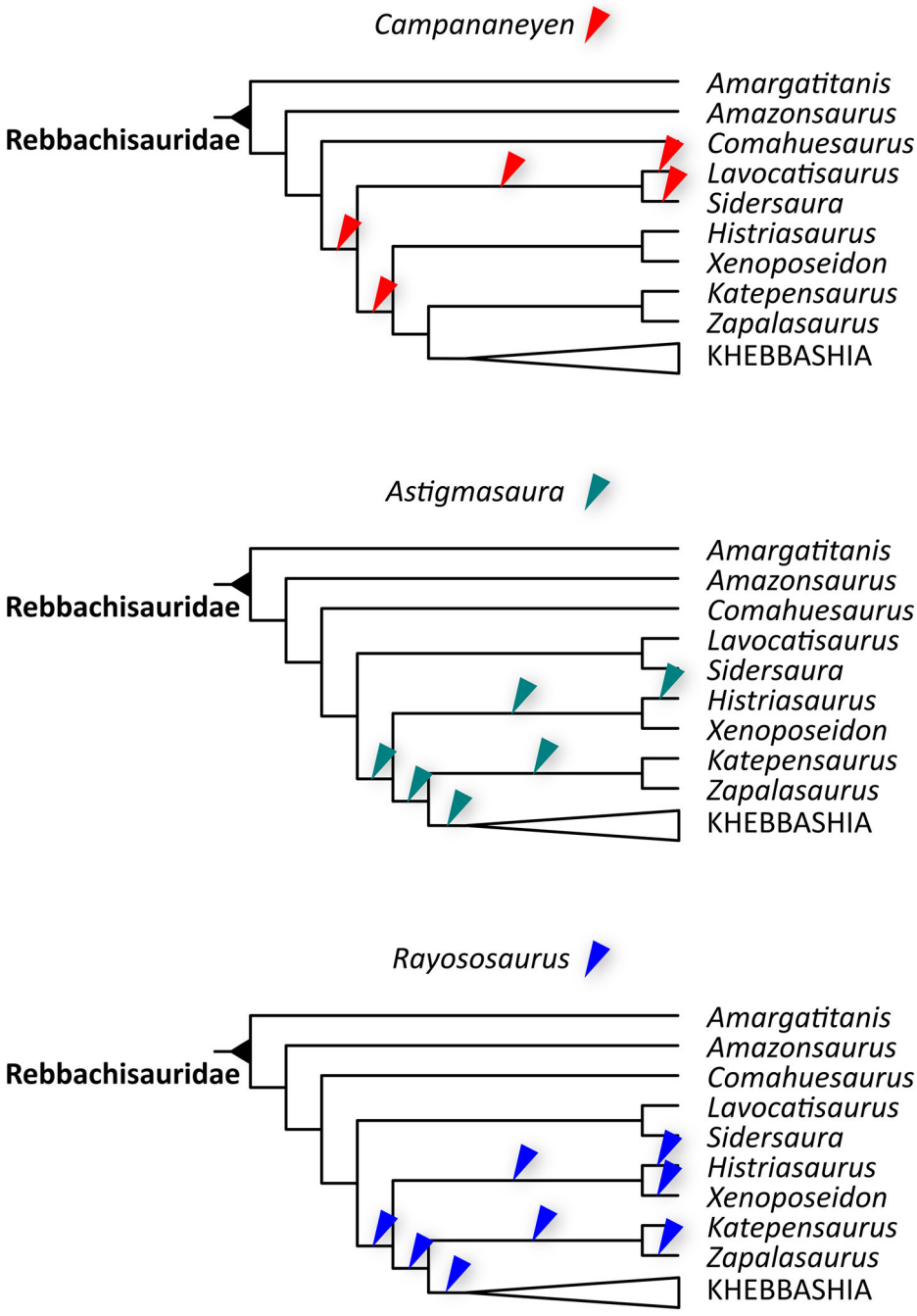

Figure 7. Equally parsimonious placements in both extended implied weights analyses (EIW12, EIW9) of the non-khebbashian rebbachisaurid OTUs, *Campananeyen*, *Astigmasaura* and *Rayososaurus*.

Amargasaurus, *Bajadasaurus*, *Brachytrachelopan* and *Dicraeosaurus*. Given the substantial topological variation characterizing other regions of Diplodocoidea, we summarize additional phylogenetic results based on homoplasy weighting scheme.

Equal weights parsimony. Maximum parsimony analysis under EQW yields ≥500,000 trees of 2746 steps. The strict consensus of this analysis is poorly resolved (Supplemental material), and 14 unstable OTUs, mostly belonging to Rebbachisauridae, were pruned to reveal underlying tree structure (Fig. 4; Table 2). *Lingwulong* and *Cetiosauriscus* are found to be stem flagellicaudatans and *Kaatedocus* is recovered as an early-branching diplodocid, but the specific flagellicaudatan affinities of *Pilmatueia*, *Smitanosaurus*, *Suuwassea* and BYU 17096

Table 2. Summary of phylogenetic results for *Tharosaurus* and various putative diplodocoids whose relationships are sensitive to the method of character weighting. Coloured cells highlight broadly similar results across analyses, reflecting rebbachisaurid (red), stem flagellicaudatan or Flagellicaudata *incertae sedis* (green), diplodocid (yellow), and dicraeosaurid affinities (blue).

OTU	Extended implied weights (k = 12)	Extended implied weights (k = 9)	Equal weights
Tharosaurus	Indeterminate eusauropod earlier branching than Turiasauria + Neosauropoda	Indeterminate eusauropod earlier branching than Turiasauria + Neosauropoda	Non-titanosauriform eusauropod in various positions, including outside Neosauropoda, an early-branching rebbachisaurid, stem flagellicaudatan, and sister to Macronaria
***Haplocanthosaurus* spp.**	Non-diplodocimorph diplodocoids (non-monophyletic)	Non-diplodocimorph diplodocoids (non-monophyletic)	In polytomous clade with *Jobaria* that is sister either to Diplodocimorpha or to *Lapparentosaurus*+ Neosauropoda
Lingwulong	Sister to *Cetiosauriscus* as stem flagellicaudatans	Sister to *Cetiosauriscus* as early-branching diplodocids	Stem flagellicaudatan
Cetiosauriscus	Sister to *Lingwulong* as stem flagellicaudatans	Sister to *Lingwulong* as early-branching diplodocids	Stem flagellicaudatan apical to *Lingwulong*
Amphicoelias altus	Non-diplodocimorph diplodocoid, stem flagellicaudatan, or earliest-branching rebbachisaurid	Non-diplodocimorph diplodocoid	In various positions, including sister *Lapparentosaurus*, sister to *Lapparentosaurus*+ Neosauropoda, sister to Rebbachisauridae, as a stem flagellicaudatan, or within Flagellicaudata
Pilmatueia	Earliest-branching diplodocid	Early-branching diplodocid	Flagellicaudatan of unclear affinity
Kaateodocus	Early-branching diplodocid	Stem flagellicaudatan	Early-branching diplodocid
BYU 17096	Early-branching dicraeosaurid	Early-branching dicraeosaurid	Flagellicaudatan of unclear affinity
Amargatitanis	Earliest-branching rebbachisaurid	Earliest-branching rebbachisaurid	In various positions within Diplodocoidea, including as the earliest rebbachisaurid, a stem flagellicaudatan, a dicraeosaurid, or a diplodocid
Amazonsaurus	Early-branching rebbachisaurid	Early-branching rebbachisaurid	Rebbachisaurid of unclear affinities
Lavocatisaurus	Sister to *Sidersaura* as non-khebbashian rebbachisaurid	Sister to *Sidersaura* as non-khebbashian rebbachisaurid	Various positions within Rebbachisauridae, including as an early-branching rebbachisaurine
Sidersaura	Sister to *Lavocatisaurus* as non-khebbashian rebbachisaurid	Sister to *Lavocatisaurus* as non-khebbashian rebbachisaurid	Several positions within Rebbachisauridae, including as an early-branching rebbachisaurine
Rayososaurus	Non-khebbashian rebbachisaurid apical to (*Sidersaura*+*Lavocatisaurus*)	Non-khebbashian rebbachisaurid apical to (*Sidersaura*+*Lavocatisaurus*)	Rebbachisaurid of unclear affinities
Xenoposeidon	Sister to *Histriasaurus* as non-khebbashian rebbachisaurid	Sister to *Histriasaurus* as non-khebbashian rebbachisaurid	In various positions within Rebbachisauridae and Flagellicaudata, or as sister to *Europasaurus*
Astigmasaura	Non-khebbashian rebbachisaurid apical to (*Sidersaura*+*Lavocatisaurus*)	Non-khebbashian rebbachisaurid apical to (*Sidersaura*+*Lavocatisaurus*)	Several positions with Rebbachisauridae, as well as sister to or within the clade *Padillsaurus* + (*Ligabuesaurus* + *Dongbeititan*)
Campananeyen	Non-khebbashian rebbachisaurid apical to *Comahuesaurus*	Non-khebbashian rebbachisaurid apical to *Comahuesaurus*	Various positions with Rebbachisauridae
Nopcsaspondylus	Rebbachisaurine	Limaysaurine	Nested rebbachisaurid within or closely related to Khebbashia
El Chocon rebbachisaurid	Rebbachisaurine	Limaysaurine	Nested rebbachisaurid within or closely related to Khebbashia

are ambiguous. Other noteworthy results include the placement of Turiasauria within Macronaria and the recovery of *Jobaria* in a clade with *Haplocanthosaurus* spp., which in a subset of MPTs is recovered as a lineage of non-diplodocimorph diplodocoids.

Extended implied weights parsimony. Maximum parsimony analyses using EIW yield ≥500,000 trees of 99.81437 (EIW12) and 118.18830 (EIW9) steps (Figs 5–7). Results of these analyses are much better resolved than those of the EQW analysis and are broadly concordant with one another (Table 2; see Supplemental material for full strict consensus trees). The ingroup relationships of Rebbachisauridae are nearly identical across EIW analyses, with *Amargatitanis*, *Amazonsaurus* and *Comahuesaurus* found to be the earliest representatives of the lineage, followed by a stepwise series of non-khebbashian rebbachisaurid lineages. *Rayososaurus*, *Campananeyen* and *Astigmasaura* belong to this grade of non-khebbashian rebbachisaurids, but their specific placements are uncertain (Fig. 7). We recover *Xenoposeidon* as a nested, non-khebbashian rebbachisaurid that is sister taxon to *Histriasaurus*. Both EIW analyses agree on the khebbashian identity of *Nopcsaspondylus* and the El Chocon rebbachisaurid, but disagree as to whether they are limaysaurines (EIW9) or rebbachisaurines (EIW12). Unlike the EQW analysis, *Suuwassea*, *Smitanosaurus* and BYU 17096 are resolved as early-diverging dicraeosaurids, and *Pilmatueia* is placed as an early-branching diplodocid.

There are also areas of disagreement between the EIW12 and EIW9 analyses regarding the placement of some non-rebbachisaurid diplodocoids (Table 2). As in the EQW results, *Lingwulong* and *Cetiosauriscus* are recovered outside of Dicraeosauridae, but they are found to be either stem flagellicaudatans (EIW12) or early-branching diplodocids (EIW9). Less severe downweighting of homoplasy (EIW12, as well as EQW) favours an early-branching diplodocid position for *Kaatedocus*, whereas this taxon is recovered as a stem flagellicaudatan under EIW9. Both EIW analyses agree that *Amphicoelias* is positioned as a relatively early-branching diplodocoid, but whereas the taxon is solely recovered as a non-diplodocimorph diplodocoid under EIW9, it is also found to be either a stem flagellicaudatan or the earliest-branching rebbachisaurid under EIW12. Finally, *Janenschia* and *Haestasaurus* are recovered as non-diplodocimorph diplodocoids under EIW9, but are found to be early-branching macronarians under EIW12.

Systematic palaeontology

Here, we provide revised diagnoses for major diplodocoid clades based on optimization of characters used in our main phylogenetic data matrix. Given the topological variation across the EQW and EIW analyses, we focus on the results from EIW analyses within which k=12. This is because: (1) this approach has been shown to strongly outperform EQW parsimony in simulation (Goloboff et al., 2018); and (2) select comparisons across k-values suggest that values between 10 and 20 are similar in accuracy, whereas performance deteriorates for values below 10 (Goloboff et al., 2018; O'Reilly et al., 2016).

All synapomorphies are unambiguously optimized, unless otherwise noted. For ambiguously optimized synapomorphies, we generally favoured accelerated transformation ('ACCTRAN'), except in instances in which a feature observed only in members of one named clade would become a synapomorphy for a more inclusive named clade. In these cases, and in select instances in which ACCTRAN optimization would result in a synapomorphy applying to an unnamed clade, we instead applied delayed transformation ('DELTRAN'). Following a modified version of the nomenclature proposed by Tschopp et al. (2015), we define synapomorphies as: (1) unique, i.e. shared by all ingroup members, and only by them (equivalent to the 'unambiguous synapomorphies' of Tschopp et al., 2015); (2) exclusive, i.e. occur only in ingroup members, but not in all of them; (3) shared, i.e. present in all ingroup members, but also occur in taxa outside the clade; and (4) highly homoplastic, i.e. neither exclusive nor shared by all ingroup members (equivalent to the 'ambiguous synapomorphies' of Tschopp et al., 2015). Where possible, all synapomorphies should be preferably evaluated in skeletally mature individuals. We provide photographs or reconstructions of scan data to illustrate examples of most unique and exclusive synapomorphies, as well as many shared ones (Figs 8–16). Numbers in parentheses below represent the character number and the state, e.g. 221:1 represents character number 221 and state 1 of that character.

Diplodocoidea Marsh, 1884

Definition. All taxa more closely related to *Diplodocus* than to *Saltasaurus* (stem-based; Wilson & Sereno, 1998).

Unique synapomorphies. None.

Exclusive synapomorphies. Sternal plate triangular in dorsal/ventral view (221:1; ACCTRAN).

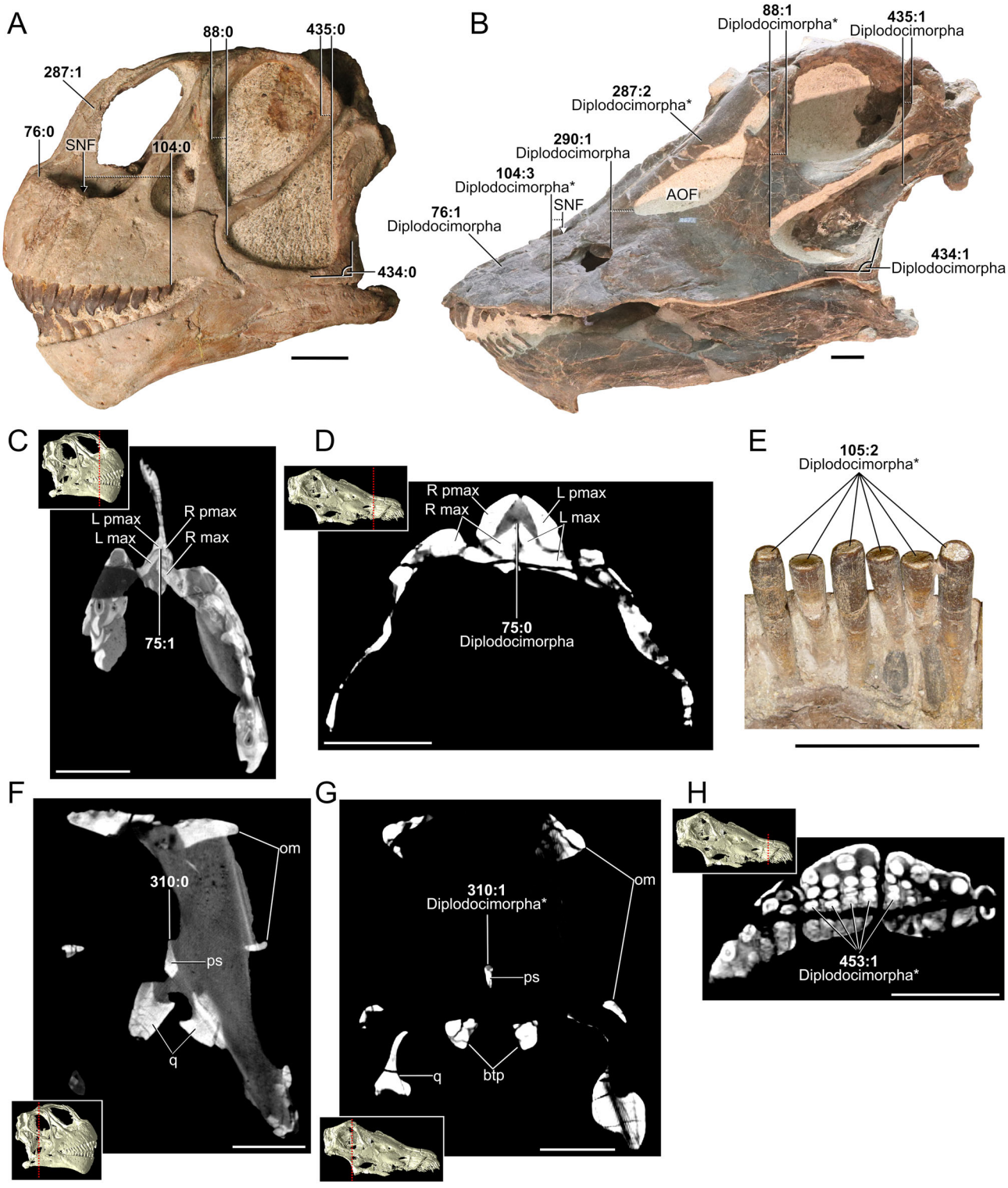
A
287:1
88:0
435:0
76:0
SNF
104:0
434:0
B
88:1
Diplodocimorpha*
435:1
Diplodocimorpha
287:2
Diplodocimorpha*
290:1
Diplodocimorpha
104:3
Diplodocimorpha*
SNF
AOF
76:1
Diplodocimorpha
434:1
Diplodocimorpha
C
L pmax
R pmax
L max
R max
75:1
D
R pmax
L pmax
R max
L max
75:0
Diplodocimorpha
E
105:2
Diplodocimorpha*
F
om
310:0
ps
q
G
310:1
Diplodocimorpha*
om
ps
q
btp
H
453:1
Diplodocimorpha*

Shared synapomorphies. Posterior ventral margin of atlantal intercentrum with ventrolateral projections (321:1; ACCTRAN); short cervical ribs that do not project far beyond their respective centrum (139:0).

Highly homoplastic synapomorphies. Postzygapophyses of posterior cervical neural arches terminate at or beyond posterior edge of centrum (328:0); weakly developed aliform processes in middle–posterior dorsal neural spines (163:0); neural spine height to centrum length ratio of posterior dorsal or sacral vertebrae $\geq$2.0 (486:0); anterior caudal centra with ventral longitudinal hollow (181:1); anterior caudal centra with distinct ventrolateral ridges (182:1); scapular acromion dorsoventral height to minimum dorsoventral height of scapular blade ratio less than 3.0 (36:0).

Diplodocimorpha Calvo & Salgado, 1995

Definition. *Diplodocus* and *Rebbachisaurus*, their most recent common ancestor, and all of its descendants (node-based; Taylor & Naish, 2005).

Unique synapomorphies. Premaxilla ascending process sub-rectilinear and directed posterodorsally (287:2; DELTRAN); infratemporal fenestra with anterior extension that reaches or surpasses the anterior margin of the orbit (88:1; DELTRAN); parasphenoid rostrum transversely thin and sheet-like in cross-section (310:1); tooth rows restricted anterior to subnarial foramen (104:3; DELTRAN); four or more replacement teeth per alveolus (453:1; DELTRAN).

Exclusive synapomorphies. Premaxillary-maxillary index greater than 75% (286:2; DELTRAN); teeth with low-angled planar wear facets (105:2; ACCTRAN); middle–posterior dorsal neural spines petal-shaped in anterior/posterior view (480:1); anterior caudal vertebrae with SPRL extending onto the lateral aspect of the neural spine (496:1); anterior-most caudal ribs with anterior surface excavated, forming a sharp-lipped fossa or foramen (503:1); anterior caudal ribs with dorsolaterally orientated dorsal margin (204:1; ACCTRAN); distal end of pubis expanded anteriorly and posteriorly (525:1).

Shared synapomorphies. Posterolateral process of premaxilla and lateral process of maxilla lack midline contact (75:0; ACCTRAN); anterior margin of premaxilla lacks a step (76:1; ACCTRAN); preantorbital fenestra lies anterior to antorbital fenestra (290:1; DELTRAN); ascending process of maxilla extends posterior to posterior end of main body (292:1; DELTRAN); external nares retracted to a position between the orbits (300:1; DELTRAN); jugal with a large contribution to the antorbital fenestra (426:2; DELTRAN); ventral process of squamosal extends past posterior margin of the orbit (435:1; DELTRAN); angle between anterior and dorsal processes of the quadratojugal $>90^{\circ}$ (434:1; DELTRAN); infratemporal fenestra linear and slit-like (301:1); basipterygoid processes angled less than 80° relative to skull roof (312:1; DELTRAN); tooth crowns aligned along jaw axis and do not overlap (106:1; DELTRAN); lower tooth crowns smaller than upper tooth crowns (107:1; DELTRAN); tooth crowns with circular cross-section at mid-crown height (109:1; DELTRAN); tooth crowns with convex lingual surface (110:1; DELTRAN); no apicobasally oriented lingual ridge on tooth crowns (111:1; DELTRAN); lateral pneumatic excavations of anterior caudal centra with sharply defined margins (179:1; DELTRAN); posterior caudal centra with average elongation index $\geq$1.7 (31:1); biconvex distal caudal centra (186:1; DELTRAN); humerus to femur proximodistal length ratio $\leq$0.7 (40:0; DELTRAN); pubic obturator foramen sub-circular in lateral view (250:0).

Highly homoplastic synapomorphies. Subnarial foramen and anterior maxillary foramen separated by a narrow isthmus (425:1; ACCTRAN); parietal lacks a contribution to the post-temporal fenestra (85:1; ACCTRAN); quadrate with shallow quadrate fossa (91:0; ACCTRAN); tooth crown slenderness index $\geq$4.0

Figure 8. Photographs and reconstructions of scan data illustrating select cranial synapomorphies supporting Diplodocimorpha, as well as the plesiomorphic condition: **A,** Skull of *Camarasaurus lentus* (CM 11338) in right lateral view (reversed). **B,** Skull of an indeterminate diplodocine (USNM 2672) in left lateral view. Coronal slices through the rostra of **C,** *Camarasaurus lentus* (CM 11338) and **D,** an indeterminate diplodocine (CM 11161) illustrating the presence (75:1) or absence (75:0) of a marked narial fossa and midline articulations between the premaxillae and maxillae. **E,** Apicolingual view of the upper dentition of an indeterminate diplodocine (CM 11161) showing low-angled planar wear facets (105:2). Coronal slices through the posterior facial skeleton of **F,** *Camarasaurus lentus* (CM 11338) and **G,** an indeterminate diplodocine (CM 11161) depicting the triangular (310:0) and sheet-like (310:1) cross-sections of the parasphenoid rostrum. **H,** CT slice through the alveoli of the premaxillae and maxillae of an indeterminate diplodocine (CM 11161) showing at least four generations of replacement teeth (453:1). Insets in parts C, D, F–H indicate the approximate location of the CT slice. Unique and exclusive synapomorphies are denoted with an asterisk. **Abbreviations: AOF**: anterior orbital fenestra; **btp**, basipterygoid process; **L**, left; **max**, maxilla; **om**, orbital margin; **pmax**, premaxilla; **ps**, parasphenoid rostrum; **q**, quadrate; **R**, right; **SNF**, subnarial foramen. Scale bar equals 50 mm in A–H. Image credit: E, Matt Lamanna/Carnegie Museum of Natural History.

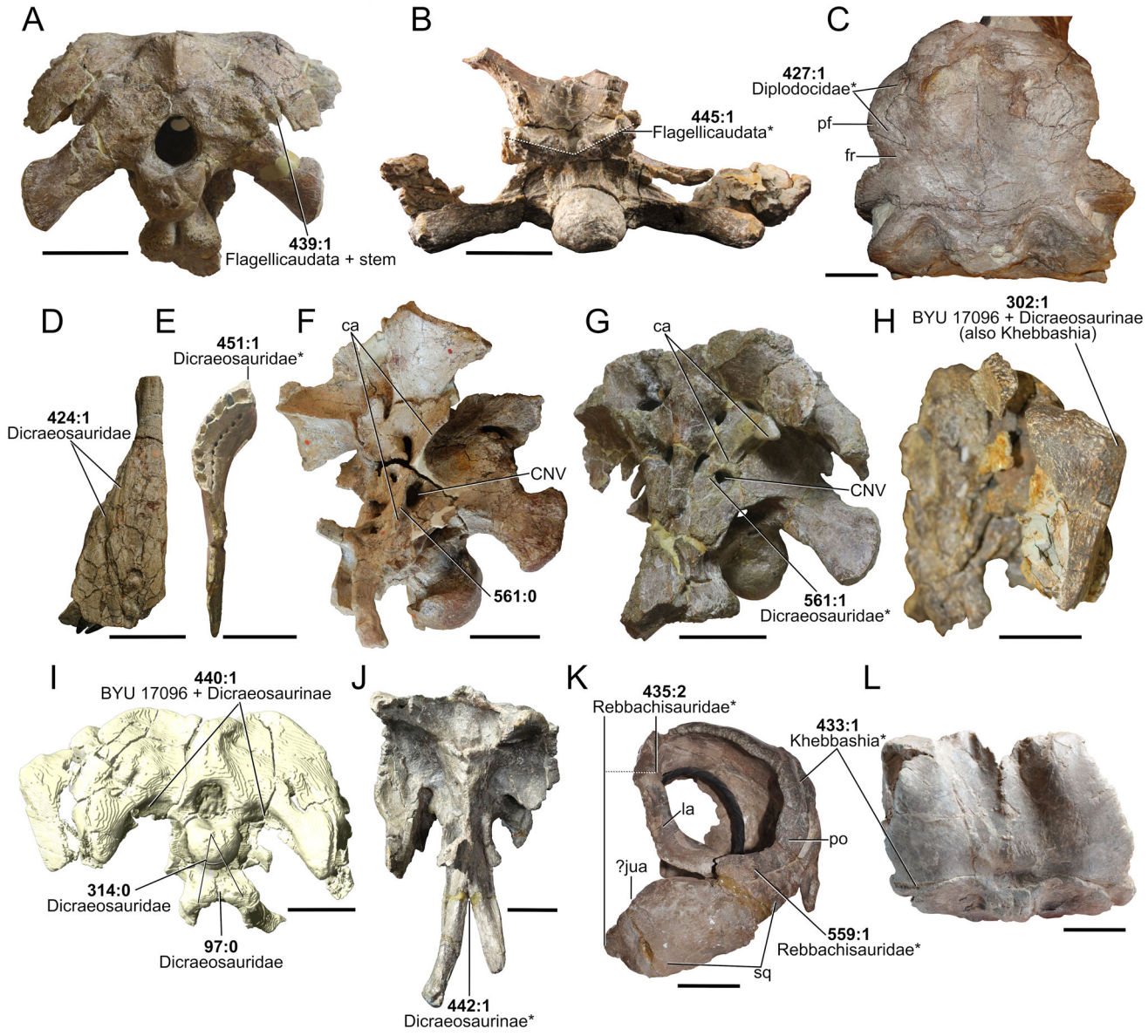

Figure 9. Photographs and reconstructions of scan data illustrating select cranial synapomorphies supporting various clades within Diplodocoidea. **A,** Braincase of *Suuwassea* (ANS 21122) in posterior view. **B,** Braincase of BYU 17096 in ventral view. **C,** Skull of an indeterminate diplodocine (CM 3452) in dorsal view. **D,** Premaxilla of *Dicraeosaurus hansemanni* (MfN MB.R. 2379) in anterior view. **E,** Dentary of *Suuwassea* (ANS 21122) in dorsal view. Braincases of **F,** *Giraffatitan* (MfN MB.R. 2180) and **G,** *Suuwassea* (ANS 21122) in left anterolateral views, illustrating the presence (561:0) or absence (561:1) of a crista antotica that extends ventrally to reach the anterior border of the foramen for cranial nerve V. **H,** Braincase of BYU 17096 in left lateral view, showing the absence of an acuminate posterior process of the postorbital (302:1) that supports BYU 17096 + Dicraeosaurinae, as well as Khebbashia. **I,** Braincase of BYU 17096 in posterior view illustrating deep, well-demarcated fossae at the ventromedial base of the paroccipital processes (440:1), as well as basal tubera with little or no divergence between them (97:0). **J,** Braincase of *Amargasaurus* (MACN PV N15) in anterior view. Braincase of *Limaysaurus* (MUCPv-205) in **K,** left lateral and **L,** dorsal views. Unique and exclusive synapomorphies are denoted with an asterisk. **Abbreviations: ca**, crista antotica; **CNV**, cranial nerve V; **fr**, frontal; **jua**, jugal articulation; **la**, lacrimal; **pf**, prefrontal; **po**, postorbital; **sq**, squamosal. Scale bar equals 50 mm in A–L. Image credits: D, Amy Campbell and Daniela Schwarz/Museum für Naturkunde, Berlin.

(11:2; ACCTRAN); average elongation index of the axis ≥2.0 (322:0); presence of a ventral midline keel in postaxial cervical centra (120:1); middle–posterior dorsal centra with flat or concave anterior articular faces (147:0); middle–posterior dorsal neural spines that do not flare distally (162:0); anterior-most caudal centra with well-defined ACDL (409:1; ACCTRAN); anterior caudal neural spines with lateral lamina (497:1;

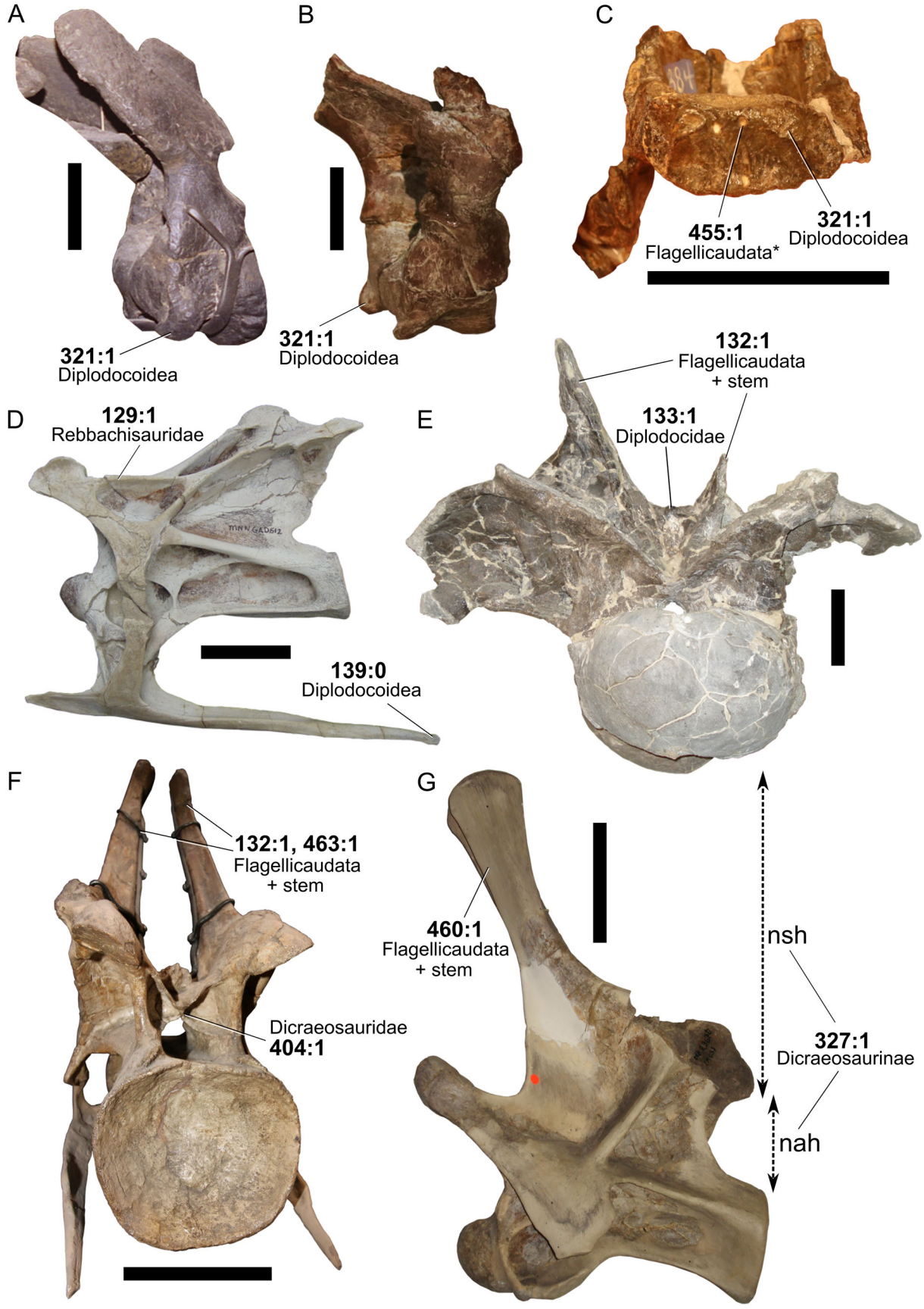
A
321:1
Diplodocoidea
B
321:1
Diplodocoidea
C
455:1
Flagellicaudata*
321:1
Diplodocoidea
D
129:1
Rebbachisauridae
139:0
Diplodocoidea
E
132:1
Flagellicaudata
+ stem
133:1
Diplodocidae
F
132:1, 463:1
Flagellicaudata
+ stem
Dicraeosauridae
404:1
G
460:1
Flagellicaudata
+ stem
nsh
327:1
Dicraeosaurinae
nah

ACCTRAN); anterior caudal ribs project mainly laterally (205:1); anterior-most caudal ribs with ventral surface directed dorsolaterally in anterior/posterior view (502:1); dorsal margin of ilium strongly convex throughout its length (520:1; ACCTRAN); projected line passing across ischial and pubic articular surfaces of the ilium passes through or dorsal to the ventral edge of the postacetabular part of the ilium (381:1); lateral edge of proximal tibia lacking 'second cnemial crest' (261:0; DELTRAN).

Remarks. Optimizing teeth with a high slenderness index (SI $\geq$ 4.0) as a synapomorphy of Diplodocimorpha (11:2) requires a secondary reversal to relatively broad crowns (11:1; SI = 2.0 to <4.0) in *Lingwulong* and potentially also *Kaatedocus* (see Saleiro & Tschopp, 2025). Under ACCTRAN, two unique synapomorphies (88:1 and 104:3) are optimized as synapomorphies of Diplodocoidea, rather than Diplodocimorpha.

Flagellicaudata Harris & Dodson, 2004

Definition. *Dicraeosaurus* and *Diplodocus*, their most recent common ancestor, and all of its descendants (node-based; Harris & Dodson, 2004).

Unique synapomorphies. Atlantal intercentrum with foramen on ventral surface, near posterior margin (455:1; DELTRAN).

Exclusive synapomorphies. Long axes of distal tips of basal tubera directed posteromedially (445:1; ACCTRAN); fibular articular surface of the astragalus faces posterolaterally (538:1; ACCTRAN).

Shared synapomorphies. Two foramina for CN XII (317:0; DELTRAN); occipital condyle positioned at an angle greater than 60° relative to horizontal plane (313:1; DELTRAN); middle–posterior dorsal neural spines with distinct pre- and postspinal laminae (167:1); middle–posterior dorsal neural spines with absent or short SPRLs that merge into the PRSL at its ventral end (342:1); ratio of mediolateral width across sacral vertebrae and ribs to average length of sacral centrum $\geq$4.0 (346:1; DELTRAN); anterior-most caudal ribs with ventrally deflected distal tip (501:1; DELTRAN); metatarsal III to metatarsal I proximodistal length ratio <1.3 (421:1).

Highly homoplastic synapomorphies. Lacrimal bears an anterior process (80:1; DELTRAN); posterior face of basal tubera flat or slightly concave (444:1); atlantal intercentrum with occipital facet expanded anteroventrally (116:1; DELTRAN); cervical centra with highest average elongation index $\geq$3.0 (15:1); middle cervical neural spines with lateral fossa at base of prezygapophyseal process (405:1); middle–posterior dorsal neural arches with single PCPL (148:1); anterior caudal centra with mildly convex posterior articular surface (27:1; ACCTRAN); ratio of mediolateral width to dorsoventral height of anterior articular surface of middle caudal centra $\geq$1.0 (28:1); scapular acromion dorsoventral height to minimum dorsoventral height of scapular blade ratio $\geq$3.0 (36:1); scapular acromion with excavated area posterior to the acromial ridge (212:1); coracoid ventral margin lacks a notch and infraglenoid lip (220:0); conjoined distal ends of the ischia are 'V'-shaped, forming an angle of 90° or less (533:0).

Remarks. Because the definition of Flagellicaudata is node-based, the above list of synapomorphies excludes those features that support *Cetiosauriscus* and *Lingwulong* as stem flagellicaudatans. Numerous unambiguous synapomorphies support the (*Cetiosauriscus*+*Lingwulong*) + Flagellicaudata clade, including: the dorsolateral margin of the exoccipital bearing a curving spur of bone that forms the dorsomedial margin of the post-temporal fenestra (439:1 [unique]); postaxial cervical centra with a small, clearly demarcated fossa on the posteroventral corner of the lateral surface (457:1 [exclusive]); postaxial cervical centra with posteriorly concave ventral surfaces (119:1 [highly homoplastic]); bifurcated neural spines in postaxial cervical and anterior dorsal vertebrae (132:1 [shared]); middle cervical neural spines anteriorly inclined (460:1 [exclusive]); bifurcated middle dorsal neural spines (161:1 [highly

Figure 10. Photographs illustrating select cervical vertebral synapomorphies supporting various clades within Diplodocoidea. **A,** *Haplocanthosaurus delfsi* atlas (CMNH 10380) in right posterolateral view. **B,** *Suuwassea* atlas (ANS 21122) in right posterolateral view. **C,** *Smitanosaurus* atlas (USNM 5384) in ventral view. **D,** Cervical vertebra 5 of *Nigersaurus* (MNN GAD 512) in left lateral view. **E,** Posterior cervical vertebra of *Brontosaurus yahnahpin* (TATE-001) in anterior view. **F,** Cervical vertebra 8 of *Dicraeosaurus hansemanni* (MfN MB.R. 4886) in posterior view. **G,** Middle cervical vertebra of *Dicraeosaurus sattleri* (MfN MB.R. 3676) in left lateral view. Several diplodocoid synapomorphies are highlighted, comprising: an atlas with ventrolateral projections (321:1) and a ventral foramen (455:1); short cervical ribs (139:0); cervical neural arches with an accessory lamina connecting the PODL to the SPRL (129:1); middle–posterior cervical neural arches with a sTPOL (404:1); anteriorly inclined (460:1) and elongate (327:1) middle cervical neural spines; and bifurcated cervical and anterior dorsal neural spines (132:1) with a median process at the base of the metapophyseal notch (133:1). Unique and exclusive synapomorphies are denoted with an asterisk. **Abbreviations: nah**, neural arch height; **nsh,** neural spine height. Scale bar equals 50 mm in A–D, and 100 mm in E–G. Image credit: F, Amy Campbell and Daniela Schwarz/Museum für Naturkunde, Berlin.

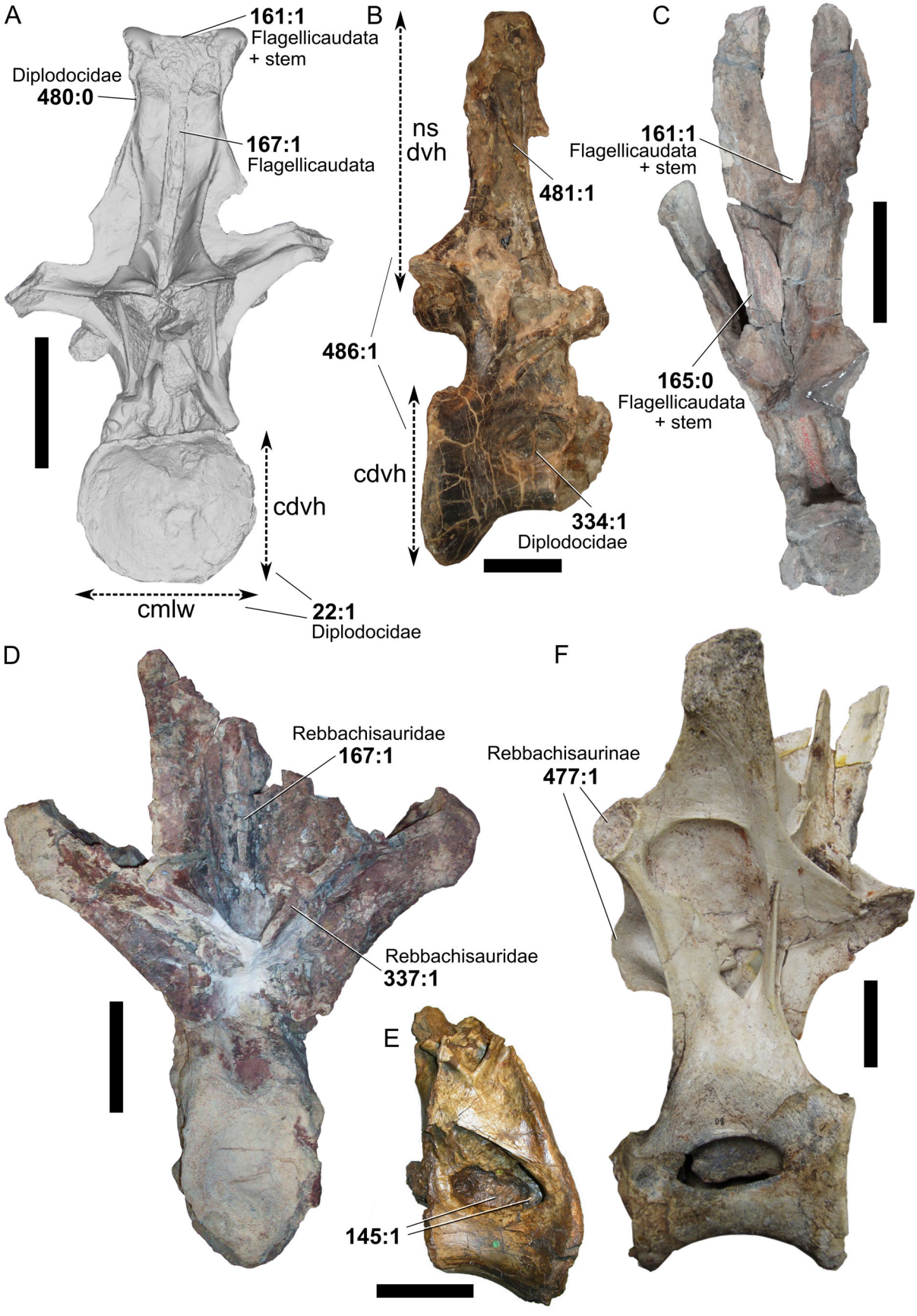
A
161:1
Flagellicaudata
+ stem
Diplodocidae
480:0
167:1
Flagellicaudata
cdvh
cmlw
22:1
Diplodocidae
B
ns
dvh
481:1
486:1
cdvh
334:1
Diplodocidae
C
161:1
Flagellicaudata
+ stem
165:0
Flagellicaudata
+ stem
D
Rebbachisauridae
167:1
Rebbachisauridae
337:1
E
145:1
F
Rebbachisaurinae
477:1

homoplastic]); anterior chevrons bridged dorsally by bone (208:1 [shared]); a scapular blade maximum to minimum dorsoventral height ratio less than 2.0 (37:1 [highly homoplastic]); a well-developed, anteriorly projecting ambiens process on pubis (522:1 [shared]); and the proximoventral corner of pedal phalanx I-1 drawn out into a thin plate underlying metatarsal I (542:1 [unique]).

Dicraeosauridae Huene, 1927

Definition. All taxa more closely related to *Dicraeosaurus* than to *Diplodocus* (stem-based; Sereno, 1998).

Unique synapomorphies. Crista antotica tapers out dorsally and does not reach the anterior border of the CNV foramen (561:1); dentary bears a tuberosity on its labial surface near the mandibular symphysis (451:1).

Exclusive synapomorphies. None.

Shared synapomorphies. External surface of premaxilla bears well-developed, anteroventrally orientated vascular grooves (424:1); presence of a frontoparietal fenestra (558:1); postparietal foramen present (432:1; DELTRAN); basioccipital with a foramen/foramina between the basal tubera and basipterygoid processes (99:0); little or no divergence between the basal tubera, such that they are cojoined along most or all of their length (97:0; DELTRAN), with their long axes forming an angle of $<50^{\circ}$ (314:0); middle–posterior cervical neural arches with a vertical midline lamina (sTPOL) or the ventral midline tip of a 'V'-shaped TPOL that divides the CPOF into two fossae (404:1).

Highly homoplastic synapomorphies. Cervical axis with ventral midline keel (117:1; ACCTRAN).

Remarks. Under DELTRAN, the postparietal foramen (431:1) is a dicraeosaurid synapomorphy, independently acquired in *Kaatedocus*. Alternatively, ACCTRAN optimization favours a scenario in which the postparietal foramen is a flagellicaudatan synapomorphy, lost in later-branching diplodocids.

Dicraeosaurinae Huene, 1927

Definition. *Dicraeosaurus* and *Bajadasaurus*, their most recent common ancestor, and all of its descendants (node-based; this study).

Unique synapomorphies. Area between basipterygoid processes forms a deep, slot-like cavity (442:1).

Exclusive synapomorphies. None.

Shared synapomorphies. Frontoparietal suture positioned at or posterior to the centre of the supratemporal fenestra (84:1); paroccipital process with a ventral non-articular process (96:1; ACCTRAN); posterior face of basal tubera convex (444:1); basipterygoid processes narrowly divergent, at an angle $<30^{\circ}$ (311:1); cervical and anterior-most dorsal vertebrae with solid internal tissue (115:0; DELTRAN); middle cervical vertebral neural spine to neural arch height ratio >2.0 (327:1; DELTRAN).

Highly homoplastic synapomorphies. None.

Remarks. The presence of a ventral non-articular process of the paroccipital process in *Bajadasaurus* is ambiguous. Solid internal vertebral architecture of cervical and anterior dorsal vertebrae (115:0) and tall middle cervical neural spines (327:1) would be synapomorphies of a slightly more inclusive clade if the taxon represented by BYU 17096 is eventually shown to share these features. Anterior dorsal vertebrae with diapophyses directed strongly dorsolaterally (153:1) might constitute an additional shared dicraeosaurine synapomorphy, but the status of this character in *Bajadasaurus* and BYU 17096 is not known.

Diplodocidae Marsh, 1884

Definition. All taxa more closely related to *Diplodocus* than to *Dicraeosaurus* (stem-based; Sereno, 1998).

Figure 11. Photographs and reconstructions of scan data illustrating select dorsal vertebral synapomorphies supporting various clades within Diplodocoidea. **A,** Dorsal vertebra 8 of *Diplodocus hallorum* (USNM V10865) in posterior view. **B,** Posterior dorsal vertebra of *Supersaurus vivianae* (WDC DMJ-021) in right lateral view. **C,** Dorsal vertebra 7 of *Brachytrachelopan* (MPEF-PV 1716) in posterior view. **D,** Anterior–middle dorsal vertebra of *Comahuesaurus* (MOZ-PV 6650) in posterior view. **E,** Middle–posterior dorsal vertebra of *Xenoposeidon* (NHMUK R2095) in left lateral view. **F,** Dorsal vertebra 8 of *Nigersaurus* (MNN GAD 100) in left lateral view. Several diplodocoid synapomorphies are highlighted, comprising: mediolaterally wide middle–posterior dorsal centra (22:1), with lateral pneumatic foramina divided by internal ridges (334:1) and set within a fossa (145:1); anterior–middle dorsal neural arches with zygapophyseal articular facets facing strongly dorsomedially (337:1); posterior dorsal neural arches with parapophyses dorsal to the prezygapophyses (477:1); bifurcated middle dorsal neural spines (161:1); middle–posterior dorsal neural spines with distinct pre- and postspinal laminae (167:1), undivided SPOLs (C165:0), an accessory lamina that connects the SPRL and SPOL (481:1), and subparallel lateral margins (480:0); and dorsoventrally short posterior dorsal neural spines (486:1). **Abbreviations: cdvh**, centrum dorsoventral height; **cmlw**, centrum mediolateral width; **nsdvh**, neural spine dorsoventral height. Scale bar equals 200 mm in A–C, 100 mm in D and E, and 50 mm in F. Image credit: A, Courtesy of the Smithsonian Institution.

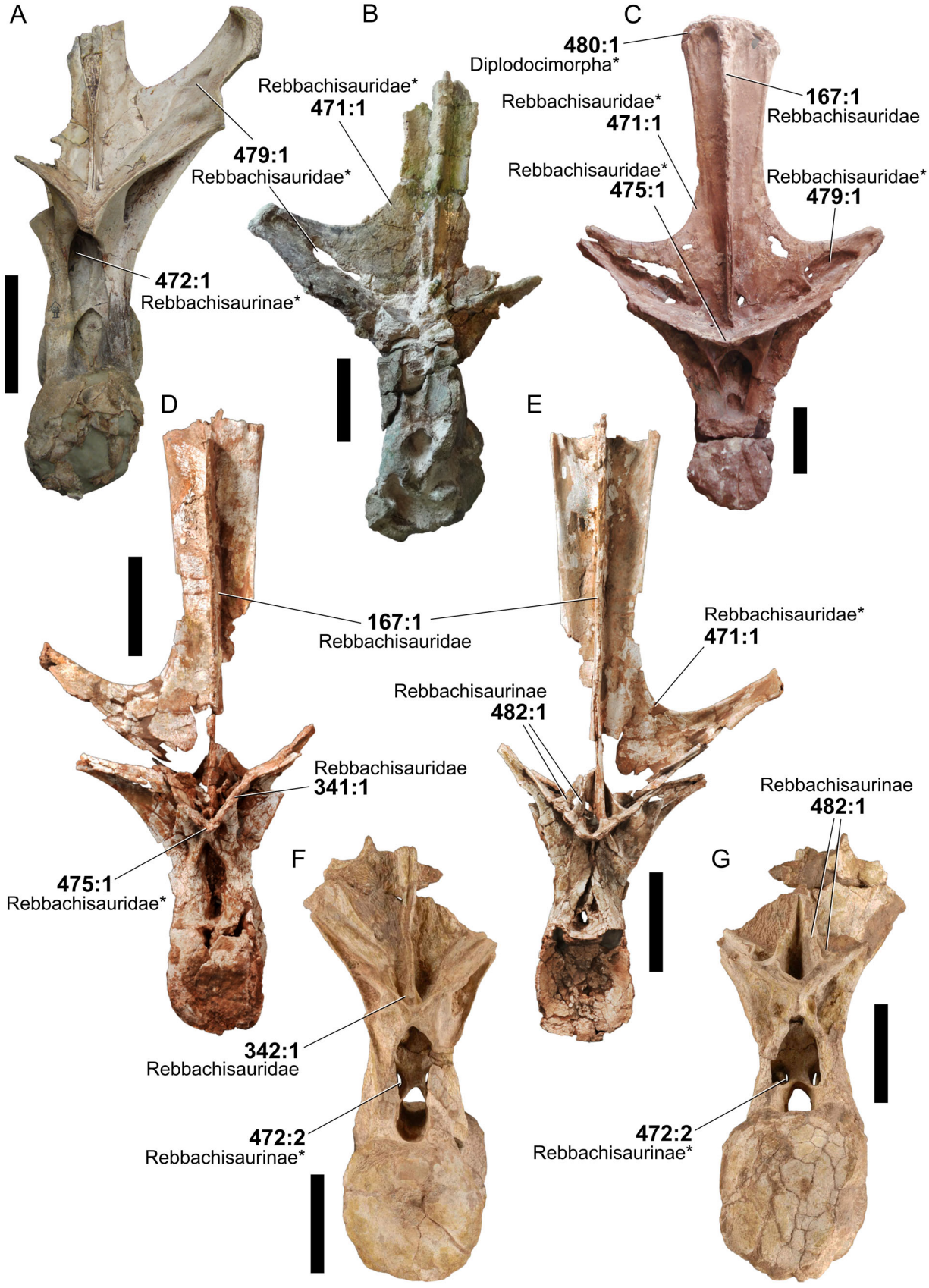
A
479:1
Rebbachisauridae*
472:1
Rebbachisaurinae*
B
Rebbachisauridae*
471:1
C
480:1
Diplodocimorpha*
167:1
Rebbachisauridae
Rebbachisauridae*
471:1
Rebbachisauridae*
475:1
Rebbachisauridae*
479:1
D
167:1
Rebbachisauridae
Rebbachisauridae
341:1
475:1
Rebbachisauridae*
E
Rebbachisauridae*
471:1
Rebbachisaurinae
482:1
F
342:1
Rebbachisauridae
472:2
Rebbachisaurinae*
G
Rebbachisaurinae
482:1
472:2
Rebbachisaurinae*

Unique synapomorphies. Anterior portion of medial margin of prefrontal and posterior process of prefrontal clasp anterolateral corner of the frontal (427:1; ACCTRAN); anterior-most caudal centra with divided ACDL (490:1; ACCTRAN).

Exclusive synapomorphies. None.

Shared synapomorphies. Prefrontal posterior process acute, with a sub-triangular outline (82:0; ACCTRAN); basioccipital without foramen or pit on posterior surface of the basal tubera (98:0; ACCTRAN); tooth crowns without labial grooves (320:1; ACCTRAN); bifurcated cervical neural spines with median process at base of metapophyseal notch (133:1); ratio of mediolateral width to dorsoventral height of the posterior articular face of middle–posterior dorsal centra $\geq$1.0 (22:1); middle–posterior dorsal neural spines rectangular throughout most of their length in anterior/posterior view (480:0, ACCTRAN); lateral pneumatic foramina of middle–posterior dorsal centra divided by internal ridge(s) (334:1; ACCTRAN); anterior-most caudal neural arches with CPRFs (492:1; ACCTRAN); ventral surface of anterior-most caudal ribs orientated laterally (502:0; ACCTRAN); lengths of anterior caudal centra increase by a factor of 1.5 or greater over the first 20 vertebrae (489:1; ACCTRAN); anterior caudal neural spines with SPRL and SPOL contacting to form prominent lateral lamina (198:1; ACCTRAN); concave lateral margin of the humeral diaphysis (224:0; ACCTRAN); distal end of pubis unexpanded posteriorly (525:0, ACCTRAN).

Highly homoplastic synapomorphies. Cervical vertebral count of at least 14 (14:1; ACCTRAN); cervical neural arches with pre-epipophyses (126:1; ACCTRAN); ratio of mediolateral width to dorsoventral height of the posterior articular face of anterior dorsal centra $\geq$1.3 (21:1); middle–posterior dorsal diapophyses directed laterally or slightly upwards (155:1).

Remarks. The number of cervical vertebrae in *Pilmatueia* is unknown. The presence of at least 14 cervical vertebrae in *Kaatedocus* supports kinship with diplodocids rather than with Dicraeosauridae, late-branching members of which have only 12. Note that optimization of tooth crowns without labial grooves (320:1) as a diplodocid synapomorphy occurs because weakly developed labial grooves are present in *Lingwulong* and *Dicraeosaurus* (Upchurch, 1998; Xu et al., 2018).

Rebbachisauridae Bonaparte, 1997

Definition. All taxa more closely related to *Rebbachisaurus* than to *Diplodocus* (stem-based; Salgado et al., 2004).

Unique synapomorphies. Ventral process of squamosal extends beyond anterior margin of the orbit (435:2; ACCTRAN); postorbital excluded from infratemporal fenestra by squamosal-jugal contact (559:1; ACCTRAN); dorsal neural spines with spinodiapophyseal lamina 'festooned' from neural spine (471:1; ACCTRAN); middle–posterior dorsal neural arches with confluent prezygapophyses (475:1; ACCTRAN); elongate, channel-like excavations on anterior surface of middle–posterior dorsal transverse processes (479:1; ACCTRAN); scapula with posteriorly directed hook-like acromion process (511:1; ACCTRAN); proximal surface of pubis and proximal third of its anterior margin meet at a right angle (521:1; ACCTRAN); pubic obturator foramen open posteriorly in adult individuals (524:1; ACCTRAN).

Exclusive synapomorphies. Articular surfaces of middle caudal centra sub-triangular (508:1; ACCTRAN).

Shared synapomorphies. Angle between long-axis of mandibular symphysis and main body of dentary approximately 90° (319:1; ACCTRAN); tooth crowns without labial grooves (320:1; ACCTRAN); cervical neural arches with accessory lamina connecting PODL to SPRL (129:1; ACCTRAN); anterior–middle dorsal neural arches with zygapophyseal articular facets facing

Figure 12. Photographs illustrating select dorsal vertebral synapomorphies supporting various clades within Diplodocoidea. **A,** Dorsal vertebra 8 of *Nigersaurus* (MNN GAD 100) in anterior view. **B,** Middle dorsal vertebra of *Katepensaurus* (UNPSJB-PV 1007-5) in anterior view. **C,** Middle–posterior dorsal vertebra of the 'El Chocon' rebbachisaurid (MMCH-Pv 49) in anterior view. Middle–posterior dorsal vertebra of *Rebbachisaurus* (MNHN-MRS 1958) in **D,** anterior and **E,** posterior views. Middle–posterior dorsal vertebra of *Demandasaurus* (MDS – RVII) in **F,** anterior and **G,** posterior views. Several diplodocoid synapomorphies are highlighted, comprising: middle–posterior dorsal neural arches with sharp-lipped fossae/foramina dorsolateral to the neural canal (472:1/2) and confluent prezygapophyses (475:1); elongate, channel-like excavations on anterior surface of middle–posterior dorsal transverse processes (479:1); dorsal neural spines with spinodiapophyseal lamina 'festooned' from neural spine (471:1); and petal-shaped (480:1) middle–posterior dorsal neural spines with distinct pre- and postspinal laminae (167:1), absent or short SPRLs that merge into the PRSL at its ventral end (342:1), and SPOLs that are divided into lateral and medial branches throughout their length (482:1). Unique and exclusive synapomorphies are denoted with an asterisk. Scale bar equals 100 mm in A–G. Image credits: D, and E, Ronan Allain and Lilian Cazes, Muséum National d'Histoire Naturelle, Paris; F, and G, Fidel Torcida Fernández-Baldor/Museo de Dinosaurios, Salas de los Infantes.

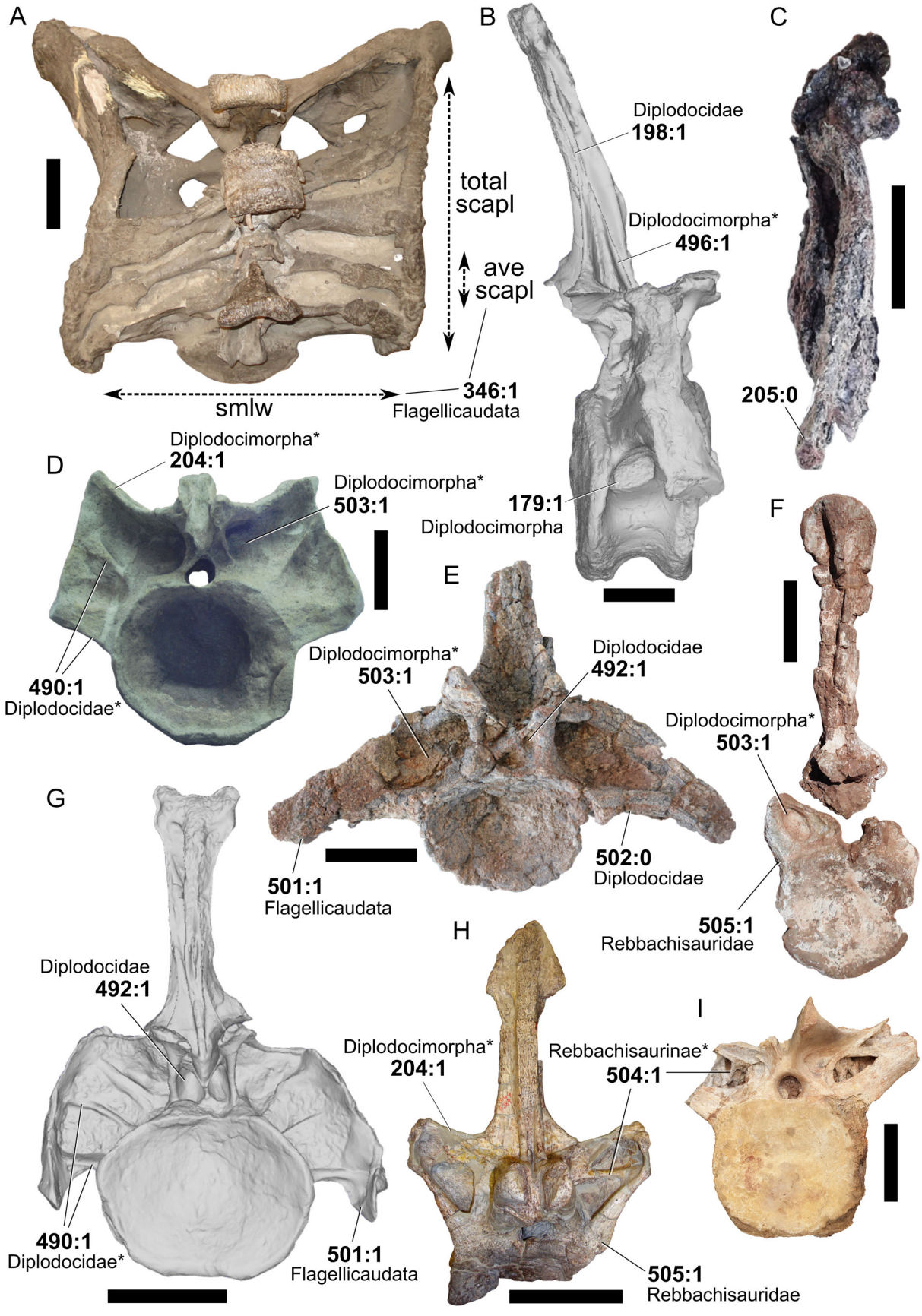
A
total scapl
ave scapl
smlw
346:1
Flagellicaudata
B
Diplodocidae
198:1
Diplodocimorpha*
496:1
179:1
Diplodocimorpha
C
205:0
D
Diplodocimorpha*
204:1
Diplodocimorpha*
503:1
490:1
Diplodocidae*
E
Diplodocimorpha*
503:1
Diplodocidae
492:1
501:1
Flagellicaudata
502:0
Diplodocidae
F
Diplodocimorpha*
503:1
505:1
Rebbachisauridae
G
Diplodocidae
492:1
490:1
Diplodocidae*
501:1
Flagellicaudata
H
Diplodocimorpha*
204:1
505:1
Rebbachisauridae
I
Rebbachisaurinae*
504:1

strongly dorsomedially (337:1; ACCTRAN); posterior dorsal neural arches with zygapophyseal articular facets facing strongly dorsomedially (341:1; ACCTRAN); middle–posterior dorsal neural spines with distinct pre- and postspinal laminae (167:1; ACCTRAN); middle–posterior dorsal neural spines with absent or short SPRLs that merge into the PRSL at its ventral end (342:1; ACCTRAN); concave posterior margin of scapular acromion (214:1; ACCTRAN); orientation of scapular blade long axis to coracoid articulation $\leq 70°$ (360:1; ACCTRAN); iliac articular surface of the pubis with anteroposterior to mediolateral width ratio ≥ 2.0 (58:1; ACCTRAN); distal end of pubis unexpanded transversely along lateral surface relative to shaft (385:1; ACCTRAN); ventral margin of proximal plate of the ischium is flat along its length (531:0; ACCTRAN); tibia to femur length ratio <0.6 (391:0; ACCTRAN).

Highly homoplastic synapomorphies. Ridge dividing lateral pneumatic foramen of postaxial cervical confluent with lateral surface of centrum (456:1; ACCTRAN); anterior-most caudal centra with lowest average elongation index ≥ 0.6 (26:1); humerus shaft eccentricity greater than 1.5 (43:0; ACCTRAN); squared humeral proximolateral corner (223:1; ACCTRAN); proximolateral margin of femur medial to the lateral margin of the distal half of the shaft (255:1).

Remarks. In analyses in which *Amargatitanis* is recovered outside of Rebbachisauridae, anterior caudal ribs restricted to the neural arch and dorsal margin of centrum (505:1) is recovered as an additional unique synapomorphy of the clade. Under EIW12, it is a synapomorphy of rebbachisaurids more derived than *Amargatitanis*.

Khebbashia Fanti, Cau, Cantelli, Hassine, & Auditore, 2015

Definition. *Rebbachisaurus*, *Nigersaurus*, *Limaysaurus*, their most recent common ancestor, and all of its descendants (node-based; Fanti et al., 2015).

Unique synapomorphies. Almost closed or absent supratemporal fenestra (433:1; DELTRAN); narrow iliac peduncle of the ischium, with a distinct 'neck' (526:1).

Exclusive synapomorphies. None.

Shared synapomorphies. 'V'-shaped frontal-nasal suture (429:1; DELTRAN); dorsal surface of frontal with grooves extending onto nasal (430:1; DELTRAN); postorbital without a pronounced, acuminate posterior process (C302:1; DELTRAN); ratio of maximum transverse width of body of the quadrate to the width of the ventral articular surface ≥ 1.7 (560:1; DELTRAN); sheet-like basal tubera (443:1; DELTRAN); basipterygoid processes narrowly divergent, at an angle $<30°$ (311:1; DELTRAN); ratio of scapula anteroposterior length to minimum blade dorsoventral height <5.5 (514:1; DELTRAN); pneumatized ilium (249:1; DELTRAN); proximolateral margin of femur narrowed to form a flange-like trochanteric shelf (256:1; DELTRAN).

Highly homoplastic synapomorphies. None.

Rebbachisaurinae Bonaparte, 1997

Definition. All taxa more closely related to *Rebbachisaurus garasbae* than to *Limaysaurus tessonei* (stem-based; Wilson & Allain, 2015).

Phylogenetic nomenclatural comments. The subfamily Rebbachisaurinae was simultaneously created when Rebbachisauridae was erected by Bonaparte (1997), but it had not been in usage until it was phylogenetically defined by Wilson and Allain (2015). Those authors defined it such that it is essentially synonymous with

Figure 13. Photographs and reconstructions of scan data illustrating select sacral and caudal vertebral synapomorphies supporting various clades within Diplodocoidea. **A,** Sacrum of *Diplodocus carnegii* (CM 94) in dorsal view. **B,** Caudal vertebra 2 of *Diplodocus hallorum* (USNM V10865) in right lateral view. **C,** Anterior caudal vertebra of *Leinkupal* (MMCH-Pv 63-6) in left lateral view. **D,** Anterior caudal vertebra of *Tornieria* (MfN MB.R. 6053) in anterior view. **E,** Anterior caudal vertebra of *Leinkupal* (MMCH-Pv 63-1) in anterior view. **F,** Caudal vertebra 2 of *Limaysaurus* (MUCPv-205) in anterior view. **G,** Caudal vertebra 2 of *Diplodocus hallorum* (USNM V10865) in anterior view. **H,** Anterior caudal vertebra of the 'Isle of Wight' rebbachisaurid (MIWG 5384) in anterior view; **I,** Anterior caudal vertebra of an indeterminate rebbachisaurine from Morocco (NHMUK R36636) in anterior view. Several diplodocoid synapomorphies are highlighted, comprising: a ratio ≥ 4.0 for the mediolateral width across sacral vertebrae and ribs to the average length of a sacral centrum (346:1); anterior-most caudal centra with divided ACDL (490:1); the presence of a sharp-lipped lateral pneumatic foramen in anterior caudal centra (179:1); ventral surface of anterior-most caudal ribs orientated laterally (502:0), with ventrally deflected distal tip (501:1); anterior-most caudal ribs with anterior surface excavated, forming a sharp-lipped fossa or foramen (503:1), internally subdivided by subvertical ridges (504:1); anterior caudal ribs curve anterolaterally (205:0), restricted to the neural arch and dorsal margin of centrum (505:1), with a dorsolaterally orientated dorsal margin (204:1); anterior-most caudal neural arches with CPRFs (492:1); and SPRL extends onto the lateral aspect of anterior caudal neural spines (496:1), contacting the SPOL to form a prominent lateral lamina (198:1). Unique and exclusive synapomorphies are denoted with an asterisk. **Abbreviations: ave**, average; **scapl**, sacral centra anteroposterior length; **smlw**, sacrum mediolateral width. Scale bar equals 200 mm in A and G, and 100 mm in B–F, H and I. Image credit: B, Courtesy of the Smithsonian Institution; C and E, Pablo Gallina.

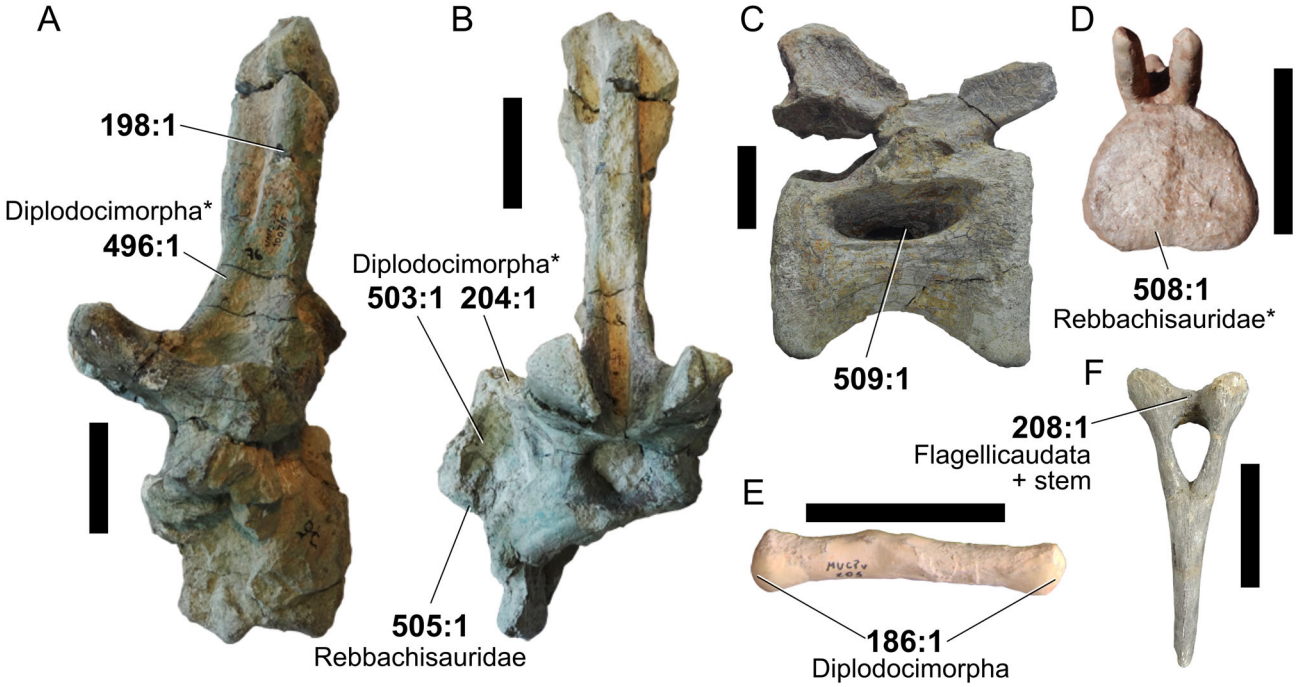

Figure 14. Photographs illustrating select caudal vertebral synapomorphies supporting various clades within Diplodocoidea. Anterior caudal vertebra of *Katepensaurus* (UNPSJB-PV 1007-7) in **A,** left lateral and **B,** anterior views. **C,** Middle caudal vertebra of *Tornieria* (MfN MB.R. 2958) in right lateral view. **D,** Middle–posterior caudal vertebra of *Limaysaurus* (MUCPv-205) in anterior view. **E,** Distal caudal vertebra of *Limaysaurus* (MUCPv-205) in left lateral view. **F,** Anterior chevron of *Amargasaurus* (MACN PV N15) in anterior view. Several diplodocoid synapomorphies are highlighted, comprising: anterior-most caudal ribs with anterior surface excavated, forming a sharp-lipped fossa (503:1); anterior caudal ribs restricted to the neural arch and dorsal margin of centrum (505:1), with a dorsolaterally orientated dorsal margin (204:1); SPRL extends onto the lateral aspect of anterior caudal neural spines (496:1), contacting the SPOL to form a prominent lateral lamina (198:1); middle caudal centra sub-triangular (508:1), with a lateral fossa (C509:1); biconvex distal caudal centra (186:1); and anterior chevrons bridged dorsally by bone (208:1). Unique and exclusive synapomorphies are denoted with an asterisk. Scale bar equals 50 mm in A–E, and 100 mm in F.

Nigersaurinae, erected by Whitlock (2011a), even though the latter clade name had begun to be widely used. Given the previously labile position of *Rebbachisaurus*, Mannion, Upchurch, Schwarz, et al. (2019) recommended the continued use of Nigersaurinae over Rebbachisaurinae. However, the developing consensus of the phylogenetic affinities of *Rebbachisaurus* (though see Lerzo, Torcida Fernández-Baldor, et al., 2025), coupled with the taxonomic priority of Rebbachisaurinae, led Mannion and Whitlock (in press) to support the usage of the latter name over Nigersaurinae, which we follow here.

Unique synapomorphies. Middle and posterior dorsal neural spines with SPOL divided into lateral and medial branches throughout its length (482:1; DELTRAN); excavated anterior surface of anterior-most caudal ribs internally subdivided by subvertical ridges (504:1; ACCTRAN); ischium with thin and sharp ridge for attachment of m. flexor tibilias internus III (530:1; ACCTRAN).

Exclusive synapomorphies. None.

Shared synapomorphies. Sharp-lipped neural arch fossae dorsolateral to the neural canal in middle–posterior dorsal vertebrae (472:1/2); posterior dorsal neural arches with parapophyses dorsal to the prezygapophyses (477:1).

Highly homoplastic synapomorphies. Parapophyses of postaxial cervical centra dorsally excavated (121:1); pre-epipophyses on cervical prezygapophyses (126:1); ratio of minimum mediolateral width to proximodistal length of the humerus <0.15 (42:1).

Remarks. Middle and posterior dorsal neural spines with SPOLs divided throughout their length (482:1) constitutes a synapomorphy of Khebbashia in the EIW9 analysis, in which the El Chocon rebbachisaurid and *Nopcsaspondylus* are instead recovered as limaysaurines. This character is optimized ambiguously in the EIW12 analysis because it cannot be scored in *Limaysaurus* or *Cathartesaura*. Thus, while fully divided SPOLs are

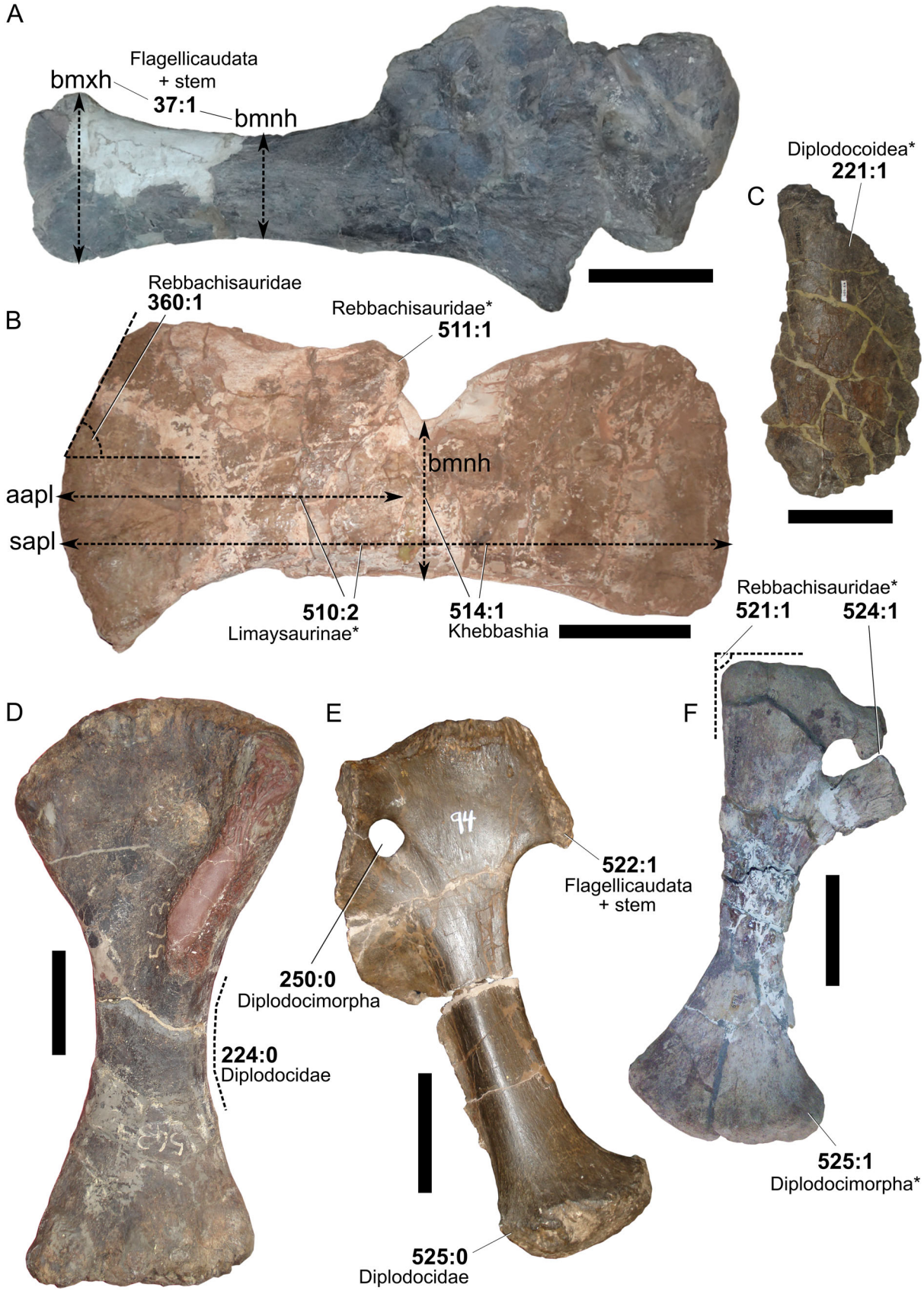
A
bmxh
Flagellicaudata
+ stem
37:1
bmnh
B
Rebbachisauridae
360:1
Rebbachisauridae*
511:1
bmnh
aapl
sapl
510:2
Limaysaurinae*
514:1
Khebbashia
C
Diplodocoidea*
221:1
D
224:0
Diplodocidae
E
250:0
Diplodocimorpha
522:1
Flagellicaudata
+ stem
525:0
Diplodocidae
F
Rebbachisauridae*
521:1
524:1
525:1
Diplodocimorpha*

recovered as a unique rebbachisaurine synapomorphy under DELTRAN optimization, this feature becomes a synapomorphy of Khebbashia under ACCTRAN optimization.

Limaysaurinae Whitlock, 2011a

Definition. All taxa more closely related to *Limaysaurus* than to *Nigersaurus* (stem-based; Whitlock, 2011a).

Unique synapomorphies. Scapular acromion anteroposterior length to total scapula length ratio ≥0.5 (510:2).

Exclusive synapomorphies. None.

Shared synapomorphies. None.

Highly homoplastic synapomorphies. None.

Remarks. Whitlock (2011a) recovered two additional unambiguous synapomorphies in support of Limaysaurinae. The first of these is the presence of an accessory lateral lamina connecting the PODL and SPRL in posterior cervical vertebrae (96:1 of that study). This feature was termed the 'suprapostzygapophyseal accessory lamina (SPZAL)' by Calvo and Salgado (1995) and Gallina and Apesteguía (2005), who identified it in *Limaysaurus* and *Cathartesaura*, respectively; however, rather than being a novel structure, the SPZAL appears to be homologous to the SPDL, which in most eusauropods is serially present only in the dorsal vertebrae. The phylogenetic character matrix used herein does not include a character for the presence of a SPDL in the posterior cervical vertebrae, and we were therefore unable to independently validate this proposed synapomorphy. Whitlock (2011a) also recovered contact between the SPRL and SPOL in anterior caudal neural spines, forming a prominent lateral lamina, as an unambiguous limaysaurine synapomorphy. Although this feature is indeed shared by *Limaysaurus* and *Cathartesaura*, it is only a synapomorphy of Limaysaurinae under DELTRAN optimization, as it is also present in the rebbachisaurids *Katepensaurus*, *Nigersaurus* and *Rebbachisaurus* (198:1) (Fig. 14A).

Discussion

Systematics of *Tharosaurus* and Middle Jurassic Indian sauropod faunas

Our reassessment of the anatomy of *Tharosaurus indicus* demonstrates that it lacks clear diplodocoid synapomorphies (Figs 1–3). This is supported by our reanalysis of the phylogenetic data matrix presented by Bajpai et al. (2023), as well as our analyses of our main data matrix, all of which instead place *Tharosaurus* as a eusauropod of unclear identity. In addition, we are unable to identify clear autapomorphies in the material assigned to *Tharosaurus*, with its fragmentary and distorted nature making it unsuitable as a type specimen and precluding its assignment to a lower taxonomic level within Eusauropoda (Figs 1–6). As such, we regard *Tharosaurus indicus* as a *nomen dubium* representing an indeterminate eusauropod of uncertain affinity.

The remains assigned to *Tharosaurus* are not the first sauropod specimens to be reported from the Middle Jurassic of India. Moser et al. (2006) described fragmentary sauropod remains from the Bajocian Khadir Formation on Khadir Island, western India. They assigned some of these remains to the macronarian clade Camarasauromorpha, which Bajpai et al. (2023) highlighted as additional evidence to support the presence of neosauropods in the Middle Jurassic of India. However, Moser et al. (2006) provided almost no reasoning for the assignment of these remains to Camarasauromorpha. In the few instances in which they discussed the distribution of anatomical features, Moser et al. (2006) also noted the presence of these characteristics in taxa outside of Neosauropoda. Given that none of the specimens display neosauropod synapomorphies, we regard the

Figure 15. Photographs illustrating select appendicular synapomorphies supporting various clades within Diplodocoidea. **A,** Right scapulocoracoid of *Amargasaurus* (MACN PV N15) in lateral view. **B,** Left scapula of *Limaysaurus* (MUCPv-205) in lateral view. **C,** Right sternal plate of *Brontosaurus yahnahpin* (TATE-001) in ventral view. **D,** Left humerus of *Brontosaurus parvus* (UWGM 15556) in anterior view. **E,** Right pubis of *Diplodocus carnegii* (CM 94) in lateral view. **F,** Left pubis of *Comahuesaurus* (MOZ-PV 6743) in medial view. Several diplodocoid synapomorphies are highlighted, comprising: orientation of scapular blade long axis to coracoid articulation ≤70° (360:1); a scapular acromion anteroposterior length to total scapula length ratio ≥0.5 (510:2); scapula anteroposterior length to minimum blade dorsoventral height ratio of <5.5 (514:1); a scapular blade maximum to minimum dorsoventral height ratio less than 2.0 (37:1); scapula with posteriorly directed hook-like acromion process (511:1); triangular sternal plate in dorsal/ventral view (221:1); concave lateral margin of the humeral diaphysis (224:0); proximal surface of pubis and proximal third of its anterior margin meet at a right angle (521:1); prominent ambiens process on pubis (522:1); pubic obturator foramen subcircular in lateral view (250:0) and open posteriorly (524:1); and an anteroposteriorly expanded (525:1) and unexpanded (525:0) distal pubis. Unique and exclusive synapomorphies are denoted with an asterisk. **Abbreviations: aapl**, acromion anteroposterior length; **bmnh**, blade minimum height; **bmxh**, blade maximum height; **sapl**, scapula anteroposterior length. Scale bar equals 200 mm in A–F.


A
526:1
Khebbashia*
530:1
Rebbachisaurinae*
531:0
Rebbachisauridae
B
C
531:1
F
256:1
Khebbashia
D
255:0
Rebbachisauridae
255:1
E
G
538:1
Flagellicaudata*
H
542:1
Flagellicaudata
+ stem

remains described by Moser et al. (2006) as belonging to an indeterminate eusauropod.

Sharma et al. (2022) described a sauropod tooth from the Bathonian Badabag Member of the Jaisalmer Formation, which overlies the Fort Member that yielded *Tharosaurus*. As demonstrated by Sharma et al. (2022), this heart-shaped tooth bears synapomorphies that support its referral to Turiasauria (see Mateus et al., 2014; Mocho et al., 2016; Royo-Torres et al., 2006; Saleiro & Tschopp, 2025), which is typically recovered as a non-neosauropod eusauropod clade (though see our EQW topology for an unusual macronarian placement for Turiasauria). Although *Tharosaurus* cannot be referred to Turiasauria, this is potentially because of its incompleteness and poor preservation, rather than features that contradict such a placement.

Other possible Early–Middle Jurassic Gondwanan neosauropods

Purported neosauropods have also been described from pre-Late Jurassic deposits from elsewhere in Gondwana. *Jobaria tiguidensis* is known from multiple individuals from the Bathonian–Callovian Tiourarén Formation of Niger (Rauhut and López-Arbarello, 2009; Sereno et al., 1999). Most analyses have recovered it as a eusauropod just outside of the neosauropod radiation (e.g. D'Emic, 2012; Mannion, Upchurch, Schwarz, et al., 2019; Wilson, 2002), although occasionally it has been placed as an early-diverging macronarian (e.g. Upchurch, Barrett, et al., 2004; Xing et al., 2015) or diplodocoid (Carballido et al., 2011; Moore et al., 2020). The latter position is supported by a subset of MPTs in our EQW analysis, in which a clade comprising *Jobaria* and *Haplocanthosaurus* spp. is the sister taxon to all other diplodocoids. Features supporting close kinship of *Jobaria* and *Haplocanthosaurus* include a relatively short cervical axis (322:1), dorsal neural spines in which the SPRL contacts the diapophysis following 'lamina capture' (470:1), a dorsomedially directed femoral head (388:1), and a femoral fourth trochanter that is visible in anterior view (258:1). In addition, *Jobaria* shares with diplodocoids a premaxilla that lacks a stepped anterior margin (76:1), as well as anterior caudal centra with a ventral longitudinal hollow (181:1). Although *Jobaria* lacks a detailed published description, it is scored based on firsthand observation in most eusauropod data matrices, including the one presented herein.

Atlasaurus imelakai, from the Bathonian Guettioua Formation of Morocco, was described as a brachiosaurid by Monbaron et al. (1999). Its position is labile across phylogenetic analyses, switching between non-neosauropod eusauropod and early-diverging macronarian placements (e.g. D'Emic, 2012; Mannion et al., 2013; Mannion, Upchurch, Schwarz, et al., 2019; Royo-Torres et al., 2006), as well as being placed as a 'basal' diplodocoid in at least one previous analysis (Ren et al., 2023). In the analyses presented herein, it is a non-titanosauriform eusauropod under EQW (either outside of Neosauropoda or an early-diverging macronarian), but a brachiosaurid under EIW (Figs 4–6). Given that it is known from much of the skeleton, *Atlasaurus* is an important taxon for understanding the early evolutionary history of Gondwanan eusauropods. However, it has received only a brief description (Monbaron et al., 1999) and is in need of revision, and no published phylogenetic analysis has yet to include it based on firsthand study.

Bindellini and Dal Sasso (2021) interpreted several isolated teeth from the Bathonian Sakahara (=Isalo III) Formation of Madagascar as belonging to a titanosauriform. Although we do not exclude this possibility, we remain cautious about taxonomic identifications based solely on teeth (see also Frauenfelder et al., 2024). Furthermore, the teeth appear similar to those of *Atlasaurus*, for which a non-neosauropod identification remains possible. Bindellini and Dal Sasso (2021) suggested that another tooth from the Sakahara Formation represents either a diplodocoid or titanosaur. However, this specimen does not appear morphologically similar to any known tooth of either clade. As such, we contend

Figure 16. Photographs illustrating select appendicular synapomorphies supporting various clades within Diplodocoidea. **A,** Left ischium of *Demandasaurus* (MDS – RVII) in lateral view. **B,** Right ischium of *Rebbachisaurus* (MNHN-MRS 2009) in lateral view. **C,** Right ischium of *Tornieria* (SMNS 12143) in lateral view. **D,** Right femur of *Tornieria* (SMNS 12140) in posterior view. **E,** Right femur of *Comahuesaurus* (MOZ-PV 6761) in posterior view. **F,** Left femur of *Demandasaurus* (MDS – RVII) in posterior view. **G,** Left astragalus of *Amargasaurus* (MACN PV N15) in posterior view. **H,** Right pedal phalanx I-1 of *Diplodocus carnegii* (CM 89) in dorsal view. Several diplodocoid synapomorphies are highlighted, comprising: narrow iliac peduncle of the ischium, with a distinct 'neck' (526:1); ischium with thin and sharp ridge for attachment of m. flexor tibilias internus III (530:1); ventral margin of proximal plate of the ischium is flat along its length (531:0); proximolateral margin of femur medial to the lateral margin of the distal half of the shaft (255:1) and narrowed to form a flange-like trochanteric shelf (256:1); fibular articular surface of the astragalus faces posterolaterally (538:1); and proximoventral corner of pedal phalanx I-1 drawn out into a thin plate underlying metatarsal I (542:1). Unique and exclusive synapomorphies are denoted with an asterisk. Scale bar equals 200 mm in A–F, and 50 mm in G and H. Image credits: A, Fidel Torcida Fernández-Baldor/Museo de Dinosaurios, Salas de los Infantes; B, Ronan Allain and Lilian Cazes, Muséum National d'Histoire Naturelle, Paris.

that this tooth cannot currently be attributed to a neosauropod. Other sauropod remains from the Middle Jurassic of Madagascar, including the named taxa *Archaeodontosaurus descouensi*, *Lapparentosaurus madagascariensis* and *Narindasaurus thevenini*, appear to belong to lineages outside of Neosauropoda, including Turiasauria (Buffetaut, 2005; Mannion, 2010; Mannion et al., 2013; Royo-Torres et al., 2021). Finally, Carballido et al. (2017) described a partial tooth from the Toarcian (upper Lower Jurassic) Cañadón Asfalto Formation of Argentina that shares some features with Titanosauriformes, but its affinities remain uncertain and more complete material is required to support such an identification.

In summary, support for pre-Late Jurassic Gondwanan neosauropods remains tenuous, and no sauropods from this spatiotemporal window can currently be referred unequivocally to Neosauropoda. Nevertheless, it remains highly possible that their near-absence is a sampling artefact, rather than a genuine signal, especially if neosauropods remained low in diversity and abundance prior to the Late Jurassic. This latter hypothesis is supported by the scarcity of neosauropods in the Middle Jurassic of Laurasia, from which body fossil remains and trackways currently assigned to Diplodocoidea (see below) or Macronaria (Dai et al., 2022; Day et al., 2002; Moreau et al., 2019; Ren et al., 2022, 2023) are extremely rare.

Implications for the evolutionary relationships and systematics of Diplodocoidea

A number of phylogenetic placements of taxa in our analyses are novel or contrast with at least some recent topologies. Below we discuss several of our phylogenetic results pertaining to Diplodocoidea. Unless otherwise stated, we focus on the results of the EIW analysis with a *k*-value of 12 (Fig. 5).

Non-diplodocimorph diplodocoids. The Upper Jurassic Morrison Formation species *Haplocanthosaurus priscus* and *Haplocanthosaurus delfsi* are consistently recovered as non-diplodocimorph diplodocoids in both EIW analyses, as in previous iterations of this data matrix (Mannion, Upchurch, Schwarz, et al., 2019; Mannion et al., 2021). However, they are recovered outside of Neosauropoda in a subset of MPTs from the EQW analysis. It remains uncertain whether *H. delfsi* is attributable to *Haplocanthosaurus* (see also analyses in Gallina & Apesteguía, 2005; Mannion, Upchurch, Schwarz, et al., 2019). The incorporation of additional remains attributed to this genus (e.g. Boisvert et al., 2025) into phylogenetic analysis might help resolve the systematics of these two species. The two *Haplocanthosaurus* species form a clade with the late Middle Jurassic North African taxon *Jobaria* in our EQW analysis (Fig. 4), which is entirely novel to our study. Support for this relationship is based on several features of the axial skeleton and femur (see above), all of which are homoplastic within Eusauropoda.

Stem flagellicaudatans. Consistent with previous studies (Gallina et al., 2019; Mannion, Upchurch, Schwarz, et al., 2019; Whitlock & Wilson Mantilla, 2020; Windholz et al., 2022; Xu et al., 2018), our analyses recover *Lingwulong shenqi* as a Middle Jurassic diplodocimorph. However, it is no longer recovered as a dicraeosaurid and instead is placed outside of the diplodocid–dicraeosaurid split as a stem flagellicaudatan (EQW and EIW12) or as an early-branching diplodocid (EIW9) (Figs 4–6), positions supported by numerous synapomorphies (see above). This revised position is primarily driven by a small number of character score changes to our *Lingwulong* OTU, including the interpretation that it lacks a deep, slot-like cavity between the basipterygoid processes (442:0), *contra* Xu et al. (2018), with the presence of this feature recovered as a unique synapomorphy of Dicraeosaurinae (Fig. 9J). *Cetiosauriscus stewarti* is recovered as the sister taxon of *Lingwulong* in both EIW analyses, but under EQW it lies either outside of Neosauropoda (immediately 'basal' to *Lapparentosaurus*), or just 'apical' to *Lingwulong* as an additional stem flagellicaudatan (Figs 4–6). This is broadly consistent with a previous iteration of this data matrix (Mannion, Upchurch, Schwarz, et al., 2019), except that *Cetiosauriscus* was placed as a dicraeosaurid therein under EIW. Flagellicaudatan affinities were also recovered for the latter species by Holwerda et al. (2019) and in some of the analyses of Tschopp et al. (2015), whereas other studies have consistently placed it as a non-neosauropod eusauropod (e.g. Moore et al., 2020, 2023; Rauhut et al., 2005).

Laurasian diplodocids. Our sampling of unequivocal diplodocids is unchanged from previous iterations of this phylogenetic data matrix (Mannion, Upchurch, Schwarz, et al., 2019; Mannion et al., 2021), with only the apatosaurine *Apatosaurus* spp. and the diplodocines *Diplodocus* spp. (possibly including material pertaining to *Galeamopus* spp. within this OTU) and *Supersaurus vivianae* included as representatives of the high species richness known from the Upper Jurassic Morrison Formation. As is the case in most previous analyses (e.g. Mannion et al., 2012; Mannion, Upchurch, Schwarz, et al., 2019; Tschopp et al., 2015; Whitlock & Wilson Mantilla, 2020), we recover a sister-taxon relationship between *Supersaurus* and *Dinheirosaurus lourinhanensis* from the upper Kimmeridgian–lower Tithonian Lourinhã Formation of Portugal (Bonaparte & Mateus, 1999; Mannion et al.,

2012) (Figs 4–6), supported by an accessory lamina on the lateral surface of middle–posterior dorsal neural spines that connects the SPRL and SPOL (481:1), as well as relatively short posterior dorsal neural spines (486:1) (Fig. 11B). Tschopp et al. (2015) proposed that *Dinheirosaurus lourinhanensis* should be regarded as a second species of *Supersaurus*, but, given the geographical separation of these two species, coupled with anatomical differences that approach the generic level cut-off value (*sensu* Tschopp et al., 2015), we follow Mannion and Whitlock (in press) in tentatively retaining *Dinheirosaurus* as a distinct genus. Tschopp and Mateus (2013) described *Kaatedocus siberi* as an additional Morrison Formation diplodocid. Initially recovered as a phylogenetically nested diplodocine (Tschopp & Mateus, 2013; Tschopp et al., 2015), it was subsequently placed as the earliest-diverging diplodocine by Tschopp and Mateus (2017) and as a 'basal' dicraeosaurid by Whitlock and Wilson Mantilla (2020). Our analyses place *Kaatedocus* in novel positions, either as a diplodocid outside of the apatosaurine–diplodocine split (EIW12, EQW) or as a stem flagellicaudatan (EIW9) (Figs 4–6). Although we remain cautious about its position within Diplodocidae given that we do not sample all Morrison Formation species of that clade, and its 'basal' placement might be impacted by the possibly subadult nature of the published material (Mannion et al., 2021; Tschopp & Mateus, 2013), our results argue against the likelihood of *Kaatedocus* representing a dicraeosaurid.

Gondwanan diplodocids. By contrast with analyses based on different underlying data matrices (e.g. Tschopp & Mateus, 2017; Whitlock & Wilson Mantilla, 2020; Windholz et al., 2022), we continue to recover a phylogenetically nested Gondwanan diplodocine clade in which *Tornieria africana*, from the Tithonian Tendaguru Formation of Tanzania (Remes, 2006), is the sister taxon of *Leinkupal laticauda*, from the upper Berriasian–Valanginian Bajada Colorada Formation of Argentina (Gallina et al., 2014) (Figs 4–6). The sister-taxon relationship between these two species is supported by a high ratio (>2) of middle cervical neural spine to arch height (327:1), the anterolateral curvature of anterior caudal ribs (205:0) (Fig. 13C), and the absence of an anteroposteriorly elongate ridge two-thirds of the way up the lateral surface of middle caudal centra (183:0). We suspect that the discrepancy between our results and those of other studies arises from the exclusion of some of these characters, as well as those that unite these species with *Diplodocus* to the exclusion of more 'basal' diplodocids, including the presence of a lateral fossa on middle caudal centra (C509:1; Fig. 14C; Mannion, Upchurch, Schwarz, et al., 2019). Furthermore, by contrast with the present study (and previous iterations of this data matrix), the analyses of Tschopp et al. (2015) and Tschopp and Mateus (2017) restricted their *Leinkupal* OTU to the type caudal vertebra and did not include additional cervical vertebrae referrable to *Tornieira* (MfN MB.R.6022, 6023; see Remes, 2007, p. 663 and fig. 7c). Although our *Leinkupal* OTU does not include the partial braincase described by Garderes et al. (2022) from the type locality, the morphology of the latter specimen is broadly consistent with the corresponding region in *Tornieria*. Nevertheless, the topological effect of including the braincase in the *Leinkupal* OTU should be tested.

Recovery of *Pilmatueia faundezi* as a diplodocid in both EIW analyses (Figs 5, 6) runs counter to all previous studies, in which it has been consistently placed as a dicraeosaurid (Coria et al., 2019; Gallina et al., 2019; Whitlock and Wilson Mantilla, 2020; Windholz et al., 2022). *Pilmatueia* shares several features with diplodocids that are absent in most or all unambiguous dicraeosaurids, including: a median process between the metapophyses of bifurcated cervical vertebrae (C133:1; independently acquired in *Dicraeosaurus* and, under EIW9, in *Kaatedocus*), relatively wide centra in anterior (C21:1) and middle–posterior dorsal vertebrae (C22:1), and laterally directed middle–posterior dorsal diapophyses (C155:1) (Figs 10E, 11A). A diplodocid affinity for *Pilmatueia* is also made possible by the basally branching position of *Lingwulong* in our analyses, which has the effect of repolarizing characters formerly considered unique to dicraeosaurids and optimizing them as synapomorphic for Flagellicaudata, with secondary transformations occurring at deeper nodes within Diplodocidae. Such 'new' flagellicaudatan synapomorphies that inform the 'basal' position of *Pilmatueia* include: anteriorly inclined middle cervical neural spines (C460:1); parallel-to-converging metapophyses in bifid posterior cervical and anterior dorsal vertebrae (463:1; also present in *Kaatedocus*); solid internal tissue in middle–posterior dorsal vertebrae (C141:0); and middle–posterior dorsal vertebrae with undivided SPOLs (C165:0) (Figs 10E–G, 11C).

It is possible that continued study of *Pilmatueia* will reinstate dicraeosaurid affinities. A natural endocast from the type locality was described as belonging to a dicraeosaurid (Paulina Carabajal et al., 2018) and was not included in our *Pilmatueia* OTU because of a lack of association. It would be interesting to test the effect of its incorporation on the placement of *Pilmatueia* in future. Nevertheless, we note that Paulina Carabajal et al. (2018) did not make anatomical comparisons with diplodocids in their description of this endocast and so it remains possible that this specimen would not support a dicraeosaurid placement. Furthermore, fragmentary remains from the *Pilmatueia* type locality have been

identified as belonging to a diplodocid (Gnaedinger et al., 2017) and thus referral of *Pilmatueia* to this clade would not be surprising, at least from a biogeographical perspective. Finally, it remains possible that *Pilmatueia* is a chimera, with the disarticulated remains of both a dicraeosaurid and diplodocid included within this species.

Laurasian dicraeosaurids. We consistently recover a sister-taxon relationship between the Morrison Formation species *Smitanosaurus agilis* and *Suuwassea emilieae*, with this clade positioned as the earliest-diverging dicraeosaurid lineage. This contrasts with the analysis of Whitlock and Wilson Mantilla (2020), in which these species were distantly related to one another. The sister-taxon relationship between these two species is supported by a single feature: well-distanced openings in the basisphenoid for cranial nerves III and VI (C315:1).

The BYU 17096 OTU is also positioned as a 'basal' dicraeosaurid and appears to be distinct from the two named Morrison Formation species of this clade. This specimen, consisting of an isolated braincase, was originally referred to *Apatosaurus* by Balanoff et al. (2010). This referral was based partly on the ubiquity of *Apatosaurus* at the Cactus Park Quarry in western Colorado from which BYU 17096 was recovered, which contains hundreds of disarticulated or partially articulated specimens that have been assigned to *Apatosaurus*, as well as a partial skeleton of *Diplodocus* and a distal ischium possibly belonging to *Camarasaurus* (Curry, 1999; Foster, 2003; R. Wilhite, pers. comm., 2024). Balanoff et al. (2010) also drew on the phylogenetic results of Wilson (2002) to identify diplodocoid synapomorphies in BYU 17096, including two basicranial features specifically supporting referral of the specimen to *Apatosaurus*: a distinct recess between the basipterygoid processes, and an angle of approximately 60–70° separating these processes. However, we find that none of the features highlighted by Balanoff et al. (2010) are sufficient to justify referring BYU 17096 to *Apatosaurus*, as discussed below.

Referencing Wilson (2002), Balanoff et al. (2010) stated that *Apatosaurus* and *Nemegtosaurus* secondarily reacquired a recess between the basipterygoid processes, which is otherwise synapomorphically absent in neosauropods owing to the development of a rounded shelf (note that appendix 3 of Wilson [2002] erroneously reverses the distribution of this feature in summarizing taxon synapomorphies). Although not described in detail by either author, the shelf in question does not so much replace the recess on the ventral surface of the parabasisphenoid as divide it into two portions: a posterior depression of variable depth that extends towards the basal tubera, and an anterior fossa that reaches the base of the parasphenoid rostrum. Following the nomenclature applied to early dinosaurs (e.g. Bronzati et al., 2018), the posterior fossa corresponds to the basisphenoid recess and the anterior depression is equivalent to the subsellar recess. Among sauropods, the ridge separating these recesses and spanning the region between the basipterygoid processes is particularly apparent in specimens of taxa such as *Europasaurus* (Schade et al., 2022, fig. 2d), *Camarasaurus* (CM 11338), *Turiasaurus* (CPT-1211), *Sarmientosaurus* (MDT-PV 2), and perhaps also *Apatosaurus ajax* (YPM VP.001860; Berman & McIntosh, 1978, fig. 11b), although this region of the braincase is incompletely preserved in the latter. By contrast, an uninterrupted ventral depression of the parabasisphenoid is present in *Bagualia* (MPEF-PV 3301/1), *Abrosaurus* (ZDM 5038), and perhaps *Kaatedocus* (AMNH FARB 7530). Contrary to Balanoff et al. (2010), we recognize in BYU 17096 a broad ridge between the basipterygoid processes anteriorly, which separates a large basisphenoid recess from a small, flat subsellar recess. This morphology is consistent with that of *Camarasaurus* (CM 11338) and diplodocine specimens such as CM 11161 and USNM 2672, and thus cannot be used as a basis for referral of BYU 17096 to a particular diplodocoid genus. As an aside, we note that the current character pertaining to this recess (C99) requires revision.

The degree of angulation between the basipterygoid processes is also unconvincing as evidence supporting an *Apatosaurus* identity for BYU 17096. Upchurch, Tomida, et al. (2004) diagnosed *Apatosaurus* as having an angle of 60° between the basipterygoid processes. Although this is an atypically large value for sauropods, it is not unique. For example, *Bellusaurus* (IVPP 8299) and *Europasaurus* (Marpmann et al., 2015, fig. 13a, c) have angles of *c*. 56° and ∼67°, respectively. For BYU 17096, Balanoff et al. (2010) approximated this measurement as 60–70°, whereas we observed a larger angle of ∼79° when measuring directly from the CT scans. Notably, the difference in angle between BYU 17096 (79°) and the *Apatosaurus* specimen CM 11162 (60°; Berman & McIntosh, 1978) is nearly as great as that between the latter taxon and the unambiguous diplodocine specimen CM 11161 (39°). Thus, rather than supporting referral of BYU 17096 to *Apatosaurus*, the strong divergence of the basipterygoid processes in BYU 17096 may instead be autapomorphic. Unfortunately, the basipterygoid processes are not preserved in either *Smitanosaurus* or *Suuwassea*, limiting comparison of this feature to other Laurasian dicraeosaurids.

BYU 17096 bears several features that support its position as a dicraeosaurid. Like *Suuwassea*, *Smitanosaurus* and dicraeosaurines, BYU 17096 has a midline foramen between the basal tubera and basipterygoid processes (C99:0), narrowly diverging basal tubera (C314:0), and a frontoparietal (pineal) foramen (C558:1). In addition, it shares several features with the wholly Gondwanan dicraeosaurines that distinguish it from the other Laurasian dicraeosaurids: a postorbital without a pronounced, acuminate posterior process (C302:1), a supratemporal fenestra with a contribution from the frontal (299:0; *contra* Balanoff et al. [2010], who described the frontal as being excluded from the supratemporal fenestra), a crista prootica with a tab-like, dorsolaterally directed process near the base of the basipterygoid process (441:1; ACCTRAN), and a deep, well-demarcated muscular fossa at the base of the paroccipital processes (C440:1; secondarily absent in *Dicraeosaurus* and convergently present in *Lingwulong*).

Dicraeosaurinae. The Gondwanan dicraeosaurids form a phylogenetically nested clade to the exclusion of Morrison Formation species. Janensch (1929a) was the first to explicitly use Dicraeosaurinae for the genus *Dicraeosaurus*, although this subfamily name was technically created when Huene (1927) erected Dicraeosauridae. Regardless, Dicraeosaurinae has rarely been mentioned in the subsequent literature (Taylor & Naish, 2005). Previous authors have found some evidence for this Gondwanan clade, but have used terms such as 'advanced dicraeosaurids' to refer to it (e.g. Xu et al., 2018). The intrarelationships of this clade have also varied substantially between analyses (Gallina et al., 2019; Mannion, Upchurch, Schwarz, et al., 2019; Whitlock & Wilson Mantilla, 2020; Windholz et al., 2022). Here, we phylogenetically define Dicraeosaurinae as a clade for the first time, using a node-based definition of the least inclusive clade containing *Dicraeosaurus hansemanni* and *Bajadasaurus pronuspinax*. This definition has the benefit that the composition of Dicraeosaurinae herein is essentially the same as that recovered in Gallina et al. (2019) and in the preferred topology of Windholz et al. (2022), despite differing intrarelationships. As noted above, Dicraeosaurinae is supported by several unique and shared synapomorphies of the braincase (Fig. 9), and potentially by features of the axial skeleton (Fig. 10G).

Non-khebbashian rebbachisaurids. Both the EIW12 and EQW analyses recover *Amphicoelias altus* as the earliest-diverging rebbachisaurid in a subset of MPTs, which is an entirely novel placement. Previous analyses have recovered it as either a non-diplodocimorph diplodocoid (a position favoured by our EIW9 analysis) or an apatosaurine diplodocid (see Mannion et al., 2021). Although a rebbachisaurid position might seem like a substantial topological change, this essentially represents a movement from the 'base' of one clade to another. Nevertheless, *Amphicoelias* is known from only a few skeletal elements, and support for a rebbachisaurid placement is based on the absence of conflicting character information, rather than the presence of unambiguous rebbachisaurid synapomorphies. As such, this result should be treated with caution. It is interesting to note, however, that *Amphicoelias* is not the only putative rebbachisaurid from the Morrison Formation (see discussion of *Maraapunisaurus* below).

Whereas recent studies have supported dicraeosaurid affinities for *Amargatitanis macni* (Bajpai et al., 2023; Gallina, 2016; Whitlock & Wilson, 2020; Windholz et al., 2022), both of our EIW analyses place it as the earliest-branching rebbachisaurid (Figs 5, 6). Two unambiguous synapomorphies support this position: relatively elongate anterior-most caudal centra (26:1; also present in *Dicraeosaurus* and *Amargasaurus*), and a femur with the proximolateral margin medial to the lateral margin of its shaft (255:1; also present in *Amargasaurus*) (Fig. 16E). However, the possession of these features by some dicraeosaurines, and the placement of *Amargatitanis* in various flagellicaudatan positions in our EQW analysis, indicate that character conflict and specimen incompleteness complicate robust placement of *Amargatitanis* (see also D'Emic, 2012; Mannion et al., 2013; Gallina, 2016), and we view its specific diplodocoid affinities as unsettled.

A rebbachisaurid placement for *Xenoposeidon proneneukos* is supported for the first time herein by a phylogenetic analysis, in which it is recovered in both EIW analyses as the sister taxon of *Histriasaurus boscarollii* (based on the presence of lateral pneumatic foramina of the dorsal centra set within a lateral fossa; 145:1; Fig. 11E), with this clade outside of Khebbashia (Figs 5, 6). A rebbachisaurid affinity for *Xenoposeidon* is further supported by a dorsally bifurcated CPRL in middle–posterior dorsal vertebrae (473:1; also present in *Comahuesaurus* among non-khebbashian rebbachisaurids), and, though not included here as a character, by an 'M'-shaped arrangement of intersecting laminae on the lateral face of the neural arch (Taylor, 2018). However, under EQW, *Xenoposeidon* is recovered in numerous other non-rebbachisaurid positions, including within Flagellicaudata and as the sister taxon to the Early Cretaceous Spanish somphospondylan *Europatitan*, likely owing to the paucity of characters that can be scored for the highly incomplete specimen (see also Mannion et al., 2013; Taylor & Naish, 2007).

Under EIW, other non-khebbashian rebbachisaurids include *Amazonsaurus maranhensis*, *Astigmasaura genuflexa*, *Campananeyen fragilissimus*, *Comahuesaurus windhauseni*, *Lavocatisaurus agrioensis* and *Rayososaurus agrioensis*. We also recover *Katepensaurus goicoecheai* in a clade with *Zapalasaurus bonapartei*, forming the sister taxon to *Khebbashia*. A position outside of *Khebbashia* for most of these taxa is largely consistent with recent analyses, although the latter two species have sometimes been recovered as limaysaurines or rebbachisaurines (Canudo et al., 2018; Fanti et al., 2015; Ibiricu et al., 2015; Lerzo, Torcida Fernández-Baldor, et al., 2025; Mannion et al., 2012; Mannion, Upchurch, Schwarz, et al., 2019; Whitlock, 2011a; Whitlock and Wilson Mantilla, 2020).

Rebbachisaurinae. The internal relationships of Rebbachisaurinae are largely unchanged from those presented in Mannion, Upchurch, Schwarz, et al. (2019). This is broadly consistent with most other recent analyses (e.g. Whitlock & Wilson Mantilla, 2020; Wilson & Allain, 2015), although it contrasts with that of Lerzo, Torcida Fernández-Baldor, et al., (2025), in which *Rebbachisaurus garasbae*, one of the clade specifiers, clustered with limaysaurines instead, essentially making Limaysaurinae synonymous with Rebbachisaurinae. Our analyses consistently recover *Itapeuasaurus cajapioensis* as an additional member of Rebbachisaurinae, as the sister taxon to a clade formed by all other rebbachisaurines, a position supported by pneumatic excavations dorsolateral to the neural canal of middle–posterior dorsal vertebrae (472:1), and posterior dorsal vertebrae with parapophyses positioned dorsal to the prezygapophysis (477:1) (Fig. 12). In their original description of *Itapeuasaurus*, Lindoso et al. (2019) also recovered it as a rebbachisaurine, whereas the only other study to incorporate it into a phylogenetic analysis placed it outside of Khebbashia (Lerzo, Torcida Fernández-Baldor, et al., 2025). Our EIW12 analysis also includes a clade comprising the El Chocon rebbachisaurid and *Nopcsaspondylus* as the earliest-branching rebbachisaurines, whereas these taxa are found to be limaysaurines under EIW9, consistent with Mannion, Upchurch, Schwarz, et al. (2019).

Limaysaurinae. The composition of Limaysaurinae is particularly sensitive to the method of weighting homoplastic characters, forming a relatively depauperate lineage comprising only *Limaysaurus* and *Cathartesaura* under EIW12 and a more diverse clade that also includes the El Chocon rebbachisaurid and *Nopcsaspondylus* under EIW9 (Figs 5–7), similar to the results of Mannion, Upchurch, Schwarz, et al. (2019). Aside from taxa such as *Katepensaurus* sometimes appearing within this clade (e.g. Lerzo, Torcida Fernández-Baldor, et al., 2025), the composition of Limaysaurinae is generally consistent between recent phylogenetic analyses, with the main difference being the greater sampling of putative limaysaurine OTUs (e.g. *Nopcsaspondylus alarconensis* and MMCH-Pv-49) in both previous and current versions of this data matrix.

The evolutionary and biogeographical history of Diplodocoidea

Based on the results of our phylogenetic analyses, below we present an updated view on the evolutionary and biogeographical history of Diplodocoidea, emphasizing the results of our EIW12 analyses unless otherwise noted. As part of this, we incorporate information from occurrences that are not included in our phylogenetic data matrix. Although interpretation of their taxonomic affinities requires caution, owing to their typically fragmentary nature, we stress that it is important to consider such remains, especially when they represent stratigraphically early possible members of diplodocoid lineages (Figs 17, 18).

Middle Jurassic. Although our re-evaluation of *Tharosaurus* as an indeterminate eusauropod removes the evidence for diplodocoids from the pre-Late Jurassic southern Gondwanan record, the possibility that *Jobaria* represents a non-diplodocimorph diplodocoid (EQW analysis) would place the clade in at least northern Gondwana by the late Middle Jurassic (Fig. 17A). The stratigraphical provenance and thus age of the Chinese stem flagellicaudatan *Lingwulong shenqi* remain uncertain, given that it either comes from the Aalenian (lower Middle Jurassic) Yan'an Formation (Xu et al., 2018; Zhang et al., 2021) or Bathonian–Callovian (upper Middle Jurassic) Zhiluo Formation (You et al., 2019). Nevertheless, its Middle Jurassic age and phylogenetic placement (i.e. outside of Dicraeosauridae) are now more compatible with one another, reducing the otherwise lengthy ghost lineages within Flagellicaudata (Mannion, Upchurch, Schwarz, et al., 2019; Xu et al., 2018). *Cetiosauriscus stewarti*, from the Callovian Oxford Clay Formation of the UK, might be an additional stem flagellicaudatan. Fragmentary vertebral remains from the Oxford Clay Formation, along with the contemporaneous Podosinkovskaya Formation in western Russia, are potentially also attributable to Flagellicaudata (Averianov & Zverkov, 2020; Holwerda et al., 2019) and could belong to a *Lingwulong*-like sauropod. If correctly interpreted, these Callovian occurrences would provide evidence for a widespread distribution of Flagellicaudata-line diplodocimorphs across

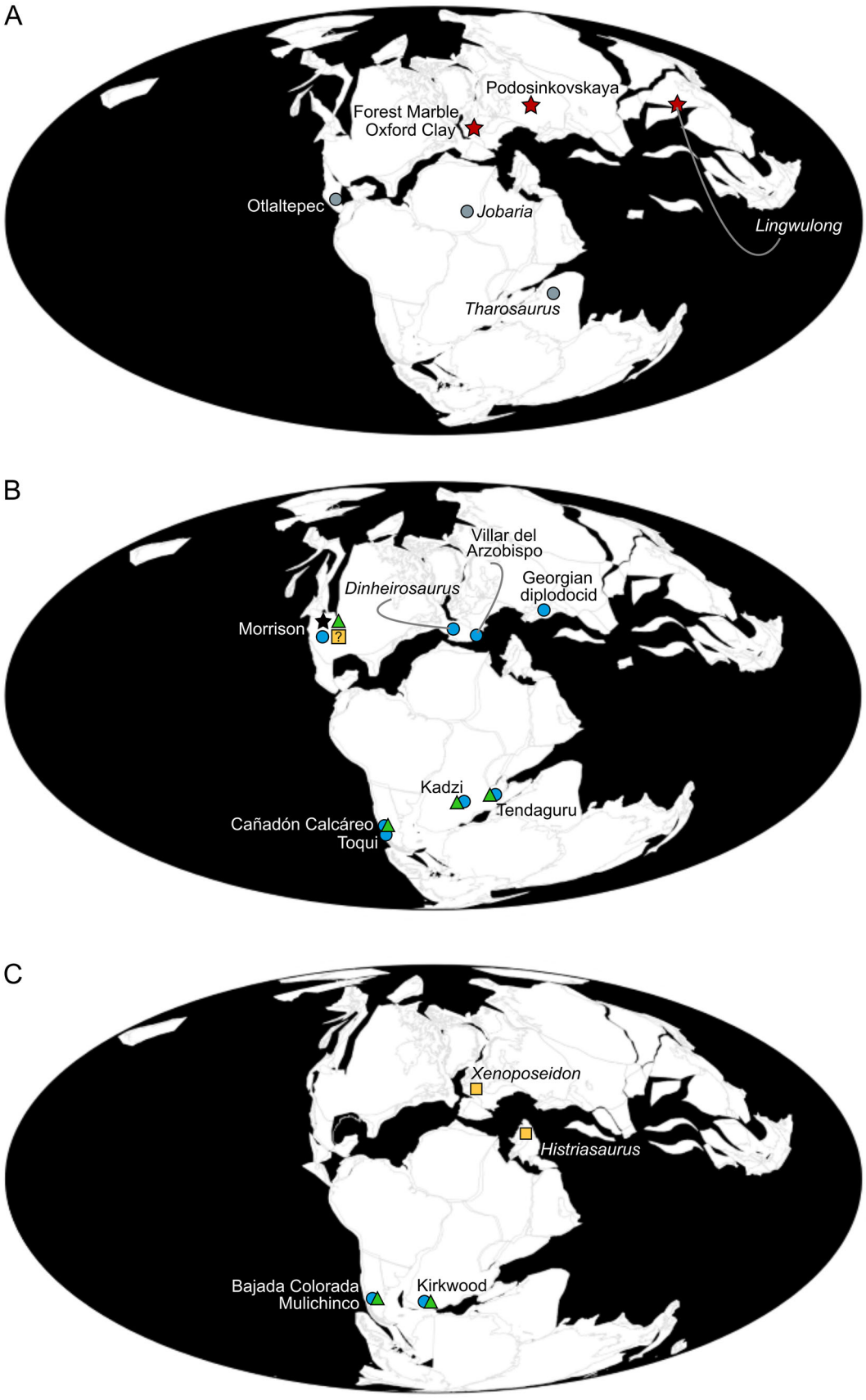
A
Podosinkovskaya
Forest Marble
Oxford Clay
Otlaltepec
Jobaria
Lingwulong
Tharosaurus
B
Villar del
Arzobispo
Georgian
diplodocid
Dinheirosaurus
Morrison
?
Kadzi
Tendaguru
Cañadón Calcáreo
Toqui
C
Xenoposeidon
Histriasaurus
Bajada Colorada
Mulichinco
Kirkwood

Eurasia at this time. Coupled with possible diplodocoid affinities for *Jobaria*, this therefore points to a distribution of Diplodocoidea across at least Eurasia and potentially North Africa by the late Middle Jurassic (Fig. 17A). Their apparent absence from North America at this time, which potentially formed the only viable connection between Eurasia and Gondwana by the late Middle Jurassic (e.g. Seton et al., 2012), can be explained by the lack of exposure of suitable dinosaur-bearing sedimentary rock outcrop. A similar explanation would account for the absence of northern South American diplodocoids.

A stratigraphically older European occurrence, consisting of nine middle–posterior caudal vertebrae from the Bathonian Forest Marble Formation of the UK, assigned to *Cetiosaurus glymptonensis* (Phillips, 1871), might represent an additional early diplodocoid (Upchurch & Martin, 2003). The presence of lateral ridges on the middle caudal centra (183:1), elongation of the posterior caudal centra (31:1), and the central placement of caudal neural arches (192:0) is a combination of features primarily observed in Diplodocoidea (Mannion et al., 2012; Upchurch & Martin, 2003). However, given that these features also characterize *Cetiosauriscus*, for which diplodocoid affinities remain uncertain, we conservatively regard *Cetiosaurus glymptonensis* as an indeterminate eusauropod (see also Whitlock, 2011a).

Rivera-Sylva and Espinosa-Arrubarrena (2020) assigned fragmentary metatarsals from the Bathonian–Callovian Otlaltepec Formation of Mexico to Flagellicaudata, which would provide evidence to support the hypothesis that diplodocoids were even more widespread across Laurasia by the late Middle Jurassic (Fig. 17A). However, the anatomical features used to assign these remains to Flagellicaudata are more broadly distributed among eusauropods and there is no basis for attributing this occurrence to Neosauropoda (Mannion & Whitlock, in press). Nevertheless, given that diplodocoids must have originated by at least the Middle Jurassic and were present in both Americas by the Kimmeridgian (middle Late Jurassic), it would not ultimately be surprising to discover diplodocoids in the late Middle Jurassic of Mexico.

Late Jurassic. The non-diplodocimorph diplodocoid clade formed by *Jobaria* and the Upper Jurassic Morrison Formation species *Haplocanthosaurus priscus* and *Haplocanthosaurus delfsi* in the EQW analysis is potentially indicative of dispersal between North Africa and North America. However, as with biogeographical explanations for close relationships between sauropods from the Morrison and Tendaguru formations, any such dispersal likely took place in the Middle Jurassic or earliest Late Jurassic (see Mannion, Upchurch, Schwarz, et al., 2019), i.e. prior to the separation of Gondwana and Laurasia (Seton et al., 2012; Scotese, 2021). Furthermore, given their spatiotemporal separation, we suggest that *Jobaria* and *Haplocanthosaurus* are likely to be members of a larger, mostly unsampled clade of early diplodocoids, rather than close relatives of one another, which is reinforced by their distant relationship in our EIW analyses.

Apatosaurinae is known only from the Morrison Formation, consisting of several species of *Apatosaurus* and *Brontosaurus* (Foster & Peterson, 2016; Tschopp et al., 2015). Late Jurassic diplodocines also predominantly come from this stratigraphical unit, comprising *Ardetosaurus viator*, *Barosaurus lentus*, *Diplodocus* spp., *Galeamopus* spp., *Kaatedocus siberi* and *Supersaurus vivianae* (Jensen, 1985; Lovelace et al., 2008; McIntosh, 2005; Tschopp & Mateus, 2013, 2017; Tschopp et al., 2015; van der Linden et al., 2024). The latter species is the sister taxon of *Dinheirosaurus lourinhanensis*, from the upper Kimmeridgian–lower Tithonian Lourinhã Formation of Portugal (Bonaparte & Mateus, 1999; Mannion et al., 2012). Dispersal between North America and Iberia appears to have been possible at this time (Brikiatis, 2016) (Fig. 17B).

Although some Morrison Formation diplodocids might conceivably date from the upper Oxfordian, most, if not all, of the remains appear to be restricted to the upper Kimmeridgian–Tithonian (e.g. Maidment, 2023; Tschopp et al., 2015). Therefore, an anterior caudal vertebral centrum from the Oxfordian of Georgia (Fig. 17B), which appears to be referrable to Diplodocinae (Gabunia et al., 1998), might represent the stratigraphically earliest known diplodocid (Mannion et al., 2012; Tschopp et al., 2015). At least one specimen (an anterior caudal centrum) from the Villar del Arzobispo Formation of Spain is also attributable to a diplodocine (Royo-Torres et al., 2009). At the time of the description of this specimen, the age of this formation was constrained to the Tithonian–Berriasian, which might have indicated that this was an example of a Jurassic/

Figure 17. Palaeogeographical distribution of Diplodocoidea, showing occurrences in the **A,** Middle Jurassic; **B,** Late Jurassic; and **C,** earliest Cretaceous (Berriasian–Hauterivian). Grey circles = putative diplodocoids; black stars = non-diplodocimorph diplodocoids; red stars = stem flagellicaudatans; blue circles = diplodocids; green triangles = dicraeosaurids; orange squares = rebbachisaurids. Palaeogeographical reconstructions utilize GPlates and were modified from *The Paleobiology Database's* Navigator (https://paleobiodb.org/navigator/). The palaeogeographical maps represent the **A**, Bathonian; **B**, Kimmeridgian; and **C**, Valanginian stages.

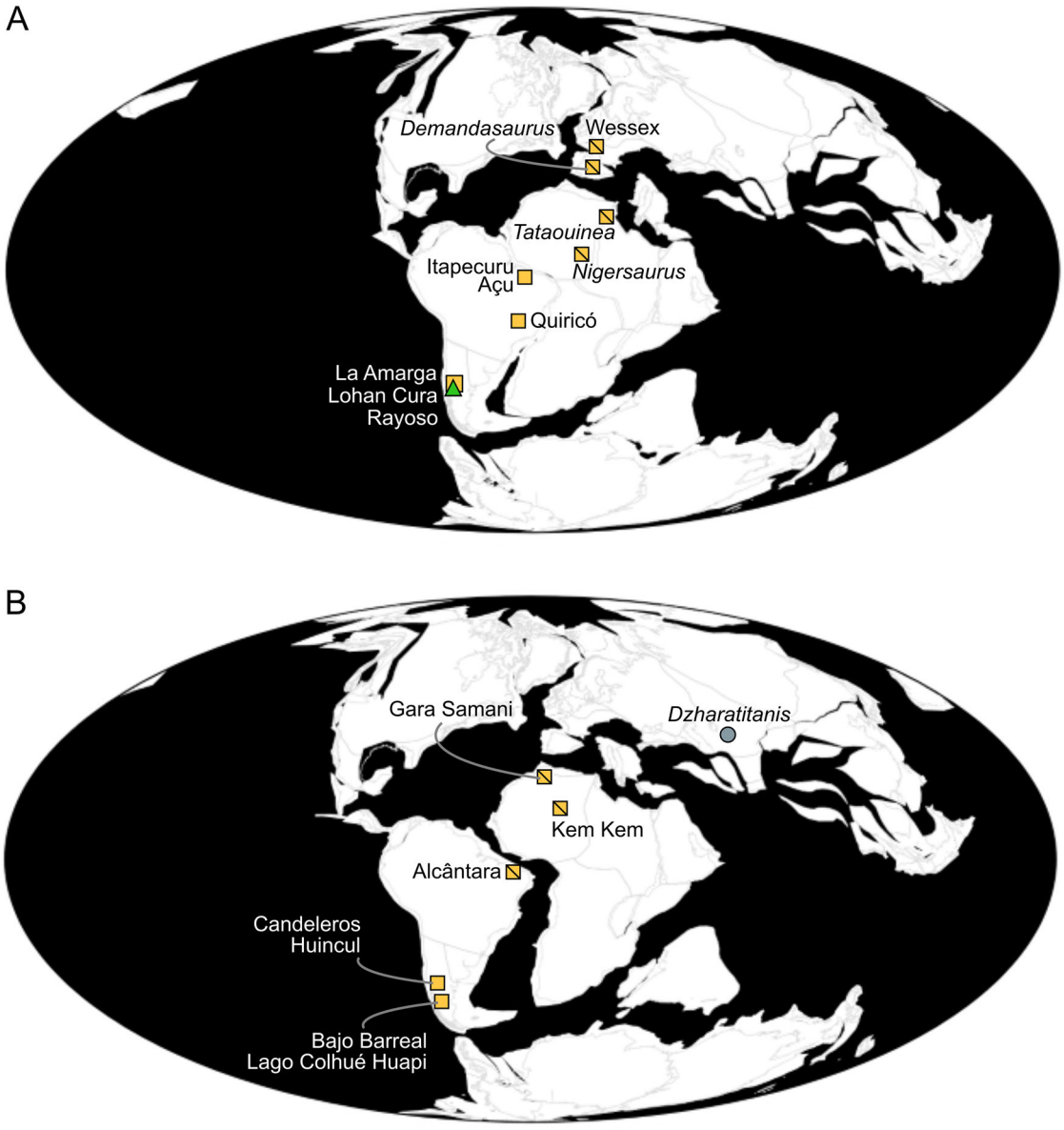

Figure 18. Palaeogeographical distribution of Diplodocoidea, showing occurrences in the **A,** late Early Cretaceous (Barremian–Albian); and **B,** early Late Cretaceous (Cenomanian–Coniacian). Grey circles = putative diplodocoids; green triangles = dicraeosaurids; orange squares = rebbachisaurids; orange square with a diagonal line = rebbachisaurines. Palaeogeographical reconstructions utilize GPlates and were modified from *The Paleobiology Database*'s Navigator (https://paleobiodb.org/navigator/). The palaeogeographical maps represent the **A**, Aptian and **B**, Cenomanian stages.

Cretaceous (J/K) boundary-crossing flagellicaudatan lineage (see below). However, the Villar del Arzobispo Formation is now dated to the Kimmeridgian–Tithonian (Campos-Soto et al., 2019). Fragmentary remains of diplodocines have also been documented from the upper Kimmeridgian–Tithonian Praia da Amoreira-Porto Novo, Bombarral, and Freixial formations in Portugal (Mannion et al., 2012; Mocho et al., 2017; Tschopp et al., 2015). It is not possible to currently determine if these Georgian and Iberian remains belong to species more closely related to *Dinheirosaurus* + *Supersaurus* than to other diplodocines.

Although too fragmentary to robustly test via phylogenetic analysis, we hypothesize that remains from the Kimmeridgian Cañadón Calcáreo of Argentina (Rauhut et al., 2015), the Tithonian Toqui Formation of Chile (Salgado et al., 2015), and the Tithonian Kadzi Formation of Zimbabwe (Raath & McIntosh, 1987)

(Fig. 17B) belong to the Gondwanan diplodocine clade formed by the Tendaguru species *Tornieria africana* (Remes, 2006) and its sister taxon, *Leinkupal laticauda*, from the upper Berriasian–Valanginian Bajada Colorada Formation of Argentina (Gallina et al., 2014) (see also McPhee et al., 2016). The Chilean material shares the presence of a lateral fossa on middle caudal centra (C509:1) with diplodocines more derived than *Dinheirosaurus* + *Supersaurus* (Fig. 14C).

Late Jurassic dicraeosaurids are present in the Morrison Formation (Fig. 17B), represented by *Smitanosaurus agilis*, *Suuwassea emilieae*, probably *Dyslocosaurus polyonychius*, and perhaps *Dystrophaeus viaemalae* (Mannion et al., 2021; Tschopp et al., 2015; Whitlock, 2011a; Whitlock & Wilson Mantilla, 2020). Additional dicraeosaurid taxa are likely present based on currently unnamed material, including BYU 17096. The remaining Late Jurassic dicraeosaurids are Gondwanan, consisting of *Dicraeosaurus* spp. from the Tendaguru Formation (Janensch, 1914) and *Brachytrachelopan mesai* from the Kimmeridgian–lower Tithonian Cañadón Calcáreo Formation of Argentina (Rauhut et al., 2005) (Fig. 17B). Our analyses suggest that the Gondwanan taxa (including Cretaceous species) form a phylogenetically nested clade (Dicraeosaurinae) and might be indicative of a Laurasian origination of Dicraeosauridae prior to dispersal into Gondwana (see also Whitlock, 2011a).

Given that our analyses recover *Kaatedocus siberi* as a 'basal' diplodocid outside of the apatosaurine–diplodocine split (or potentially as a stem flagellicaudatan), that Apatosaurinae is restricted to the Morrison Formation, and that the earliest diverging dicraeosaurids also come from this stratigraphical unit, this might provide evidence that the flagellicaudatan divergence occurred in North America (e.g. Whitlock & Wilson Mantilla, 2020). However, we urge caution in this interpretation given the widespread distribution of diplodocids and dicraeosaurids in the Late Jurassic (Fig. 17B), which suggests that major intraclade divergences occurred prior to our sampling of the stratigraphically earliest known occurrences. The Morrison Formation might capture an unusually rich ecosystem and diplodocids and dicraeosaurids might have radiated here; however, it is also conceivable that the Morrison Formation is only unusual in terms of the quality and quantity of our sampling of it and that other ecosystems would be similarly diverse if sampled to the same extent (Mannion, 2024).

Cope (1878) erected *Amphicoelias fragillimus* based on a middle–posterior dorsal neural arch from the Morrison Formation. Despite the subsequent loss or destruction of this specimen, Carpenter (2018) interpreted it to represent a rebbachisaurid based on the solitary drawing in posterior view presented in Cope (1878), erecting the new genus *Maraapunisaurus*. Although subsequent authors have been wary of this interpretation (e.g. Bellardini et al., 2022; Lerzo, Torcida Fernández-Baldor, et al., 2025; Mannion et al., 2021; Salgado et al., 2022; Whitlock & Wilson Mantilla, 2020), the available information on the anatomy of the dorsal neural arch is at least consistent with a rebbachisaurid identification (Carpenter, 2018). Coupled with the recovery of *Amphicoelias altus* as a rebbachisaurid in a subset of MPTs in our EIW12 and EQW analyses (Table 2), it is therefore plausible that rebbachisaurids were present in the Morrison Formation (Fig. 17B). If true, such a scenario would cast doubt on repeated assertions that rebbachisaurids originated in South America (see below). Regardless of the affinities of *Amphicoelias and Maraapunisaurus*, we should expect to find rebbachisaurids in the Late Jurassic (and earlier), given that the group must have been present in the Middle Jurassic based on its sister-taxon relationship with *Flagellicaudata*. Furthermore, rebbachisaurids should be present in Laurasia at this time given the distribution of the earliest stem flagellicaudatans and non-diplodocimorph diplodocoids on this landmass (Figs 17A, B). Finally, the pre-Cretaceous absence of unequivocal rebbachisaurids is potentially indicative of a genuine rarity of this clade in the Jurassic, perhaps reflecting low diversity and abundance. As such, it remains possible that the fragmentary remains from which *Amphicoelias and Maraapunisaurus* are known is all we have currently found of this clade in the well-sampled Morrison Formation because members of Rebbachisauridae were genuinely rare. This potentially parallels the record of Brachiosauridae in the Morrison Formation, with remains belonging to this clade exceedingly scarce in comparison to those of diplodocids (e.g. Foster, 2003).

Early Cretaceous. Prior to the relatively recent discovery of Cretaceous representatives in Gondwana (Gallina et al., 2014), diplodocids were thought to have gone extinct at the J/K boundary (Upchurch & Barrett, 2005). A number of remains from the Cretaceous of Eurasia have been assigned to Flagellicaudata, but these assignments have all been convincingly refuted (Mannion et al., 2012; Upchurch & Mannion, 2009; Whitlock et al., 2011). A partial hind limb from the Barremian Wessex Formation of the UK could potentially represent a flagellicaudatan, but most likely belongs to a somphospondylan titanosauriform (Higgins et al., 2024).

The continued absence of unequivocal diplodocids and dicraeosaurids from the Cretaceous Laurasian record (Fig. 17C) suggests that they might have become extirpated at the J/K boundary in the Northern Hemisphere.

However, the relative scarcity of lowermost Cretaceous deposits, especially outside of Europe (Tennant et al., 2017), combined with the skeletal incompleteness of most sauropod specimens from this time interval (Cashmore et al., 2020), means that support for this must remain tentative. For example, until recently, the dearth of pre-Barremian terrestrial deposits in North America meant that it was impossible to determine whether the Morrison Formation diplodocoids died out at the J/K boundary or afterwards (D'Emic & Foster, 2016). However, the revised chronostratigraphical framework for the Yellow Cat Member of the Cedar Mountain Formation in Utah dates this stratigraphical unit to the upper Berriasian–Valanginian (Joeckel et al., 2023). Given the preservation of titanosauriforms and turiasaurians in this unit (Kirkland et al., 2024; Royo-Torres et al., 2017; Tidwell et al., 1999), this suggests that the absence of diplodocoids is genuine, and provides some support that the demise of Laurasian representatives of the clade occurred at or close to the J/K boundary (Mannion, 2024). One possible exception is a partial skeleton from the upper Valanginian–lower Hauterivian Sao Khua Formation of Thailand, which might represent a flagellidautan (Eiamlaor et al., 2025); however, this material is yet to be described.

Flagellicaudata is currently therefore known with certainty only from Gondwana in the Cretaceous (Figs 17C, 18). Unequivocal diplodocid remains are restricted to the Berriasian–Valanginian, emanating from the Bajada Colorada and Mulichinco formations of Argentina (Gallina et al., 2014; Garderes et al., 2022; Gnaedinger et al., 2017) and the Kirkwood Formation of South Africa (McPhee et al., 2016) (Fig. 17C). Currently, generically diagnostic remains are limited to *Leinkupal laticauda*, from the Bajada Colorada Formation (Gallina et al., 2014), and, according to the analyses presented herein, *Pilmatueia faundezi* from the Mulichinco Formation (Coria et al., 2019). As noted above, our phylogenetic analyses support previous iterations of this matrix (Mannion, Upchurch, Schwarz, et al., 2019) in recovering *Leinkupal* as the sister taxon of *Tornieria*, which is consistent with a lineage of Gondwanan diplodocine diplodocids crossing the J/K boundary. The diplodocid specimen from the Kirkwood Formation is a partial caudal vertebra that is too incomplete to robustly test its phylogenetic affinities, but it appears to belong to the same diplodocine clade as *Leinkupal* + *Tornieria* (e.g. McPhee et al., 2016). If correctly assigned to Diplodocidae, *Pilmatueia* would represent a second J/K boundary-crossing diplodocid lineage.

Bandeira et al. (2025) interpreted two isolated vertebrae from the Early Cretaceous of north-eastern Brazil as diplodocines. One of these, from the Valanginian–Hauterivian Marfim Formation, preserves the posterior portion of a centrum, as well as part of the base of the corresponding neural arch, and was described as a middle–posterior caudal vertebra. Bandeira et al. (2025) only made comparisons with diplodocoids and so it is not clear on what anatomical basis the referral to Diplodocoidea was made; however, it is likely that the presence of an extensive lateral fossa and a ventral longitudinal hollow were the primary contributing features in this identification. In diplodocines that are characterized by a lateral fossa, this opening tends to be deep and positioned dorsally on the lateral surface of the centrum (e.g. Fig. 3G), whereas the opening on the Brazilian specimen is shallower and more centrally positioned. The ventral longitudinal hollow is potentially more compelling evidence of diplodocine affinities, but this feature also characterizes many somphospondylans (e.g. Mannion, Upchurch, Schwarz, et al., 2019). Given the poor preservation and limited nature of the specimen, we consider it more conservative to interpret it as an indeterminate neosauropod, although it is not clear that it unequivocally represents a sauropod dinosaur at all. The second specimen described by Bandeira et al. (2025) is from the Berriasian–Barremian Salvador Formation and preserves a complete centrum and its corresponding neural arch, which those authors interpreted as a posterior caudal vertebra. Comparisons were only made with diplodocines, but this identification was probably based primarily on the occurrence of a small fossa positioned at midheight and midlength on each lateral surface of the centrum, as well as the presence of ventrolateral ridges. The latter feature characterizes numerous somphospondylans (see above), as well as some diplodocids, and so does not support attribution to the latter clade by itself. An equivalent lateral fossa has not been described in a caudal vertebra this distal in the tail in any sauropod, to our knowledge, but characterizes both diplodocoids and somphospondylans in the more proximal region of the tail (e.g. Wilson, 2002; Mannion, Upchurch, Schwarz, et al., 2019). As such, this feature also cannot be used to support referral to Diplodocidae. Finally, we remain uncertain that this specimen unequivocally represents a sauropod, given that it also has similarities to the posterior caudal vertebrae of some coelurosaurian theropods (e.g. Weishampel et al., 2004). Consequently, we conservatively assign it to an indeterminate saurischian.

Dicraeosaurids are known from the same three Berriasian–Valanginian stratigraphical units as Cretaceous unequivocal diplodocids (Gallina et al., 2019; Garderes et al., 2024; McPhee et al., 2016; Paulina Carabajal et al., 2018) (Fig. 17C), but their

distribution also extends into the Barremian La Amarga Formation of Argentina (Gallina, 2016; Gallina et al., 2022; Paulina Carabajal et al., 2014; Salgado & Bonaparte, 1991; Salgado & Calvo, 1992; Windholz et al., 2021) (Fig. 18A). The material from the Kirkwood Formation is too incomplete to diagnose to genus level, but it appears to be from a close relative of *Dicraeosaurus* (McPhee et al., 2016). Within Dicraeosauridae, it appears that only members of Dicraeosaurinae survived into the Cretaceous. Generically diagnostic remains comprise *Bajadasaurus pronuspinax* from the Bajada Colorada Formation (Gallina et al., 2019) and *Amargasaurus cazaui* from the La Amarga Formation (Salgado & Bonaparte, 1991). *Amargatitanis macni* is an additional species from the latter stratigraphical unit that might represent another dicraeosaurine, but it is known from fragmentary, incomplete remains (Apesteguía, 2007; Gallina, 2016) and its phylogenetic affinities are uncertain, with some of our analyses supporting a rebbachisaurid placement instead (Table 2).

The stratigraphically oldest known unequivocal rebbachisaurid is *Xenoposeidon proneneukos* from the upper Berriasian–lower Valanginian Ashdown Formation of the UK (Taylor, 2018) (Fig. 17C). The confirmation of *Xenoposeidon* as a rebbachisaurid, which is supported herein via phylogenetic analysis for the first time, means that the J/K extinction of Laurasian diplodocoids was restricted to flagellicaudatans and taxa outside of Diplodocimorpha. Previous authors have not only not included *Xenoposeidon* in their phylogenetic analyses, but have typically ignored it in discussions of biogeography too (e.g. Lerzo, Torcida Fernández-Baldor, et al., 2025). Instead, a Gondwanan origin for rebbachisaurids has been argued for based on the sampled taxa recovered at the base of topologies (e.g. the Aptian–Albian Brazilian taxon *Amazonsaurus*; see discussion in Salgado et al., 2022). Yet these 'basal' rebbachisaurids are from stratigraphically younger deposits (late Hauterivian/early Barremian onwards) than *Xenoposeidon*. Although we should not denote a centre of origin based solely on the stratigraphically oldest occurrence of a clade, and *Xenoposeidon* is not recovered as the earliest diverging rebbachisaurid in our analyses, the most substantial problem with a proposed Gondwanan origin for the clade is that this ignores the long ghost lineage for Rebbachisauridae that extends back to the Middle Jurassic (potentially punctuated by the Late Jurassic Laurasian taxa *Amphicoelias* and *Maraapunisaurus*; see above): we contend that there is little reason to reconstruct a Gondwanan origin for the clade based on a large number of species on this landmass *c*. 40 million years later. Furthermore, given that the earliest known occurrences of stem flagellicaudatans are from the Middle Jurassic of Laurasia (Fig. 17A), we would expect that the sister taxon of this clade, Rebbachisauridae, would also first appear there in the fossil record. The presence of *Xenoposeidon* in the earliest Cretaceous of Europe also cannot be explained as a geologically recent dispersal from Gondwana given that the latter landmass had separated from Laurasia by the early Late Jurassic (see above) (Fig. 17B). It remains possible that rebbachisaurids were restricted to Laurasia prior to landbridges reconnecting it with Gondwana in the Barremian, which is the stratigraphical age of the earliest occurrences of this clade on that landmass. However, we suggest a more likely explanation is that rebbachisaurids were already more widespread and that their Late Jurassic–earliest Cretaceous Gondwanan absence reflects a combination of genuine rarity and sampling failure.

As noted by Dalla Vecchia (1998, 2005), the Croatian rebbachisaurid *Histriasaurus boscarollii*, from an unnamed stratigraphical unit dated to the upper Hauterivian–lower Barremian, should be regarded as a Gondwanan, rather than a Laurasian occurrence, given that this region was part of the Afro-Arabian plate at this time (Fig. 17C). Its sister-taxon relationship with the stratigraphically older species *Xenoposeidon* is potentially indicative of dispersal between Europe and Africa for this non-khebbashian lineage, which would have been viable via the Apulian route, at least in the Barremian (Canudo et al., 2009; Dalla Vecchia, 2005; Torcida Fernández-Baldor et al., 2011). With the exception of *Xenoposeidon*, Cretaceous Laurasian rebbachisaurids consist of the rebbachisaurine *Demandasaurus darwini* from the upper Barremian–lower Aptian Castrillo de la Reina Formation of Spain (Pereda Suberbiola et al., 2003; Fernández-Baldor et al., 2011), as well as indeterminate remains of a closely related species from the Barremian Wessex Formation of the UK (Sereno & Wilson, 2005; Mannion, 2009; Mannion et al., 2011) (Fig. 18A).

Rebbachisaurines were also present on the African continent during the Early Cretaceous (Fig. 18A). *Nigersaurus taqueti* was erected by Sereno et al. (1999) for material from the Aptian–Albian Elrhaz Formation of Niger (see also Sereno & Wilson, 2005; Sereno et al., 2007). Remains documented from here earlier by Taquet (1976) likely also belong to this species. *Tataouinea hannibalis*, from the lower Albian Aïn el Guettar Formation of Tunisia, demonstrates the presence of a second Early Cretaceous North African rebbachisaurine species (Fanti et al., 2013, 2015). Indeterminate rebbachisaurid remains from this formation are too fragmentary to determine if they also belong to

Rebbachisaurinae (Fanti et al., 2014; Holwerda, 2020). This Afro-European clade of rebbachisaurine khebbashians is not closely related to *Xenoposeidon* + *Histriasaurus*, but it is probable that its distribution can be attributed to the same Apulian dispersal route between Africa and Europe that was likely available in the Barremian–Albian.

Lerzo (2024) reinterpreted a rebbachisaurid dorsal neural arch (MACN PV 35) from the Barremian La Amarga Formation of Argentina, previously described by Apesteguía (2007), as a rebbachisaurine. This was primarily based on the presence of a mediolaterally elongate, channel-like laterodiapophyseal fossa that the specimen shares with the lower Upper Cretaceous Argentinean species *Katepensaurus goicoecheai* (Ibiricu et al., 2013), which has sometimes been recovered within Rebbachisaurinae. However, Mannion, Upchurch, Schwarz, et al. (2019) demonstrated that a laterodiapophyseal fossa (or fenestra; C479-1) is more widespread amongst rebbachisaurids (Fig. 12), given that it is also present in some possible limaysaurines (i.e. the lower Upper Cretaceous Argentinean species *Nopcsaspondylus alarconensis* and MMCH-Pv-49), in addition to the unequivocal rebbachisaurine *Nigersaurus*. It has also been recognized in the lower Upper Cretaceous Argentinean species *Campananeyen fragilissimus* (Lerzo, Torcida Fernández-Baldor, et al., 2025), which we recover as a non-khebbashian rebbachisaurid. As such, we do not consider a rebbachisaurine position for MACN PV 35 as robustly supported and we regard it is an indeterminate rebbachisaurid.

The remaining diversity of Early Cretaceous rebbachisaurids is from South America and appears to lie outside of Khebbashia (Fig. 18A). This includes *Amazonsaurus maranhensis*, from the Aptian–Albian Itapecuru Formation of Brazil (Carvalho et al., 2003), which is recovered as one of the earliest-branching rebbachisaurids. Other remains from this formation are too fragmentary to determine if they are referrable to *Amazonsaurus*, but can be assigned to Rebbachisauridae (Castro et al., 2007). Fragmentary specimens from the Barremian–Aptian Quiricó Formation (Carvalho & Santucci, 2018) and Albian–Cenomanian Açu Formation (Costa Pereira et al., 2020) of Brazil (Fig. 18A) are also too incomplete to identify beyond Rebbachisauridae. Early Cretaceous Argentinean non-khebbashian rebbachisaurids are represented by: *Zapalasaurus bonapartei*, from the Barremian La Amarga Formation; *Lavocatisaurus agrioensis* from the Aptian–lower Albian Rayoso Formation (Canudo et al., 2018; Salgado et al., 2012); and *Comahuesaurus windhauseni* from the upper Aptian–Albian section of the Lohan Cura Formation (Carballido et al., 2012; Salgado et al., 2004) (Fig. 18A). Although not included in our phylogenetic analysis, it seems likely that *Agustinia ligabuei*, from a stratigraphically higher (Albian) section of the Lohan Cura Formation (Bonaparte, 1999), is another non-khebbashian rebbachisaurid (Bellardini et al., 2023).

Late Cretaceous. Rauhut (1999) referred remains from the Wadi Milk Formation of Sudan to Dicraeosauridae. At the time, this formation was regarded as Cenomanian, but it has since been dated to the Campanian–Maastrichtian (Owusu Agyemang et al., 2019). Although some authors have continued to list this Sudanese occurrence as evidence for the survival of Dicraeosauridae into the Late Cretaceous (e.g. Windholz et al., 2021, 2022), Mannion and Barrett (2013) re-evaluated these remains and demonstrated that they represent indeterminate somphospondylans. As such, the stratigraphically youngest remains that can be attributed to Dicraeosauridae are from the Barremian (Fig. 18A).

Averianov and Sues (2021) erected *Dzharatitanis kingi* for a caudal vertebra from the Turonian Bissekty Formation of Uzbekistan (Fig. 18B). Those authors referred *Dzharatitanis* to Rebbachisauridae, which would make it the stratigraphically youngest Laurasian member of the clade, and the first Eurasian occurrence recovered from east of western Europe. However, Averianov and Sues (2021) utilized a phylogenetic data matrix containing very few non-diplodocoid taxa and, as demonstrated by Lerzo et al. (2021), *Dzharatitanis* lacks rebbachisaurid synapomorphies (Figs 13, 14). Lerzo et al. (2021) proposed that *Dzharatitanis* instead belongs to Somphospondyli, as part of the lognkosaurian titanosaurian radiation. Although we agree that *Dzharatitanis* is a somphospondylan, rather than a rebbachisaurid, Lerzo et al. (2021) made no comparisons with contemporaneous Eurasian taxa, such as *Dongyangosaurus*, which it greatly resembles (Sues et al., 2015). As such, we follow Díez Díaz et al. (2025) in suggesting that *Dzharatitanis* is more likely to belong to a clade of Eurasian somphospondylans close to the titanosaurian radiation (e.g. Mannion, Upchurch, Jin, et al., 2019; Han et al., 2024), rather than a member of the primarily Gondwanan Lognkosauria. Regardless, Cretaceous Laurasian rebbachisaurids are therefore currently known only from western Europe and from deposits no younger than the lower Aptian (Figs 17, 18).

Late Cretaceous occurrences of Rebbachisauridae are known only from Gondwana (Fig. 18B). Numerous remains have been documented from the lower Cenomanian Kem Kem Group of Morocco, comprising the rebbachisaurine *Rebbachisaurus garasbae* (Lavocat, 1954; Wilson & Allain, 2015) and indeterminate material that might belong to this species (Holwerda et al., 2018; Ibrahim et al., 2020; Mannion and Barrett, 2013;

Russell, 1996). Lapparent (1960) erected a second species of *Rebbachisaurus* (*R. tamesnensis*) for material from numerous Cretaceous localities within the 'Continental Intercalaire' of northern Africa. Although the stratigraphical ages of these deposits vary and are typically poorly constrained, only a single specimen amongst this generically undiagnostic material preserves rebbachisaurid synapomorphies (MNHN unnumbered, PDM pers. obs., 2016). This specimen comes from the Djoua Valley of Algeria and is likely from the lower Cenomanian Gara Samani Formation or a lateral correlate (e.g. Benyoucef et al., 2022). Lapparent (1960, p. 33 and pl. 7, fig. 3) identified this specimen as a dorsal vertebra, but it is clearly an anterior caudal vertebra. It can be assigned to Rebbachsauridae based on a number of features, including the restriction of ribs to the neural arch and dorsal margin of the centrum (Figs 13, 14) (see Mannion et al., 2011; Mannion, Upchurch, Schwarz, et al., 2019). Unfortunately, it does not overlap anatomically with remains assignable to *Rebbachisaurus garasbae*. However, it shares the presence of a large and deep lateral pneumatic foramen on the upper third of the centrum with an isolated rebbachisaurid anterior caudal vertebra from the Kem Kem Group (Mannion & Barrett, 2013); given that *Rebbachisaurus garasbae* is the only currently recognized rebbachisaurid from this stratigraphical unit, this provides circumstantial evidence that *Rebbachisaurus tamesnensis* represents a rebbachisaurine. Regardless, we consider this species a *nomen dubium*. As with their Early Cretaceous distribution, early Late Cretaceous rebbachisaurids are only known from north-western Africa (Fig. 18), with the Trans-Saharan Seaway potentially representing a barrier to dispersal to the remainder of the continent (Mannion & Barrett, 2013).

The remaining known Late Cretaceous diversity comes from South America (Fig. 18B). An abundance of specimens, representing numerous species, have been described from the Cenomanian–Turonian of Argentina, along with rare remains from the Cenomanian of Brazil. Several species appear to lie outside of Khebbashia, consisting of: *Campananeyen fragilissimus* (Lerzo, Torcida Fernández-Baldor, et al., 2025; Paulina Carabajal et al., 2016) and *Rayososaurus agrioensis* (Bonaparte, 1996, 1997; Carballido et al., 2010) from the lower Cenomanian Candeleros Formation; *Astigmasaura genuflexa*, *Cienciargentina sanchezi* and *Sidersaura marae* from the upper Cenomanian–lower Turonian Huincul Formation (Bellardini et al., 2025; Lerzo, Gallina, et al., 2025; Simón & Salgado, 2025); and *Katepensaurus goicoecheai* from the upper Cenomanian–Turonian Bajo Barreal Formation (Ibiricu et al., 2013, 2015, 2017). Additional remains from the latter formation have been suggested to be referrable to Limaysaurinae (Ibiricu et al., 2012, 2015), but might be best regarded as indeterminate rebbachisaurids (Ibiricu et al., 2020). Some authors have commented upon this survival of 'basal' lineages of rebbachisaurids into the Late Cretaceous (e.g. Lerzo, Gallina, et al., 2025); however, this partly reflects how we choose to illustrate and visualize phylogenetic topologies and decide that one lineage is 'basal' and the other is 'derived' (e.g. see Bronzati, 2017). Ultimately, the survival of these non-khebbashian lineages into the Late Cretaceous is no more unexpected than the survival of rebbachisaurines.

Windholz et al. (2024) described a well-preserved anterior caudal vertebra (MDPA-Pv 007) from the Candeleros Formation, which they recovered within Rebbachisaurinae. However, the feature that united MDPA-Pv 007 with rebbachisaurines in their analyses is also present in taxa recovered outside of Khebbashia in ours: the presence of triangular lateral processes near the apex of anterior caudal neural spines characterizes *Katepensaurus* (Ibiricu et al., 2013) and is also incipiently present in *Zapalasaurus* (Salgado et al., 2006). As such, we consider it more prudent to regard MDPA-Pv 007 as an indeterminate rebbachisaurid. Bellardini et al. (2022) described several rebbachisaurid specimens from the Huincul Formation; of these, one specimen seemed to show rebbachisaurine affinities. However, given that this was based on similarities with *Katepensaurus* (see above), we regard all of these remains as belonging to Rebbachisauridae. Although we suggest that those generically indeterminate remains cannot be referred to Rebbachisaurinae, our EIW analyses place *Itapeuasaurus cajapioensis*, from the Cenomanian Alcântara Formation of north-eastern Brazil (Lindoso et al., 2019), as an early-diverging member of this clade. This would expand the known distribution of this clade (Fig. 18B), but is consistent with faunal similarities between North Africa and north-eastern Brazil observed in other contemporaneous terrestrial vertebrate clades (e.g. Candeiro et al., 2011; Medeiros et al., 2014). Furthermore, dispersal between these regions was likely possible until the late Albian or early Cenomanian (Granot & Dyment, 2015).

Limaysaurinae appears to have been endemic to South America (Fig. 18B), but its taxonomic composition and relative diversity vary across analyses (Fanti et al., 2015; Mannion, Upchurch, Schwarz, et al., 2019; Salgado et al., 2022). In addition to the Argentinean species *Limaysaurus tessonei*, which is known from the lower Cenomanian Candeleros Formation, as well as possibly the upper Cenomanian–lower Turonian Huincul formation too (Calvo, 1999; Calvo & Salgado, 1995; Paulina Carabajal & Calvo, 2021), Limaysaurinae includes *Cathartesaura anaerobica* (Gallina & Apesteguía, 2005),

and might also contain *Nopcsaspondylus alarconensis* (Apesteguía, 2007) from the Candeleros Formation, and MMCH-Pv-49 (Apesteguía et al., 2010; Haluza et al., 2012) from the Huincul Formation. Indeterminate material from the Alcântara Formation of Brazil is also potentially referrable to Limaysaurinae (Ribeiro et al., 2024). Currently, Limaysaurinae is absent from the Early Cretaceous record, despite its khebbashian sister clade, Rebbachisaurinae, first appearing in the Barremian (Fig. 18A). The apparent restriction of Limaysaurinae to South America, coupled with the South American provenance of the earliest-branching rebbachisaurines (i.e. *Itapeuasaurus*, and possibly also *Nopcsaspondylus* and MMCH-Pv-49), potentially suggests that Khebbashia diverged on this continent. However, the long ghost lineages for these early khebbashian divergences, as well as the stratigraphically oldest remains emanating from Europe and north Africa, indicate that this biogeographical scenario should be interpreted with caution.

An undescribed caudal vertebral series from the Coniacian Lago Colhué Huapi Formation of Argentina might represent the stratigraphically youngest known rebbachisaurid, and thus diplodocoid, known globally (Casal et al., 2015). Given good sampling of middle Cretaceous deposits in Australia, including numerous remains of somphospondylan titanosauriforms, it appears that rebbachisaurids did not reach East Gondwana, possibly as a consequence of palaeoenvironmental barriers to high-latitude dispersal (Poropat et al., 2021). With the well-established interpretation of nemegtosaurids as titanosaurs, rather than diplodocoids (e.g. Curry Rogers & Forster, 2001; Jacobs et al., 1993; Salgado et al., 1997; Wilson, 2005), no members of any lineage of Diplodocoidea are known from the latest Cretaceous, with the clade seemingly undergoing a spatiotemporally staggered extinction during the middle Cretaceous (Fig. 18).

Conclusions

We present a revised view on the evolutionary and biogeographical history of diplodocoid sauropod dinosaurs, including new diagnoses for major clades. Detailed anatomical comparisons and phylogenetic analysis indicate that the Middle Jurassic Indian sauropod dinosaur *Tharosaurus* is an indeterminate eusauropod that lacks diplodocoid synapomorphies. The Upper Jurassic Morrison Formation sauropod *Haplocanthosaurus* is recovered as a non-diplodocimorph diplodocoid. Previously regarded as a dicraeosaurid, the Middle Jurassic Chinese diplodocoid *Lingwulong* is placed as a stem flagellicaudatan, outside of the diplodocid–dicraeosaurid split. We recover a diverse Dicraeosauridae, with Morrison Formation taxa as its earliest-branching members. Phylogenetically more-nested dicraeosaurids are all Late Jurassic–Early Cretaceous Gondwanan taxa, for which we formally define the clade Dicraeosaurinae. Early-diverging rebbachisaurids include Gondwana taxa, as well as the earliest Cretaceous UK taxon *Xenoposeidon*. Within the rebbachisaurid clade Khebbashia, Limaysaurinae is restricted to South America, whereas Rebbachisaurinae is more widespread, present in Europe, North Africa, and South America. The stratigraphically youngest known flagellicaudatans are from the Barremian, whereas rebbachisaurids survived until the Turonian or Coniacian. Our results reinforce the view that Flagellicaudata (and probably also Rebbachisauridae) likely originated in Laurasia. Nevertheless, the presence of diplodocoids in Eurasia in the Middle Jurassic suggests a potentially widespread distribution early in their evolutionary history that is likely obscured by sampling failure.

Acknowledgements

We are grateful to Roger Benson and Carl Mehling (AMNH), Ned Gilmore (ANS), Brooks Britt and Rod Scheetz (BYU), Martin Ezcurra (MACN), Paul Barrett (NHMUK), and Matt Carrano, Amanda Millhouse, and Holly Little (USNM) for providing access to specimens newly incorporated or substantially revised in the phylogenetic data matrix in this contribution. Bajpai Sunil and Debajit Datta kindly provided us with high-resolution versions of the figures of the anatomy of *Tharosaurus*. Flavio Bellardini is thanked for kindly providing measurements and photographs of two rebbachisaurid specimens. We are also grateful to the following colleagues and their respective institutions for providing us with photographs and surface scan data that we were able to use in our figures: Amy Campbell and Daniela Schwarz (Museum für Naturkunde, Berlin), Fidel Torcida Fernández-Baldor (Museo de Dinosaurios, Salas de los Infantes, Burgos), Larry Witmer (Ohio University), Matt Lamanna (Carnegie Museum of Natural History, Pittsburgh), and Ronan Allain and Lilian Cazes (Muséum National d'Histoire Naturelle, Paris). Ray Wilhite and Brian Curtice provided valuable information on the history of the Cactus Park Quarry and we also thank John D'Angelo and Ale Chiarenza for discussion of the anatomy of *Tharosaurus* and theropod dinosaurs, respectively. We also thank Emanuel Tschopp, the anonymous reviewer and the handling editor Kimi Chapelle, for their comments which improved this work. We gratefully acknowledge the Willi Hennig Society,

which has sponsored the development and free distribution of TNT. PDM's research was supported by funding from The Royal Society (UF160216, URF\R\221010, RGF\EA\201037).

Author contributions

Both authors contributed equally to this manuscript.

Disclosure Statement

No potential conflict of interest was reported by the author(s).

Supplemental material

Supplemental material for this article can be accessed here: https://doi.org/10.1080/14772019.2025.2550760

ORCID

Philip D. Mannion http://orcid.org/0000-0002-9361-6941
Andrew J. Moore http://orcid.org/0000-0002-3023-2502

Data availability

The data that support the findings of this study are openly available from Morphobank at https://doi.org/10.7934/P5968 (Mannion & Moore, 2025).

References

Allain, R., & **Aquesbi, N.** (2008). Anatomy and phylogenetic relationships of *Tazoudasaurus naimi* (Dinosauria, Sauropoda) from the late Early Jurassic of Morocco. *Geodiversitas*, *30*, 345–424.

Apesteguía, S. (2007). The sauropod diversity of the La Amarga Formation (Barremian), Neuquén (Argentina). *Gondwana Research*, *12*, 533–546. https://doi.org/10.1016/j.gr.2007.04.007

Apesteguía, S., **Gallina, P. A.**, & **Haluza, A.** (2010). Not just a pretty face: anatomical peculiarities in the postcranium of rebbachisaurids (Sauropoda: Diplodocoidea). *Historical Biology*, *22*, 165–174. https://doi.org/10.1080/08912960903411580

Averianov, A. O., & **Sues, H.-D.** (2021). First rebbachisaurid sauropod dinosaur from Asia. *PLoS ONE*, *16*, e0246620. https://doi.org/10.1371/journal.pone.0246620

Averianov, A. O., & **Zverkov, N. G.** (2020). New diplodocoid sauropod dinosaur material from the Middle Jurassic of European Russia. *Acta Palaeontologica Polonica*, *65*, 499–509. https://doi.org/10.4202/app.00724.2020

Bajpai, S., **Datta, D.**, **Pandey, P.**, **Ghosh, T.**, **Kumar, K.**, & **Bhattcharya, D.** (2023). Fossils of the oldest diplodocoid dinosaur suggest India was a major centre for neosauropod radiation. *Scientific Reports*, *13*, 12680. https://doi.org/10.1038/s41598-023-39759-2

Balanoff, A. M., **Bever, G. S.**, **Ikejiri, T.** (2010). The braincase of *Apatosaurus* (Dinosauria: Sauropoda) based on computed tomography of a new specimen with comments on variation and evolution in sauropod neuroanatomy. *American Museum Novitates, 3677*, 1–32.

Bandeira, K. L. N., **Navarro, B. A.**, **Pêgas, R. V.**, **Brilhante, N. S.**, **Brum, A. S.**, **de Souza, L. G.**, **da Silva, R. C.**, & **Gallo, V.** (2025). A reassessment of the historical fossil findings from Bahia State (Northeast Brazil) reveals a diversified dinosaur fauna in the Lower Cretaceous of South America. *Historical Biology*, *37*, 548–589. https://doi.org/10.1080/08912963.2024.2318406

Bandyopadhyay, S., **Gillette, D. D.**, **Ray, S.**, & **Sengupta, D. P.** (2010). Osteology of *Barapasaurus tagorei* (Dinosauria: Sauropoda) from the Early Jurassic of India. *Palaeontology*, *53*, 533–569. https://doi.org/10.1111/j.1475-4983.2010.00933.x

Bellardini, F., **Coria, R. A.**, **Windholz, G. J.**, **Martinelli, A. G.**, & **Baiano, M. A.** (2023). Revisiting the Early Cretaceous sauropod *Agustinia ligabuei* (Dinosauria: Diplodocoidea) from southern Neuquén basin (Patagonia, Argentina), with implications on the early evolution of rebbachisaurids. *Historical Biology*, *35*, 2408–2434. https://doi.org/10.1080/08912963.2022.2142911

Bellardini, F., **Filippi, L. S.**, **Carballido, J. L.**, **Garrido, A. C.**, & **Baiano, M. A.** (2024). Exploring rebbachisaurid hind-limb anatomy on the basis of a new articulated specimen from the Huincul Formation (upper Cenomanian) of Neuquén Basin, Patagonia, Argentina. *Historical Biology*, *36*, 2587–2603. https://doi.org/10.1080/08912963.2023.2268638

Bellardini, F., **Filippi, L. S.**, **Carballido, J. L.**, **Garrido, A. C.**, & **Baiano, M. A.** (2025). Side by side with titans: a new rebbachisaurid dinosaur from the Huincul Formation (upper Cenomanian) of Patagonia, Argentina. *Cretaceous Research*, *176*, 106188. https://doi.org/10.1016/j.cretres.2025.106188

Bellardini, F., **Filippi, L. S.**, **Garrido, A. C.**, **Carballido, J. L.**, & **Baiano, M. A.** (2022). New rebbachisaurid remains from the Huincul Formation (Middle Cenomanian–Early Turonian) of the Central Neuquén Basin, Patagonia, *Argentina. Publicación Electrónica de la Asociación Paleontológica Argentina*, *22*, 1–24.

Benyoucef, M., **Pérez-García, A.**, **Bendella, M.**, **Ortega, F.**, **Vullo, R.**, **Bouchemla, I.**, & **Ferré, B.** (2022). The "mid"-Cretaceous (Lower Cenomanian) continental vertebrates of Gara Samani, Algeria. Sedimentological framework and palaeodiversity. *Frontiers in Earth Science*, *10*, 927059. https://doi.org/10.3389/feart.2022.927059

Berman, D. S., & **McIntosh, J. S.** (1978). Skull and relationships of the Upper Jurassic sauropod *Apatosaurus* (Reptilia, Saurischia). *Bulletin of Carnegie Museum of Natural History*, *8*, 1–35. https://doi.org/10.5962/p.228587

Bindellini, G., & **Dal Sasso, C.** (2021). Sauropod teeth from the Middle Jurassic of Madagascar, and the oldest record of Titanosauriformes. *Papers in Palaeontology*, *7*, 137–161. https://doi.org/10.1002/spp2.1282

Boisvert, C., **Bivens, G. T.**, **Curtice, B.**, **Wilhite, R.**, & **Wedel, M.** (2025). Census of currently known specimens of the Late Jurassic sauropod *Haplocanthosaurus* from the Morrison Formation, USA. *Geology of the Intermountain West*, *12*, 1–23. https://doi.org/10.31711/giw.v12.pp1-23

Bonaparte, J. F. (1996). Cretaceous tetrapods of Argentina. *Münchner Geowissenschaften Abhandlungen*, *30*, 73–130.

Bonaparte, J. F. (1997). *Rayososaurus agrioensis* Bonaparte 1995. *Ameghiniana*, *34*, 116.

Bonaparte, J. F. (1999). An armoured sauropod from the Aptian of northern Patagonia, Argentina. *National Science Museum Monographs*, *15*, 1–12.

Bonaparte, J. F., & **Mateus, O.** (1999). A new diplodocid, *Dinheirosaurus lourinhanensis* gen. et sp. nov., from the Late Jurassic beds of Portugal. *Revista del Museo Argentino de Ciencias Naturales "Bernardino Rivadavia" e Instituto Nacional de Investigación de las Ciencias Naturales, Paleontología*, *5*, 13–29.

Brikiatis, L. (2016). Late Mesozoic North Atlantic land bridges. *Earth-Science Reviews*, *159*, 47–57. https://doi.org/10.1016/j.earscirev.2016.05.002

Bronzati, M. (2017). Should the terms 'basal taxon' and 'transitional taxon' be extinguished from cladistic studies with extinct organisms? *Palaeontologia Electronica*, *20*, 2.3 E.

Bronzati, M., **Langer, M. C.**, & **Rauhut, O. W. M.** (2018). Braincase anatomy of the early sauropodomorph *Saturnalia tupiniquim* (Late Triassic, Brazil). *Journal of Vertebrate Paleontology*, *38*, e1559173. https://doi.org/10.1080/02724634.2018.1559173

Buffetaut, E. (2005). A new sauropod dinosaur with prosauropod-like teeth from the Middle Jurassic of Madagascar. *Bulletin de la Societé Géologique de France*, *176*, 467–473.

Calvo, J. O. (1999). Dinosaurs and other vertebrates of the Lake Ezequiel Ramos Mexía area, Neuquén-Patagonia, Argentina. *National Science Museum Monographs*, *15*, 13–45.

Calvo, J. O., & **Salgado, L.** (1995). *Rebbachisaurus tessonei* sp. nov. a new Sauropoda from the Albian–Cenomanian of Argentina; new evidence on the origin of the Diplodocidae. *Gaia*, *11*, 13–33.

Campos-Soto, S., **Benito, M. I.**, **Cobos, A.**, **Caus, E.**, **Quijada, I. E.**, **Suarez-Gonzalez, P.**, **Mas, R.**, **Royo-Torres, R.**, & **Alcalá, L.** (2019). Revisiting the age and palaeoenvironments of the Upper Jurassic–Lower Cretaceous? dinosaur-bearing sedimentary record of eastern Spain: implications for Iberian palaeogeography. *Journal of Iberian Geology*, *45*, 471–510. https://doi.org/10.1007/s41513-019-00106-y

Candeiro, C. R. A., **Fanti, F.**, **Therrien, F.**, & **Lamanna, M. C.** (2011). Continental fossil vertebrates from the mid-Cretaceous (Albian–Cenomanian) Alcântara Formation, Brazil, and their relationship with contemporaneous faunas from North Africa. *Journal of African Earth Sciences*, *60*, 79–92. https://doi.org/10.1016/j.jafrearsci.2011.02.004

Canudo, J. I., **Barco, J. L.**, **Pereda – Suberbiola, X.**, **Ruiz – Omeñaca, J. I.**, **Salgado, L.**, **Torcida Fernández-Baldor, F.**, & **Gasulla, J. M.** (2009). What Iberian dinosaurs reveal about the bridge said to exist between Gondwana and Laurasia in the Early Cretaceous. *Bulletin de la Société Géologique de France*, *180*, 5–11.

Canudo, J. I., **Carballido, J. L.**, **Garrido, A.**, & **Salgado, L.** (2018). A new rebbachisaurid sauropod from the Aptian–Albian, Lower Cretaceous Rayoso Formation, Neuquén, Argentina. *Acta Palaeontologica Polonica*, *63*, 679–691. https://doi.org/10.4202/app.00524.2018

Carballido, J. L., **Garrido, A. C.**, **Canudo, J. L.**, & **Salgado, L.** (2010). Redescription of *Rayososaurus agrioensis* Bonaparte (Sauropoda, Diplodocoidea), a rebbachisaurid from the early Late Cretaceous of Neuquén. *Geobios*, *43*, 493–503. https://doi.org/10.1016/j.geobios.2010.01.004

Carballido, J. L., **Holwerda, F. M.**, **Pol, D.**, & **Rauhut, O. W. M.** (2017). An Early Jurassic sauropod tooth from Patagonia (Cañadón Asfalto Formation): implications for sauropod diversity. *Publicación Electrónica de la Asociación Paleontológica Argentina*, *17*, 50–57. https://doi.org/10.5710/PEAPA.17.11.2017.249

Carballido, J. L., **Rauhut, O. W. M.**, **Pol, D.**, & **Salgado, L.** (2011). Osteology and phylogenetic relationships of *Tehuelchesaurus benitezii* (Dinosauria, Sauropoda) from the Upper Jurassic of Patagonia. *Zoological Journal of the Linnean Society*, *163*, 605–662. https://doi.org/10.1111/j.1096-3642.2011.00723.x

Carballido, J. L., **Salgado, L.**, **Pol, D.**, **Canudo, J. I.**, & **Garrido, A.** (2012). A new basal rebbachisaurid (Sauropoda, Diplodocoidea) from the Early Cretaceous of the Neuquén Basin; evolution and biogeography of the group. *Historical Biology*, *24*, 631–654. https://doi.org/10.1080/08912963.2012.672416

Carpenter, K. (2018). *Maraapunisaurus fragillimus*, N.G. (Formerly *Amphicoelias fragillimus*), A basal rebbachisaurid from the Morrison Formation (Upper Jurassic) of Colorado. *Geology of the Intermountain West*, *5*, 227–244. https://doi.org/10.31711/giw.v5.pp227-244

Carvalho, I. S., **Avilla, L. S.**, & **Salgado, L.** (2003). *Amazonsaurus maranhensis* gen. et sp. nov. (Sauropoda, Diplodocoidea) from the Lower Cretaceous (Aptian-Albian) of Brazil. *Cretaceous Research*, *24*, 697–713. https://doi.org/10.1016/j.cretres.2003.07.005

Carvalho, J. C., & **Santucci, R. M.** (2018). New dinosaur remains from the Quiricó Formation, Sanfranciscana Basin (Lower Cretaceous), southwestern Brazil. *Cretaceous Research*, *85*, 20–27. https://doi.org/10.1016/j.cretres.2017.12.017

Casal, G. A., **Allard, J. O.**, & **Foix, N.** (2015). Análisis estratigráfico y paleontológico del Cretácico Superior en la Cuenca del Golfo San Jorge: nueva unidad litoestratigráfica para el Grupo Chubut. *Revista de la Asociación Geológica Argentina*, *72*, 77–95.

Cashmore, D. D., **Mannion, P. D.**, **Upchurch, P.**, & **Butler, R. J.** (2020). Ten more years of discovery: revisiting the quality of the sauropodomorph dinosaur fossil record. *Palaeontology*, *63*, 951–978. https://doi.org/10.1111/pala.12496

Castro, D. F., **Bertini, R. J.**, **Santucci, R. M.**, & **Medeiros, M. A.** (2007). Sauropods of the Itapecuru Group (lower/middle Albian), São Luis-Grajaú Basin, Maranhão State,

Brazil. *Revista Brasileira de Paleontologia*, *10*, 195–200. https://doi.org/10.4072/rbp.2007.3.06

Cope, E. D. (1878). A new species of *Amphicoelias*. *The American Naturalist*, *12*, 563–565.

Coria, R. A., **Windholz, F. J.**, **Ortega, F.**, & **Currie, P. J.** (2019). A new dicraeosaurid sauropod from the Lower Cretaceous (Mulichinco Formation, Valanginian, Neuquén Basin) of Argentina. *Cretaceous Research*, *93*, 33–48. https://doi.org/10.1016/j.cretres.2018.08.019

Costa Pereira, P. V. L. G., **Veiga, I. M. M. G.**, **Ribeiro, T. B.**, **Bezerra Cardozo, R. H.**, **Candeiro, C. R. A.**, & **Bergqvist, L. P.** (2020). The path of giants: a new occurrence of Rebbachisauridae (Dinosauria, Diplodocoidea) in the Açu Formation, NE Brazil, and its paleobiogeographic implications. *Journal of South American Earth Sciences*, *100*, 10251. https://doi.org/10.1016/j.jsames.2020.102515

Curry, K. A. (1999). Ontogenetic histology of *Apatosaurus* (Dinosauria: Sauropoda): new insights on growth rates and longevity. *Journal of Vertebrate Paleontology*, *19*, 654–665. https://doi.org/10.1080/02724634.1999.10011179

Curry Rogers, K., & **Forster, C.** (2001). The last of the dinosaur titans: a new sauropod from Madagascar. *Nature*, *412*, 530–534. https://doi.org/10.1038/35087566

Curtice, B. D., & **Stadtman, K. L.** (2001). The demise of *Dystylosaurus edwini* and a revision of *Supersaurus vivianae*. *Mesa Southwest Museum Bulletin*, *8*, 33–40.

Dai, H., **Tan, C.**, **Xiong, C.**, **Ma, Q.**, **Li, N.**, **Yu, H.**, **Wei, Z.**, **Wang, P.**, **Yi, J.**, **Wie, G.**, **You, H.**, & **Ren, X.** (2022). New macronarian from the Middle Jurassic of Chongqing, China: phylogenetic and biogeographic implications for neosauropod dinosaur evolution. *Royal Society Open Science*, *9*, 220794. https://doi.org/10.1098/rsos.220794

Dalla Vecchia, F. M. (1998). Remains of Sauropoda (Reptilia, Saurischia) in the Lower Cretaceous (Upper Hauterivian/Lower Barremian) limestones of SW Istria (Croatia). *Geologica Croatica*, *51*, 105–134.

Dalla Vecchia, F. M. (1999). Atlas of the sauropod bones from the upper Hauterivian–lower Barremian of Valle/Bale (SW Istria, Croatia). *Natura Nacosta*, *18*, 6–41.

Dalla Vecchia, F. M. (2005). Between Gondwana and Laurasia: Cretaceous sauropods in an intraoceanic carbonate platform. In K. Carpenter & V. Tidwell (Eds.), *Thunder-Lizards: The Sauropodomorph Dinosaurs* (pp. 395–429). Indiana University Press.

Day, J. J., **Upchurch, P.**, **Norman, D. B.**, **Gale, A. S.**, & **Powell, H. P.** (2002). Sauropod trackways, evolution, and behavior. *Science*, *296*, 1659. https://doi.org/10.1126/science.1070167

D'Emic, M. D. (2012). The early evolution of titanosauriform sauropod dinosaurs. *Zoological Journal of the Linnean Society*, *166*, 624–671.

D'Emic, M. D., & **Foster, J. R.** (2016). The oldest Cretaceous North American sauropod dinosaur. *Historical Biology*, *28*, 470–478. https://doi.org/10.1080/08912963.2014.976817

Díez Díaz, V., **Mannion, P. D.**, **Csiki-Sava, Z.**, & **Upchurch, P.** (2025). Revision of Romanian sauropod dinosaurs reveals high titanosaur diversity and body-size disparity on the latest Cretaceous Haţeg Island, with implications for titanosaurian biogeography. *Journal of Systematic Palaeontology*, *23*, 2441516. https://doi.org/10.1080/14772019.2024.2441516

Eiamlaor, K., **Suteethorn, S.**, **Chanthasit, P.**, **Suteethorn, V.**, & **Suraprasit, K.** (2025) Pneumatic structures of sauropod cervical vertebrae from the Lower Cretaceous Sao Khua Formation of northeastern Thailand. *Cretaceous Research*, *176*, 106189. https://doi.org/10.1016/j.cretres.2025.106189

Ezcurra, M. D. (2024). Exploring the effects of weighting against homoplasy in genelogies of paleontological phylogenetic matrices. *Cladistics*, *40*, 242–281. https://doi.org/10.1111/cla.12581

Fanti, F., **Cau, A.**, **Cantelli, L.**, **Hassine, M.**, & **Auditore, M.** (2015). New information on *Tataouinea hannibalis* from the Early Cretaceous of Tunisia and implications for the tempo and mode of rebbachisaurid sauropod evolution. *PLoS ONE*, *10*, e0123475. https://doi.org/10.1371/journal.pone.0123475

Fanti, F., **Cau, A.**, & **Hassine, M.** (2014). Evidence of titanosauriforms and rebbachisaurids (Dinosauria: Sauropoda) from the Early Cretaceous of Tunisia. *Journal of African Earth Sciences*, *90*, 1–8. https://doi.org/10.1016/j.jafrearsci.2013.10.010

Fanti, F., **Cau, A. Hassine, M.**, & **Contessi, M.** (2013). A new sauropod dinosaur from the Early Cretaceous of Tunisia with extreme avian-like pneumatization. *Nature Communications*, *4*, 2080. https://doi.org/10.1038/ncomms3080

Foster, J. R. (2003). Paleoecological analysis of the vertebrate fauna of the Morrison Formation (Upper Jurassic), Rocky Mountain region, U.S.A. *New Mexico Museum of Natural History and Science Bulletin*, *23*, 1–95.

Foster, J. R., & **Peterson, J. E.** (2016). First report of *Apatosaurus* (Diplodocidae: Apatosaurinae) from the Cleveland-Lloyd Quarry in the Upper Jurassic Morrison Formation of Utah: Abundance, distribution, paleoecology, and taphonomy of an endemic North American sauropod clade. *Palaeoworld*, *25*, 431–443. https://doi.org/10.1016/j.palwor.2015.11.006

Fraas, E. (1908). Ostafrikanische Dinosaurier. *Palaeontographica*, *55*, 105–144.

Frauenfelder, T. G., **Birch, S. A.**, **Bell, P. R.**, & **Campione, N. E.** (2024). Revealing the use of dental indices to infer taxonomic variation in sauropod dinosaurs. *Palaeontology*, *67*, e12725. https://doi.org/10.1111/pala.12725

Gabunia, L. K., **Mchedlidze, G.**, **Chkhikvadze, V. M.**, & **Lucas, S. G.** (1998). Jurassic sauropod dinosaur from the Republic of Georgia. *Journal of Vertebrate Paleontology*, *18*, 233–236. https://doi.org/10.1080/02724634.1998.10011047

Gallina, P. A. (2016). Reappraisal of the Early Cretaceous sauropod dinosaur *Amargatitanis macni* (Apesteguía, 2007), from northwestern Patagonia, Argentina. *Cretaceous Research*, *64*, 79–87. https://doi.org/10.1016/j.cretres.2016.04.002

Gallina, P. A., & **Apesteguía, S.** (2005). *Cathartesaura anaerobica* gen. et sp. nov., a new rebbachisaurid (Dinosauria, Sauropoda) from the Huincul Formation (Upper Cretaceous), Río Negro, Argentina. *Revista del Museo Argentino de Ciencias Naturales, nuevo serie*, **7**, 153–166. https://doi.org/10.22179/REVMACN.7.332

Gallina, P. A., **Apesteguía, S.**, **Canale, J. I.**, & **Haluza, A.** (2019). A new long-spined dinosaur from Patagonia sheds light on sauropod defense system. *Scientific Reports*, *9*, 1392. https://doi.org/10.1038/s41598-018-37943-3

Gallina, P. A., **Apesteguía, S.**, **Carballido, J. L.**, & **Garderes, J. P.** (2022). Southernmost spiny backs and whiplash tails: Flagellicaudatans from South America. In A. Otero, J. L., Carballido, & D. Pol (Eds.), *South American sauropodomorph dinosaurs: Record, diversity and evolution* (pp. 209–236). Springer.

Gallina, P. A., **Apesteguía, S.**, **Haluza, A.**, **Canale, J. I.** (2014). A diplodocid sauropod survivor from the Early Cretaceous of South America. *PLoS ONE*, *9*, e97128. https://doi.org/10.1371/journal.pone.0097128

Garderes, J. P., **Gallina, P. A.**, **Whitlock, J. A.**, & **Toledo, N.** (2022). Neuroanatomy of a diplodocid sauropod dinosaur from the Lower Cretaceous of Patagonia, Argentina. *Cretaceous Research*, *129*, 105024. https://doi.org/10.1016/j.cretres.2021.105024

Garderes, J. P., **Gallina, P. A.**, **Whitlock, J. A.**, & **Toledo, N.** (2024). Cranial osteology of *Bajadasaurus pronuspinax* (Sauropoda, Dicraeosauridae). *Historical Biology*, *36*, 1343–1367. https://doi.org/10.1080/08912963.2023.2212389

Gilmore, C. W. (1936). Osteology of *Apatosaurus*: with special reference to specimens in the Carnegie Museum. *Memoirs of the Carnegie Museum*, *11*, 175–300. https://doi.org/10.5962/p.234849

Gnaedinger, S., **Coria, R. A.**, **Koppelhus, E.**, **Casadío, S.**, **Tunik, M.** & **Currie, P.** (2017). First Lower Cretaceous record of Podocarpaceae wood associated with dinosaur remains from Patagonia, Neuquén Province, Argentina. *Cretaceous Research*, *78*, 228–239.

Goloboff, P. (2014). Extended implied weighting. *Cladistics*, *30*, 260–272. https://doi.org/10.1111/cla.12047

Goloboff, P., & **Morales, M.** (2023). TNT version 1.6, with a graphical interface for MacOS and Linux, including new routines in parallel. *Cladistics*, *39*, 144–153. https://doi.org/10.1111/cla.12524

Goloboff, P., **Torres, A.**, & **Arias, J. S.** (2018). Weighted parsimony outperforms other methods of phylogenetic inference under models appropriate for morphology. *Cladistics*, *34*, 407–437. https://doi.org/10.1111/cla.12205

Gomez, K. L., **Carballido, J. L.**, & **Pol, D.** (2021). The axial skeleton of *Bagualia alba* (Dinosauria: Eusauropoda) from the Early Jurassic of Patagonia. *Palaeontologia Electronica*, *24*, A37. https://doi.org/10.26879/1176

Granot, R., & **Dyment, J.** (2015). The Cretaceous opening of the South Atlantic Ocean. *Earth and Planetary Science Letters*, *414*, 156–163. https://doi.org/10.1016/j.epsl.2015.01.015

Haluza, A., **Canale, J. I.**, **Otero, A.**, **Peréz, L. M.**, & **Scanferla, C. A.** (2012). Changes in vertebral laminae across the cervicodorsal transition of a well-preserved rebbachisaurid (Dinosauria, Sauropoda) from the Cenomanian of Patagonia, Argentina. *Journal of Vertebrate Paleontology*, *32*, 219–224. https://doi.org/10.1080/02724634.2012.620674

Han, F., **Yang, L.**, **Lou, F.**, **Sullivan, C.**, **Xu, X.**, **Qiu, W.**, **Liu, H.**, **Yu, J.**, **Wu, R.**, **Ke, Y.**, **Xu, M.**, **Huban, J.**, & **Lu, P.** (2024). A new titanosaurian sauropod, *Gandititan cavocaudatus* gen. et sp. nov., from the Late Cretaceous of southern China. *Journal of Systematic Palaeontology*, *22*, 2293038. https://doi.org/10.1080/14772019.2023.2293038

Harris, J. D. (2006a). The axial skeleton of the dinosaur *Suuwassea emilieae* (Sauropoda: Flagellicaudata) from the Upper Jurassic Morrison Formation of Montana, USA. *Palaeontology*, *49*, 1091–1121. https://doi.org/10.1111/j.1475-4983.2006.00577.x

Harris, J. D. (2006b). Cranial osteology of *Suuwassea emilieae* (Sauropoda: Diplodocoidea: Flagellicaudata) from the Upper Jurassic Morrison Formation of Montana, USA. *Journal of Vertebrate Paleontology*, *26*, 88–102. https://doi.org/10.1671/0272-4634(2006)26[88:COOSES]2.0.CO;2

Harris, J. D. (2006c). The significance of *Suuwassea emilieae* (Dinosauria: Sauropoda) for flagellicaudatan intrarelationships and evolution. *Journal of Systematic Palaeontology*, *4*, 185–198. https://doi.org/10.1017/S1477201906001805

Harris, J. D., & **Dodson, P.** (2004). A new diplodocoid sauropod dinosaur from the Upper Jurassic Morrison Formation of Montana, USA. *Acta Palaeontologica Polonica*, *49*, 197–210.

Hatcher, J. B. (1901). *Diplodocus* (Marsh): its osteology, taxonomy, and probable habits, with a restoration of the skeleton. *Memoirs of the Carnegie Museum*, *1*, 1–63. https://doi.org/10.5962/p.234818

Hatcher, J. B. (1903). Osteology of *Haplocanthosaurus*, with description of a new species, and remarks on the probable habits of the Sauropoda and the age and origin of the *Atlantosaurus* beds. *Memoirs of the Carnegie Museum*, *2*, 1–72. https://doi.org/10.5962/p.234822

He, X., **Li, K.**, & **Cai, K.** (1988). *The Middle Jurassic dinosaur fauna from Dashanpu, Zigong, Sichuan. IV. Sauropod dinosaurs (2). Omeisaurus tianfuensis*. Sichuan Publishing House of Science and Technology, Chengdu, 143 pp.

Higgins, R. R., **Mannion, P. D.**, **Barrett, P. M.**, & **Upchurch, P.** (2024). A new sauropod dinosaur hindlimb from the Lower Cretaceous Wessex Formation, Isle of Wight, UK. *Royal Society Open Science*, *11*, 240642. https://doi.org/10.1098/rsos.240642

Holland, W. J. (1906). The osteology of *Diplodocus* Marsh. *Memoirs of the Carnegie Museum*, *2*, 225–264. https://doi.org/10.5962/p.234827

Holland, W. J. (1910). A review of some recent criticisms of the restorations of sauropod dinosaurs existing in the museums of the United States, with special reference to that of *Diplodocus carnegiei* in the Carnegie Museum. *The American Naturalist*, *44*, 259–283. https://doi.org/10.1086/279138

Holland, W. J. (1924). The skull of *Diplodocus*. *Memoirs of the Carnegie Museum*, *9*, 379–403. https://doi.org/10.5962/p.234841

Holwerda, F. M. (2020). Sauropod dinosaur fossils from the Kem Kem and extended 'Continental Intercalaire' of North Africa: A review. *Journal of African Earth Sciences*, *163*, 103738. https://doi.org/10.1016/j.jafrearsci.2019.103738

Holwerda, F. M., **Díez Díaz, V.**, **Blanco, A.**, **Montie, R.**, & **Reumer, J. W. F.** (2018). Late Cretaceous sauropod tooth morphotypes may provide supporting evidence for faunal connections between North Africa and Southern Europe. *PeerJ*, *6*, e5925. https://doi.org/10.7717/peerj.5925

Holwerda, F. M., **Evans, M.**, & **Liston, J. J.** (2019). Additional sauropod dinosaur material from the Callovian Oxford Clay Formation, Peterborough, UK: evidence for higher sauropod diversity. *PeerJ*, *7*, e6404. https://doi.org/10.7717/peerj.6404

Holwerda, F. M., **Rauhut, O. W. M.**, & **Pol, D.** (2021). Osteological revision of the holotype of the Middle

Jurassic sauropod dinosaur *Patagosaurus fariasi* Bonaparte, 1979 (Sauropoda: Cetiosauridae). *Geodiversitas*, *43*, 575–643. https://doi.org/10.5252/geodiversitas2021v43a16

Huene, F. von. (1927). Short review of the present knowledge of the Sauropoda. *Memoirs of the Queensland Museum*, *9*, 121–126.

Ibiricu, L. M., **Casal, G. A.**, **Lamanna, M. C.**, **Harris, J. D.**, & **Lacovara, K. J.** (2012). The southernmost records of Rebbachisauridae (Sauropoda: Diplodocoidea), from early Late Cretaceous deposits in central Patagonia. *Cretaceous Research*, *34*, 220–232. https://doi.org/10.1016/j.cretres.2011.11.003

Ibiricu, L. M., **Casal, G. A.**, **Martínez, R. D.**, **Alvarez, B. N.**, & **Poropat, S. F.** (2020). New materials and an overview of Cretaceous vertebrates from the Chubut Group of the Golfo San Jorge Basin, central Patagonia, Argentina. *Journal of South American Earth Sciences*, *98*, 102460. https://doi.org/10.1016/j.jsames.2019.102460

Ibiricu, L. M., **Casal, G. A.**, **Martinez, R. D.**, **Lamanna, M. C.**, **Luna, M.**, & **Salgado, L.** (2013). *Katepensaurus goicoecheai*, gen. et sp. nov., a Late Cretaceous rebbachisaurid (Sauropoda, Diplodocoidea) from central Patagonia, Argentina. *Journal of Vertebrate Paleontology*, *33*, 1351–1366. https://doi.org/10.1080/02724634.2013.776562

Ibiricu, L. M., **Casal, G. A.**, **Martínez, R. D.**, **Lamanna, M. C.**, **Luna, M.**, & **Salgado, L.** (2015). New material of *Katepensaurus goicoecheai* (Sauropoda: Diplodocoidea) and its significance for the morphology and evolution of Rebbachisauridae. *Ameghiniana*, **52**, 430–446. https://doi.org/10.5710/AMGH.24.04.2015.2830

Ibiricu, L. M., **Lamanna, M. C.**, **Martínez, R. D. F.**, **Casal, G. A.**, **Cerda, I. A.**, **Martínez, G.**, & **Salgado, L.** (2017). A novel form of postcranial skeletal pneumaticity in a sauropod dinosaur: Implications for the paleobiology of Rebbachisauridae. *Acta Palaeontologica Polonica*, *62*, 221–236. https://doi.org/10.4202/app.00316.2016

Ibrahim, N., **Sereno, P. C.**, **Varricchio, D. J.**, **Martill, D. M.**, **Dutheil, D. B.**, **Unwin, D. M.**, **Baidder, L.**, **Larsson, H. C. E.**, **Zouhri, S.**, & **Kaoukaya, A.** (2020) Geology and paleontology of the Upper Cretaceous Kem Kem Group of eastern Morocco. *ZooKeys*, *928*, 1–216. https://doi.org/10.3897/zookeys.928.47517

Jacobs, L. L., **Winkler, D. A.**, **Downs, W. R.**, & **Gomani, E. M.** (1993). New material of an Early Cretaceous titanosaurid sauropod dinosaur from Malawi. *Palaeontology*, *36*, 523–534.

Janensch, W. (1914). Übersicht über die Wirbeltierfauna der Tendaguru-Schichten. *Archiv für Biontologie*, *3*, 81–110.

Janensch, W. (1929a). Material und Formegehalt der Sauropoden in der Ausbeute der Tendaguru-Expedition, 1909–1912. *Palaeontographica (Supplement VII)*, *2*, 3–34.

Janensch, W. (1929b). Die Wirbelsäule der Gattung *Dicraeosaurus*. *Palaeontographica (Supplement VII)*, **2**, 37–133.

Janensch, W. (1935–1936). Die Schädel der Sauropoden *Brachiosaurus*, *Barosaurus*, und *Dicraeosaurus*. *Palaeontographica (Supplement VII)*, *2*, 147–298.

Janensch, W. (1961). Die gliedmaszen und gliedmaszengürtel der Sauropoden der Tendaguru-Schichten. *Palaeontographica (Supplement VII)*, *3*, 177–235.

Jensen, J. A. (1985). Three new sauropod dinosaurs from the Upper Jurassic of Colorado. *The Great Basin Naturalist*, *45*, 697–709.

Joeckel, R. M., **Suarez, C. A.**, **McLean, N. M.**, **Möller, A.**, **Ludvigson, G. A.**, **Suarez, M. B.**, **Kirkland, J. I.**, **Andrew, J.**, **Kiessling, S.**, & **Hatzell, G. A.** (2023). Berriasian–Valanginian Geochronology and Carbon-Isotope Stratigraphy of the Yellow Cat Member, Cedar Mountain Formation, Eastern Utah, USA. *Geosciences*, *13*, 32.

Kirkland, J. I., **Sertich, J. J. W.**, & **Titus, A. L.** (2024). Dinosaur biostratigraphy of the non-marine Cretaceous of Utah. *Geological Society, London*, *Special Publications*, 545. https://doi.org/10.1144/SP545-2023-211

Lapparent, A. F. de. (1960). Les Dinosauriens du "Continental intercalaire" du Saharal central. *Mémoires de la Société géologique de France, nouvelle série*, *39*, 1–57.

Lavocat, R. (1954). Sur les dinosauriens du Continental Intercalaire des Kem-Kem de la Daoura. *Congrés Géologique International, Comptes Rendus de la Dix-Neuvième Session*, *Section 13*, *15*, 65–68.

Lerzo, L. N. (2024). Redescription of the key specimen MACN PV 35: Laminar anatomy and hyposphene-hypantrum in an early rebbachisaurid (Dinosauria, Sauropoda) from Patagonia, Argentina. *Cretaceous Research*, **153**, 105689.

Lerzo, L. N., **Carballido, J. L.**, & **Gallina, P. A.** (2021). Rebbachisaurid sauropods in Asia? A re-evaluation of the phylogenetic position of *Dzharatitanis kingi* from the Late Cretaceous of Uzbekistan. *Publicación Electrónica de la Asociación Paleontológica Argentina*, *21*, 18–27.

Lerzo, L. N., **Gallina, P. A.**, **Canale, J. I.**, **Otero, A.**, **Carballido, J. L.**, **Apesteguía, S.**, & **Makovicky, P. J.** (2025). The last of the oldies: a basal rebbachisaurid (Sauropoda, Diplodocoidea) from the early Late Cretaceous (Cenomanian–Turonian) of Patagonia, Argentina. *Historical Biology*, *37*, 208–233.

Lerzo, L. N., **Torcida Fernández-Baldor, F.**, **Canale, J. I.**, **Whitlock, J. A.**, **Otero, A.**, & **Gallina, P. A.** (2025). They all floated in the Cretaceous: new rebbachisaurid (Sauropoda, Diplodocoidea) with a highly pneumatized skeleton from the Upper Cretaceous (lower Cenomanian) of Patagonia, Argentina. *Historical Biology*, *37*, 1795–1808. https://doi.org/10.1080/08912963.2024.2383708

Lindoso, R. M., **Medeiros, M. A. A.**, **Carvalho, I. S.**, **Pereira, A. A.**, **Mendes, I. D.**, **Iori, F. V.**, **Sousa, E. P.**, **Arcanjo, S. H. S.**, & **Silva, T. C. M.** (2019). A new rebbachisaurid (Sauropoda: Diplodocoidea) from the middle Cretaceous of northern Brazil. *Cretaceous Research*, *104*, 104191. https://doi.org/10.1016/j.cretres.2019.104191

Lovelace, D. M., **Hartman, S. A.**, & **Wahl, W. R.** (2008). Morphology of a specimen of *Supersaurus* (Dinosauria, Sauropoda) from the Morrison Formation of Wyoming, and a re-evaluation of diplodocoid phylogeny. *Arquivos do Museu Nacional*, *Rio de Janeiro*, *65*, 527–544.

Maidment, S. C. R. (2023). Diversity through time and space in the Upper Jurassic Morrison Formation, western U.S.A. *Journal of Vertebrate Paleontology*, *43*, e2326027. https://doi.org/10.1080/02724634.2024.2326027

Mannion, P. D. (2009). A rebbachisaurid sauropod from the lower Cretaceous of the Isle of Wight, England. *Cretaceous Research*, *30*, 521–526. https://doi.org/10.1016/j.cretres.2008.09.005

Mannion, P. D. (2010). A revision of the sauropod dinosaur genus '*Bothriospondylus*' with a redescription of the type material of the Middle Jurassic form '*B. madagascariensis*'. *Palaeontology*, *53*, 277–296. https://doi.org/10.1111/j.1475-4983.2009.00919.x

Mannion, P. D. (2024). The spatiotemporal distribution of Mesozoic dinosaur diversity. *Biology Letters*, **20**, 20240443. https://doi.org/10.1098/rsbl.2024.0443

Mannion, P. D., & **Barrett, P. M.** (2013). Additions to the sauropod dinosaur fauna of the Cenomanian (early Late Cretaceous) Kem Kem beds of Morocco: Palaeobiogeographical implications of the mid-Cretaceous African sauropod fossil record. *Cretaceous Research*, *45*, 49–59. https://doi.org/10.1016/j.cretres.2013.07.007

Mannion, P. D., & **Moore, A. J.** (2025) Project 5968 [dataset]. *Morphobank*. https://doi.org/10.7934/P5968

Mannion, P. D., **Tschopp, E.**, & **Whitlock, J. A.** (2021). Anatomy and systematics of the diplodocoid *Amphicoelias altus* supports high sauropod dinosaur diversity in the Upper Jurassic Morrison Formation of the USA. *Royal Society Open Science*, *8*, 210377. https://doi.org/10.1098/rsos.210377

Mannion, P. D., **Upchurch, P.**, & **Hutt, S.** (2011). New rebbachisaurid (Dinosauria: Sauropoda) material from the Wessex Formation (Barremian, Early Cretaceous), Isle of Wight, United Kingdom. *Cretaceous Research*, *32*, 774–780. https://doi.org/10.1016/j.cretres.2011.05.005

Mannion, P. D., **Upchurch, P.**, **Barnes, R. N.**, & **Mateus, O.** (2013). Osteology of the Late Jurassic Portuguese sauropod dinosaur *Lusotitan atalaiensis* (Macronaria) and the evolutionary history of basal titanosauriforms. *Zoological Journal of the Linnean Society*, *168*, 98–206. https://doi.org/10.1111/zoj.12029

Mannion, P. D., **Upchurch, P.**, **Jin, X.**, & **Zheng, W.** (2019). New information on the Cretaceous sauropod dinosaurs of Zhejiang Province, China: impact on Laurasian titanosauriform phylogeny and biogeography. *Royal Society Open Science*, *6*, 191057. https://doi.org/10.1098/rsos.191057

Mannion, P. D., **Upchurch, P.**, **Mateus, O.**, **Barnes, R. N.**, **Jones, M. E. H.** (2012). New information on the anatomy and systematic position of *Dinheirosaurus lourinhanensis* (Sauropoda: Diplodocoidea) from the Late Jurassic of Portugal, with a review of European diplodocoids. *Journal of Systematic Paleontology*, *10*, 521–551. https://doi.org/10.1080/14772019.2011.595432

Mannion, P. D., **Upchurch, P.**, **Schwarz, D.**, & **Wings, O.** (2019). Taxonomic affinities of the putative titanosaurs from the Late Jurassic Tendaguru Formation of Tanzania: phylogenetic and biogeographic implications for eusauropod dinosaur evolution. *Zoological Journal of the Linnean Society*, *185*, 784–909. https://doi.org/10.1093/zoolinnean/zly068

Mannion, P. D., & **Whitlock, J. A.** (In press). Diplodocoidea. In D. B. Weishampel, P. M. Barrett, M. T. Carrano & P. J. Makovicky (Eds.), *The Dinosauria* (3rd ed. Cambridge University Press.

Marpmann, J. S., **Carballido, J. L.**, **Sander, P. M.**, & **Knötschke, N.** (2015). Cranial anatomy of the Late Jurassic dwarf sauropod *Europasaurus holgeri* (Dinosauria, Camarasauromorpha): ontogenetic changes and size dimorphism. *Journal of Systematic Palaeontology*, *13*, 221–263. https://doi.org/10.1080/14772019.2013.875074

Marsh, O. C. (1884). Principal characters of American Jurassic dinosaurs. Part VII. On the Diplodocidae, a new family of the Sauropoda. *American Journal of Science (series 3), 27*, 160–168.

Mateus, O., **Mannion, P. D.**, & **Upchurch, P.** (2014). *Zby atlanticus*, a new turiasaurian sauropod (Dinosauria, Eusauropoda) from the Late Jurassic of Portugal. *Journal of Vertebrate Paleontology*, *34*, 618–634. https://doi.org/10.1080/02724634.2013.822875

McIntosh, J. S. (1990). Sauropoda. In D. B. Weishampel, P. Dodson & H. Osmolska (Eds.), *The Dinosauria* (pp. 345–401). University of California Press.

McIntosh, J. S. (2005). The genus *Barosaurus* Marsh (Sauropoda, Diplodocidae). In V. Tidwell & K. Carpenter (Eds.), *Thunder lizards: The sauropodomorph dinosaurs* (pp. 38–77). Indiana University Press.

McIntosh, J. S., & **Berman, D. S.** (1975). Description of the palate and lower jaw of the sauropod dinosaur *Diplodocus* (Reptilia: Saurischia) with remarks on the nature of the skull of *Apatosaurus*. *Journal of Paleontology*, *49*, 187–199.

McIntosh, J. S., & **Williams, M. E.** (1988). A new species of sauropod dinosaur, *Haplocanthosaurus delfsi* sp. nov., from the Upper Jurassic Morrison Formation of Colorado. *Kirtlandia*, *43*, 3–26.

McPhee, B. W., **Mannion, P. D.**, **Klerk, W. J.**, & **Choiniere, J. N.** (2016). High diversity in the sauropod dinosaur fauna of the Lower Cretaceous Kirkwood Formation of South Africa: implications for the Jurassic-Cretaceous transition. *Cretaceous Research*, *59*, 228–248. https://doi.org/10.1016/j.cretres.2015.11.006

Medeiros, M. A., **Lindoso, R. M.**, **Mendes, I. D.**, & **Carvalho, I. D. S.** (2014). The Cretaceous (Cenomanian) continental record of the Laje do Coringa flagstone (Alcântara Formation), northeastern South America. *Journal of South American Earth Sciences*, **53**, 50–58. https://doi.org/10.1016/j.jsames.2014.04.002

Mocho, P., **Royo-Torres, R.**, **Escaso, F.**, **Malafaia, E.**, **de Miguel Chaves, C.**, **Narváez, I.**, **Pérez-García, A.**, **Pimentel, N.**, **Silva, B. C.**, & **Ortega, F.** (2017). Upper Jurassic sauropod record in the Lusitanian Basin (Portugal): Geographical and lithostratigraphical distribution. *Palaeontologia Electronica*, *20*, 27A. https://doi.org/10.26879/662

Mocho, P., **Royo- Torres, R.**, **Malafai, E.**, **Escaso, F.**, **Silva, B.**, & **Ortega, F.** (2016). Turiasauria-like teeth from the Upper Jurassic of the Lusitanian Basin, Portugal. *Historical Biology*, *29*, 151–169. https://doi.org/10.1080/08912963.2015.1049948

Monbaron, M., **Russell, D. A.**, & **Taquet, P.** (1999). *Atlasaurus imelakei*, n. g., n. sp., a brachiosaurid-like sauropod from the Middle Jurassic of Morocco. *Comptes Rendus de l'Académie des Sciences, Paris*, *329*, 519–526. https://doi.org/10.1016/S1251-8050(00)80026-9

Mook, C. C. (1917). The fore and hind limbs of *Diplodocus*. *Bulletin of the American Museum of Natural History*, *37*, 815–819.

Moore, A. J., **Barrett, P. M.**, **Upchurch, P.**, **Liao, C. C.**, **Ye, Y.**, **Hao, B.**, & **Xu, X.** (2023). Re-assessment of the Late Jurassic eusauropod *Mamenchisaurus sinocanadorum* Russell and Zheng, 1993, and the evolution of exceptionally long necks in mamenchisaurids. *Journal of Systematic Palaeontology*, *21*, 2171818. https://doi.org/10.1080/14772019.2023.2171818

Moore, A. J., **Upchurch, P.**, **Barrett, P. M.**, **Clark, J. M.**, & **Xu, X.** (2020). Osteology of *Klamelisaurus gobiensis* (Dinosauria, Eusauropoda) and the evolutionary history of Middle–Late Jurassic Chinese sauropods. *Journal of Systematic Palaeontology*, *18*, 1299–1393. https://doi.org/10.1080/14772019.2020.1759706

Moreau, J.-D., **Trincal, V.**, **Fara, E.**, **Baret, L.**, **Jacquet, A.**, **Barbini, C.**, **Flament, R.**, **Wienin, M.**, **Bourel, B.**, & **Jean, A.** (2019). Middle Jurassic tracks of sauropod dinosaurs in a deep karst cave in France. *Journal of Vertebrate Paleontology*, *39*, e1728286. https://doi.org/10.1080/02724634.2019.1728286

Moser, M., **Mathur, U. B.**, **Fürsich, F. T.**, **Pandey, D. K.**, & **Mathur, N.** (2006). Oldest camarasauromorph sauropod (Dinosauria) discovered in the Middle Jurassic (Bajocian) of the Khadir Island, Kachchh, Western India. *Paläontologische Zeitschrift*, *80*, 34–51. https://doi.org/10.1007/BF02988396

Nopcsa, F. (1902). Notizen uber Cretacischen Dinosaurier. Pt. 3. Wirbel eines sudamerikanischen Sauropoden. *Akademie der Wissenschaften*, *3*, 108–114.

O'Reilly, J. E., **Puttick, M. N.**, **Parry, L.**, **Tanner, A. R.**, **Tarver, J. E.**, **Fleming, J.**, **Pisani, D.**, & **Donoghue, P. C. J.** (2016). Bayesian methods outperform parsimony but at the expense of precision in the estimation of phylogeny from discrete morphological data. *Biology Letters*, *12*, 20160081. https://doi.org/10.1098/rsbl.2016.0081

Osborn, H. F., & **Mook, C. C.** (1921). *Camarasaurus*, *Amphicoelias*, and other sauropods of Cope. *Memoirs of the American Museum of Natural History, New Series*, *3*, 247–387.

Ostrom, J. O., & **McIntosh, J. S.** (1966). *Marsh's Dinosaurs: The collection from Como Bluff*. New Haven, CO: Yale University Press.

Owusu Agyemang, P. C., **Roberts, E. M.**, **Bussert, R.**, **Evans, D.**, & **Müller, J.** (2019). U-Pb detrital zircon constraints on the depositional age and provenance of the dinosaur-bearing Upper Cretaceous Wadi Milk formation of Sudan. *Cretaceous Research*, *97*, 52–72. https://doi.org/10.1016/j.cretres.2019.01.005

Paulina Carabajal, A., & **Calvo, J. O.** (2021). Re-description of the braincase of the rebbachisaurid sauropod *Limaysaurus tessonei* and novel endocranial information based on CT scans. *Anais da Academia Brasileira de Ciências*, *93*, e20200762.

Paulina Carabajal, A., **Canale, J. I.**, & **Haluza, A.** (2016). New rebbachisaurid cranial remains (Sauropoda, Diplodocoidea) from the Cretaceous of Patagonia, Argentina, and the first endocranial description for a South American representative of the clade. *Journal of Vertebrate Paleontology*, *36*, e1167067. https://doi.org/10.1080/02724634.2016.1167067

Paulina Carabajal, A., **Carballido, J. L.**, & **Currie, P. J.** (2014). Braincase, neuroanatomy, and neck posture of *Amargasaurus cazaui* (Sauropoda, Dicraeosauridae) and its implications for understanding head posture in sauropods. *Journal of Vertebrate Paleontology*, *34*, 870–882. https://doi.org/10.1080/02724634.2014.838174

Paulina Carabajal, A., **Coria, R. A.**, **Currie, P. J.**, & **Koppelhus, E. B.** (2018). A natural cranial endocast with possible dicraeosaurid (Sauropoda, Diplodocoidea) affinities from the Lower Cretaceous of Patagonia. *Cretaceous Research*, *84*, 437–441. https://doi.org/10.1016/j.cretres.2017.12.001

Peng, G., **Ye, Y.**, **Gao, Y.**, **Shu, C.**, & **Jiang, S.** (2005). *Jurassic dinosaur faunas in Zigong*. Sichuan People's Publishing House.

Pereda Suberbiola, X., **Torcida, F.**, **Izquierdo, L. A.**, **Huerta, P.**, **Montero, D.**, & **Pérez, G.** (2003). First rebbachisaurid dinosaur (Sauropoda, Diplodocoidea) from the early Cretaceous of Spain: palaeobiogeographical implications. *Bulletin de la Societie Géologiques de France*, *174*, 471–479. https://doi.org/10.2113/174.5.471

Phillips, J. (1871). *Geology of Oxford and the Valley of the Thames*. Clarendon Press.

Poropat, S. F., **Kundrát, M.**, **Mannion, P. D.**, **Upchurch, P.**, **Tischler, T. T.**, & **Elliott, D. A.** (2021). Second specimen of the Late Cretaceous Australian sauropod dinosaur *Diamantinasaurus matildae* provides new anatomical information on the skull and neck of early titanosaurs. *Zoological Journal of the Linnean Society*, *192*, 610–674. https://doi.org/10.1093/zoolinnean/zlaa173

Poropat, S. F., **Mannion, P. D.**, **Rigby, S. L.**, **Duncan, R. J.**, **Pentland, A. H.**, **Bevitt, J. J.**, **Sloan, T.**, & **Elliott, D. A.** (2023). A nearly complete skull of the sauropod dinosaur *Diamantinasaurus matildae* from the Upper Cretaceous Winton Formation of Australia and implications for the early evolution of titanosaurs. *Royal Society Open Science*, *10*, 221618. https://doi.org/10.1098/rsos.221618

Raath, M. A., & **McIntosh, J. S.** (1987). Sauropod dinosaurs from the central Zambezi Valley, Zimbabwe, and the age of the Kadzi Formation. *South African Journal of Geology*, *90*, 107–119.

Rauhut, O. W. M. (1999). A dinosaur fauna from the Late Cretaceous (Cenomanian) of northern Sudan. *Palaeontologia Africana*, **35**, 61–84.

Rauhut, O. W. M., **Carballido, J. L.**, & **Pol, D.** (2015). A diplodocid sauropod dinosaur from the Late Jurassic Cañadón Calcáreo Formation of Chubut, Argentina. *Journal of Vertebrate Paleontology*, **35**, e982798. https://doi.org/10.1080/02724634.2015.982798

Rauhut, O. W. M., & **López-Arbarello, A.** (2009). Considerations on the age of the Tiouaren Formation (Iullemmeden Basin, Niger, Africa): Implications for Gondwanan Mesozoic terrestrial vertebrate faunas. *Palaeogeography, Palaeoclimatology, Palaeoecology*, *271*, 259–267. https://doi.org/10.1016/j.palaeo.2008.10.019

Rauhut, O. W. M., **Remes, K.**, **Fechner, R.**, **Cladera, G.**, & **Puerta, P.** (2005). Discovery of a short-necked sauropod dinosaur from the Late Jurassic period of Patagonia. *Nature*, *435*, 670–672. https://doi.org/10.1038/nature03623

Remes, K. (2006). A revision of the Tendaguru sauropod dinosaur *Tornieria africana* (Fraas) and its relevance for sauropod paleobiogeography. *Journal of Vertebrate Paleontology*, *26*, 651–669. https://doi.org/10.1671/0272-4634(2006)26[651:ROTTSD]2.0.CO;2

Remes, K. (2007). A second Gondwanan diplodocid dinosaur from the Upper Jurassic Tendaguru Beds of Tanzania, East Africa. *Palaeontology*, *50*, 653–667. https://doi.org/10.1111/j.1475-4983.2007.00652.x

Remes, K. (2009). Taxonomy of Late Jurassic diplodocid sauropods from Tendaguru (Tanzania). *Fossil Record*, *12*, 23–46. https://doi.org/10.1002/mmng.200800008

Ren, X.-X., **Jiang, S.**, **Wang, X.-R.**, **Peng, G.-Z.**, **Ye, Y.**, **Jia, L.**, & **You, H.-L.** (2023). Re-examination of *Dashanpusaurus dongi* (Sauropoda: Macronaria) supports

an early Middle Jurassic global distribution of neosauropod dinosaurs. *Palaeogeography, Palaeoclimatology, Palaeoecology*, *610*, 111318. https://doi.org/10.1016/j.palaeo.2022.111318

Ren, X.-X., **Jiang, S.**, **Wang, X.-R.**, **Peng, G.-Z.**, **Ye, Y.**, **King, L.**, & **You, H.-L.** (2022). Osteology of *Dashanpusaurus dongi* (Sauropoda: Macronaria) and new evolutionary evidence from Middle Jurassic Chinese sauropods. *Journal of Systematic Palaeontology*, *20*, 1–72. https://doi.org/10.1080/14772019.2022.2132886

Ribeiro, T. B., **Brito, P. M. M.**, & **Costa Pereira, P. V. L. G.** (2024). The predominance of teeth in the non-avian dinosaur record from Cretaceous Brazil: a review. *Historical Biology*, **36**, 2019–2034. https://doi.org/10.1080/08912963.2023.2238965

Rivera-Sylva, H. E., & **Espinosa-Arrubarrena, L.** (2020). Remains of a diplodocid (Sauropoda: Flagellicaudata) from the Otlaltepec Formation Middle Jurassic (Bathonian-Callovian) from Puebla, Mexico. *Paleontología Mexicana*, *9*, 145–150. https://doi.org/10.22201/igl.05437652e.2020.9.2.173

Royo-Torres, R., **Cobos, A.** & **Alcala, L.** (2006). A giant European dinosaur and a new sauropod clade. *Science*, *314*, 1925–1927. https://doi.org/10.1126/science.1132885

Royo-Torres, R., **Cobos, A.**, **Luque, L.**, **Aberasturi, A.**, **Espílez, E.**, **Fierro, I.**, **González, A.**, **Mampel, L.**, & **Alcalá, L.** (2009). High European sauropod dinosaur diversity during Jurassic-Cretaceous transition in Riodeva (Teruel, Spain). *Palaeontology*, *52*, 1009–1027. https://doi.org/10.1111/j.1475-4983.2009.00898.x

Royo-Torres, R., **Cobos, A.**, **Mocho, P.**, & **Alcalá, L.** (2021). Origin and evolution of turiasaur dinosaurs set by means of a new 'rosetta' specimen from Spain. *Zoological Journal of the Linnean Society*, *191*, 201–227. https://doi.org/10.1093/zoolinnean/zlaa091

Royo-Torres, R., **Upchurch, P.**, **Kirkland, J. I.**, **DeBlieux, D. D.**, **Foster, J. R.**, **Cobos, A.**, & **Alcalá, L.** (2017). Descendants of the Jurassic turiasaurs from Iberia found refuge in the Early Cretaceous of western USA. *Scientific Reports*, *7*, 14311. https://doi.org/10.1038/s41598-017-14677-2

Russell, D. A. (1996). Isolated dinosaur bones from the Middle Cretaceous of the Tafilalt, Morocco. *Bulletin du Muséum National d'Histoire Naturelle, Paris, 4e Série*, *18*, 349–402.

Russell, D. A., & **Zheng, Z.** (1993). A large mamenchisaurid from the Junggar Basin, Xinjiang, People's Republic of China. Canadian *Journal of Earth Science, 30*, 2082–2095.

Saleiro, A., & **Tschopp, E.** (2025). New sauropod teeth from the Upper Jurassic of Portugal and their implications for sauropod dental evolution. *Papers in Palaeontology*, *11*, e70001. https://doi.org/10.1002/spp2.70001

Salgado, L., & **Bonaparte, J. F.** (1991). Un nuevo saurópodo Dicraeosauridae, *Amargasaurus cazaui* gen. et sp. nov., de la Formacion La Amarga, Neocomiano de la Provincia del Neuquén, Argentina. *Ameghiniana*, *28*, 333–346.

Salgado, L., & **Calvo, J. O.** (1992). Cranial osteology of *Amargasaurus cazaui* Salgado & Bonaparte (Sauropoda, Dicraeosauridae) from the Neocomian of Patagonia. *Ameghiniana*, *29*, 33–46.

Salgado, L., **Canudo, J. I.**, **Garrido, A. C.**, & **Carballido, J. L.** (2012). Evidence of gregariousness in rebbachisaurids (Dinosauria, Sauropoda, Diplodocoidea) from the Early Cretaceous of Neuquén (Rayoso Formation), Patagonia, Argentina. *Journal of Vertebrate Paleontology*, *32*, 603–613. https://doi.org/10.1080/02724634.2012.661004

Salgado, L., **Carvalho, I.**, & **Garrido, A. C.** (2006). *Zapalasaurus bonapartei*, un neuvo saurópodo de La Formación La Amarga (Cretacico Inferior), noroeste de Patagonia, Provincia de Neuquén, Argentina. *Geobios*, *39*, 695–707. https://doi.org/10.1016/j.geobios.2005.06.001

Salgado, L., **Coria, R. A.**, & **Calvo, J. O.** (1997). Evolution of titanosaurid sauropods. I: phylogenetic analysis based on the postcranial evidence. *Ameghiniana*, *34*, 3–32.

Salgado, L., **Gallina, P. A.**, **Lerzo, L. N.**, & **Canudo, J. I.** (2022). Highly specialized diplodocoids: The Rebbachisauridae. In A. Otero, J. L., Carballido, and D. Pol (Eds.), *South American sauropodomorph dinosaurs: Record, diversity and evolution* (pp. 165–208). Springer.

Salgado, L., **Garrido, A. C.**, **Cocca, S. E.**, & **Cocca, J. R.** (2004). Lower Cretaceous rebbachisaurid sauropods from Cerro Aguada del León, Neuquén Province, northwestern Patagonia, Argentina. *Journal of Vertebrate Paleontology*, *24*, 903–912. https://doi.org/10.1671/0272-4634(2004)024[0903:LCRSFC]2.0.CO;2

Salgado, L., **Novas, F. E.**, **Suarez, M.**, **Cruz, R.**, **Isasi, M.**, **Rubilar-Rogers, D.**, & **Vargas, A. O.** (2015). Late Jurassic sauropods in Chilean Patagonia. *Ameghiniana*, *52*, 418–429. https://doi.org/10.5710/AMGH.07.05.2015.2883

Schade, M., **Knötschke, N.**, **Hörnig, M. K.**, **Paetzel, C.**, & **Stumpf, S.** (2022). Neurovascular anatomy of dwarf dinosaur implies precociality in sauropods. *eLife*, *11*, e82190. https://doi.org/10.7554/eLife.82190

Schwarz, D., **Frey, E.**, & **Meyer, C. A.** (2007). Pneumaticity and soft-tissue reconstructions in the neck of diplodocid and dicraeosaurid sauropods. *Acta Palaeontologica Polonica*, *52*, 167–188.

Schwarz-Wings, D., & **Böhm, N.** (2014). A morphometric approach to the specific separation of the humeri and femora of *Dicraeosaurus* from the Late Jurassic of Tendaguru/Tanzania. *Acta Palaeontologica Polonica*, *59*, 81–98.

Scotese, C. R. (2021). An atlas of Phanerozoic paleogeographic maps: The seas come in and the seas go out. *Annual Review of Earth and Planetary Sciences*, *49*, 679–728. https://doi.org/10.1146/annurev-earth-081320-064052

Sereno, P. C. (1998). A rationale for phylogenetic definitions, with application to the higher-level taxonomy of Dinosauria. *Neues Jahrbuch für Geologie und Paläontologie – Abhandlungen*, *210*, 41–83. https://doi.org/10.1127/njgpa/210/1998/41

Sereno, P. C., **Beck, A. L.**, **Dutheil, D. B.**, **Larsson, H. C. E.**, **Lyon, G. H.**, **Moussa, B.**, **Sadleir, R. W.**, **Sidor, C. A.**, **Varricchio, D. J.**, **Wilson, G. P.**, & **Wilson, J. A.** (1999). Cretaceous sauropods from the Sahara and the uneven rate of skeletal evolution among dinosaurs. *Science*, *286*, 1342–1347. https://doi.org/10.1126/science.286.5443.1342

Sereno, P. C., **Wilson, J. A.** (2005). Structure and evolution of a sauropod tooth battery. In K. A. Curry Rogers & J. A. Wilson (Eds.), *The sauropods: Evolution and paleobiology* (pp. 157–177). University of California Press.

Sereno, P. C., **Wilson, J. A.**, **Witmer, L. M.**, **Whitlock, J. A.**, **Maga, A.**, **Ide. O.**, & **Rowe, T. A.** (2007).

Structural extremes in a Cretaceous dinosaur. *PLoS ONE*, *2*, e1230. https://doi.org/10.1371/journal.pone.0001230

Seton, M., **Müller, R. D.**, **Zahirovic, S.**, **Gaina, C.**, **Torsvik, T. H.**, **Shephard, G.**, **Talsma, A.**, **Gurnis, M.**, **Turner, M.**, **Maus, S.**, & **Chandler, M.** (2012). Global continental and ocean basin reconstructions since 200 Ma. *Earth-Science Reviews*, *113*, 212–270. https://doi.org/10.1016/j.earscirev.2012.03.002

Sharma, A., **Singh, S.**, & **Satheesh, S. R.** (2022). The first turiasaurian sauropod of India reported from the Middle Jurassic (Bathonian) sediments of Jaisalmer Basin, Rajasthan, India. *Neues Jahrbuch für Geologie und Paläontologie, Abhandlungen*, *304*, 187–203. https://doi.org/10.1127/njgpa/2022/1064

Simón, M. E., & **Salgado, L.** (2025). New rebbachisaurid (Dinosauria, Sauropoda) from the Huincul Formation (upper Cenomanian–Turonian) of Villa El Chocón (Neuquén Province, Argentina). *Cretaceous Research*, *173*, 106137. https://doi.org/10.1016/j.cretres.2025.106137

Sues, H.-D., **Averianov, A.**, **Ridgely, R. C.**, & **Witmer, L. M.** (2015). Titanosauria (Dinosauria, Sauropoda) from the Upper Cretaceous (Turonian) Bissekty Formation of Uzbekistan. *Journal of Vertebrate Paleontology*, *35*, e889145. https://doi.org/10.1080/02724634.2014.889145

Tan, C., **Dai, H.**, **He, J.-J.**, **Zhang, F.**, **Hu, X.-F.**, **Yu, H.-D.**, **Li, N.**, **Wei, G.-B.**, **Peng, G.-Z.**, **Ye, Y.**, **Zhang, Q.-N.**, **Ren, X.-X.**, & **You, H.-L.** (2019). Discovery of Omeisaurus (Dinosauria: Sauropoda) in the Middle Jurassic Shaximiao Formation of Yunyang, Chongqing, China. *Vertebrata Palasiatica*, *57*, 105–116.

Taquet, P. (1976). *Géologie et paléontologie du gisement de Gadoufaoua (Aptien du Niger)*. Cahiers de Paléontologie.

Taylor, M. P. (2018). *Xenoposeidon* is the earliest known rebbachisaurid sauropod dinosaur. *PeerJ*, *6*, e5212. https://doi.org/10.7717/peerj.5212

Taylor, M. P., & **Naish, D.** (2005). The phylogenetic taxonomy of Diplodocoidea (Dinosauria: Sauropoda). *PaleoBios*, *25*, 1–7.

Taylor, M. P., & **Naish, D.** (2007). An unusual new neosauropod dinosaur from the Lower Cretaceous Hastings Beds Group of East Sussex, England. *Palaeontology*, **50**, 1547–1564. https://doi.org/10.1111/j.1475-4983.2007.00728.x

Tennant, J. P., **Mannion, P. D.**, **Upchurch, P.**, **Sutton, M. D.**, & **Price, G. D.** (2017). Biotic and environmental dynamics across the Late Jurassic–Early Cretaceous transition: evidence for a protracted period of faunal and ecological turnover. *Biological Reviews*, *92*, 776–814. https://doi.org/10.1111/brv.12255

Tidwell, V., **Carpenter, K.**, & **Brooks, W.** (1999). New sauropod from the Lower Cretaceous of Utah, USA. *Oryctos*, *2*, 21–37.

Torcida Fernández-Baldor, F. (2012). *Sistemática, filogenia y análisis paleobiogeográfico de Demandasaurus darwini (Sauropoda, Rebbachisauridae) del Barremiense Superior–Aptiense de Burgos (España) [Unpublished PhD Thesis]*. Universidad Zaragoza.

Torcida Fernández-Baldor, F., **Canudo, J. I.**, **Huerta, P.**, **Montero, D.**, **Pereda Suberbiola, X.**, & **Salgado, L.** (2011). *Demandasaurus darwini*, a new rebbachisaurid sauropod from the Early Cretaceous of the Iberian Peninsula. *Acta Palaeontologica Polonica*, *56*, 535–552. https://doi.org/10.4202/app.2010.0003

Tschopp, E., & **Mateus, O.** (2013). The skull and neck of a new flagellicaudatan sauropod from the Morrison Formation and its implication for the evolution and ontogeny of diplodocid dinosaurs. *Journal of Systematic Palaeontology*, *11*, 853–888. https://doi.org/10.1080/14772019.2012.746589

Tschopp, E., & **Mateus, O.** (2017). Osteology of *Galeamopus pabsti* sp. nov. (Sauropoda: Diplodocidae), with implications for neurocentral closure timing, and the cervico-dorsal transition in diplodocids. *PeerJ*, *5*, e3179. https://doi.org/10.7717/peerj.3179

Tschopp, E., **Mateus, O.**, & **Benson, R. B. J.** (2015). A specimen-level phylogenetic analysis and taxonomic revision of Diplodocidae (Dinosauria, Sauropoda). *PeerJ*, *3*, e857. https://doi.org/10.7717/peerj.857

Upchurch, P. (1995). The evolutionary history of sauropod dinosaurs. *Philosophical Transactions of the Royal Society B*, *349*, 365–390.

Upchurch, P. (1998). The phylogenetic relationships of sauropod dinosaurs. *Zoological Journal of the Linnean Society*, *124*, 43–103. https://doi.org/10.1111/j.1096-3642.1998.tb00569.x

Upchurch, P., & **Barrett, P. M.** (2005). A phylogenetic perspective on sauropod diversity. In K. A. Curry Rogers & J. A. Wilson (Eds.), *The sauropods: Evolution and paleobiology* (pp. 104–124). University of California Press.

Upchurch, P., **Barrett, P. M.**, & **Dodson, P.** (2004). Sauropoda. In D. B. Weishampel, P. Dodson & H. Osmolska (Eds.), *The Dinosauria* (2nd ed., pp. 259–322). University of California Press.

Upchurch, P., & **Mannion, P. D.** (2009). The first diplodocid from Asia and its implications for the evolutionary history of sauropod dinosaurs. *Palaeontology*, *52*, 1195–1207. https://doi.org/10.1111/j.1475-4983.2009.00909.x

Upchurch, P., **Mannion, P. D.**, **Xu, X.**, & **Barrett, P. M.** (2021). Re-assessment of the Late Jurassic eusauropod dinosaur *Hudiesaurus sinojapanorum* Dong, 1997, from the Turpan Basin, China, and the evolution of hyper-robust antebrachia in sauropods. *Journal of Vertebrate Paleontology*, *41*, e1994414. https://doi.org/10.1080/02724634.2021.1994414

Upchurch, P., & **Martin, J.** (2003). The anatomy and taxonomy of *Cetiosaurus* (Saurischia: Sauropoda) from the Middle Jurassic of England. *Journal of Vertebrate Paleontology*, *23*, 208–231. https://doi.org/10.1671/0272-4634(2003)23[208:TAATOC]2.0.CO;2

Upchurch, P., **Tomida, Y.**, & **Barrett, P. M.** (2004). A new specimen of Apatosaurus ajax (Sauropoda: Diplodocidae) from the Morrison Formation (Upper Jurassic) of Wyoming, USA. *National Science Museum Monographs, Tokyo*, *26*, 1–108.

van der Linden, T., **Tschopp, E.**, **Sookias, R.**, **Wallaard, J.**, **Holwerda, F.**, & **Schulp, A.** (2024). A new diplodocine sauropod from the Morrison Formation, Wyoming, USA. *Palaeontologia Electronica*, **27**, A48.

Wedel, M. J. (2003). The evolution of vertebral pneumaticity in sauropod dinosaurs. *Journal of Vertebrate Paleontology*, *23*, 344–357. https://doi.org/10.1671/0272-4634(2003)023[0344:TEOVPI]2.0.CO;2

Wedel, M. J., & **Taylor, M. P.** (2013). Caudal pneumaticity and pneumatic hiatuses in the sauropod dinosaurs *Giraffatitan* and *Apatosaurus*. *PLoS ONE*, *8*, e78213. https://doi.org/10.1371/journal.pone.0078213

Weishampel, D. B., **Dodson, P.**, & **Osmolska, H.** (2004). *The Dinosauria* (2nd ed.) University of California Press.

Whitlock, J. A. (2011a). A phylogenetic analysis of Diplodocoidea (Saurischia: Sauropoda). *Zoological Journal of the Linnean Society*, *161*, 872–915. https://doi.org/10.1111/j.1096-3642.2010.00665.x

Whitlock, J. A. (2011b). Re-evaluation of *Australodocus bohetii*, a putative diplodocoid sauropod from the Tendaguru Formation of Tanzania, with comment on Late Jurassic sauropod faunal diversity and palaeoecology. *Palaeogeography, Palaeoclimatology, Palaeoecology*, *309*, 333–341. https://doi.org/10.1016/j.palaeo.2011.07.001

Whitlock, J. A., **D'Emic, M. D.**, & **Wilson, J. A.** (2011). Cretaceous diplodocids in Asia? Re-evaluating the phylogenetic affinities of a fragmentary specimen. *Palaeontology*, *54*, 351–364. https://doi.org/10.1111/j.1475-4983.2010.01029.x

Whitlock, J. A., & **Harris, J. D.** (2010). The dentary of *Suuwassea emilieae* (Sauropoda: Diplodocoidea). *Journal of Vertebrate Paleontology*, *30*, 1637–1641. https://doi.org/10.1080/02724634.2010.501452

Whitlock, J. A., & **Wilson Mantilla, J. A.** (2020). The Late Jurassic sauropod dinosaur '*Morosaurus*' *agilis* Marsh, 1889 reexamined and reinterpreted as a dicraeosaurid. *Journal of Vertebrate Paleontology*, *40*, e1780600. https://doi.org/10.1080/02724634.2020.1780600

Wilson, J. A. (2002). Sauropod dinosaur phylogeny: critique and cladistic analysis. *Zoological Journal of the Linnean Society*, *136*, 217–276. https://doi.org/10.1046/j.1096-3642.2002.00029.x

Wilson, J. A. (2005). Redescription of the Mongolian sauropod *Nemegtosaurus mongoliensis* Nowinski (Dinosauria: Saurischia) and comments on Late Cretaceous sauropod diversity. *Journal of Systematic Palaeontology*, *3*, 283–318. https://doi.org/10.1017/S1477201905001628

Wilson, J. A., & **Allain, R.** (2015). Osteology of *Rebbachisaurus garasbae* Lavocat, 1954, a diplodocoid (Dinosauria, Sauropoda) from the early Late Cretaceous-aged Kem Kem beds of southeastern Morocco. *Journal of Vertebrate Paleontology*, *35*, e1000701. https://doi.org/10.1080/02724634.2014.1000701

Wilson, J. A., & **Sereno, P. C.** (1998). Early evolution and higher-level phylogeny of sauropod dinosaurs. *Memoir of the Society of Vertebrate Paleontology*, *5*, 1–79.

Wilson, J. A., & **Upchurch, P.** (2009). Redescription and reassessment of the phylogenetic affinities of *Euhelopus zdanskyi* (Dinosauria: Sauropoda) from the Early Cretaceous of China. *Journal of Systematic Palaeontology*, *7*, 199–239. https://doi.org/10.1017/S1477201908002691

Windholz, G. J., **Baiano, M. A.**, **Bellardini, F**, & **Garrido, A.** (2021). New Dicraeosauridae (Sauropoda, Diplodocoidea) remains from the La Amarga Formation (Barremian–Aptian, Lower Cretaceous), Neuquén Basin, Patagonia, Argentina. *Cretaceous Research*, *117*, 104629.

Windholz, G. J., **Coria, R. A.**, **Bellardini, F.**, **Baiano, M. A.**, **Pino, D.**, **Ortega, F.**, & **Currie, P. J.** (2022). On a dicraeosaurid specimen from the Mulichinco Formation (Valanginian, Neuquén Basin) of Argentina and phylogenetic relationships of the South American dicraeosaurids (Sauropoda, Diplodocoidea). *Comptes Rendus Palevol*, *21*, 991–1019. https://doi.org/10.5852/cr-palevol2022v21a45

Windholz, G. J., **Coria, R. A.**, **Zurriaguz, V. L.** (2020). Vertebral pneumatic structures in the Early Cretaceous sauropod dinosaur *Pilmatueia faundezi* from northwestern Patagonia, Argentina. *Lethaia*, *53*, 369–381. https://doi.org/10.1111/let.12363

Windholz, G. J., **Porfiri, J. D.**, **Dos Santos, D.**, **Bellardini, F.**, & **Wedel, M. J.** (2024). A well-preserved vertebra provides new insights into rebbachisaurid (Sauropoda, Diplodocoidea) caudal anatomical and pneumatic features. *Acta Palaeontologica Polonica*, *69*, 39–47. https://doi.org/10.4202/app.01104.2023

Xing, L., **Miyashita, T.**, **Zhang, J.**, **Li, D.**, **Te, Y.**, **Sekiya, T.**, **Wang, F.**, & **Currie, P. J.** (2015). A new sauropod dinosaur from the Late Jurassic of China and the diversity, distribution, and relationships of mamenchisaurids. *Journal of Vertebrate Paleontology*, *35*, e889701. https://doi.org/10.1080/02724634.2014.889701

Xu, X., **Upchurch, P.**, **Mannion, P. D.**, **Barrett, P. M.**, **Regalado-Fernandez, O. R.**, **Mo, J.**, **Ma, J.**, & **Liu, H.** (2018). A new Middle Jurassic diplodocoid suggests an earlier dispersal and diversification of sauropod dinosaurs. *Nature Communications*, *9*, 2300. https://doi.org/10.1038/s41467-018-05128-1

You, S., **Li, Z.**, & **Li, Y.** (2019). The stratigraphical characteristics and sedimentary environment of dinosaurs in Lingwu, Ningxia. *Acta Geologica Sichuan*, *39*, 31–35.

Zhang, X.-Q., **Li, D.-Q.**, **Xie, Y.**, & **You, H.-L.** (2020). Redescription of the cervical vertebrae of the mamenchisaurid sauropod *Xinjiangtitan shanshanesis* Wu et al. 2013. *Historical Biology*, *32*, 803–822. https://doi.org/10.1080/08912963.2018.1539970

Zhang, Z., **Wang, T.**, **Ramezani, J.**, **Lv, D.**, & **Wang, C.** (2021). Climate forcing of terrestrial carbon sink during the Middle Jurassic greenhouse climate: Chronostratigraphic analysis of the Yan'an Formation, Ordos Basin, North China. *GSA Bulletin*, *133*, 1723–1733. https://doi.org/10.1130/B35765.1

Associate Editor: Kimberley Chapelle